Role of Climate, Land Use/Cover and Water Quality on West Nile Virus Incidence: A Modeling Approach

by

Navideh Noori

A dissertation submitted to the Graduate Faculty of
Auburn University
in partial fulfillment of the
requirements for the Degree of
Doctor of Philosophy

Auburn, Alabama
August 1st, 2015

Keywords: West Nile Virus, water quality, climate variables, mosquito habitat, urbanization, prediction.

Approved by

Latif Kalin, Chair, Professor, School of Forestry and Wildlife Sciences
B. Graeme Lockaby, Associate Dean and Professor, School of Forestry and Wildlife Sciences
Hanqin Tian, Professor, School of Forestry and Wildlife Sciences
Puneet Srivastava, Professor, Biosystems Engineering Department

Abstract

West Nile virus (WNV), a vector-borne infectious disease, has been a major public health concern in North America since 1999. This virus is transmitted to susceptible mosquitoes when they feed on infected birds. Infected mosquitoes spread the virus to humans and other animals when they bite. To control mosquito-borne diseases, it is necessary to identify the locations of mosquito breeding sites and to monitor changes in mosquito population under different environmental conditions. The focus of this study was to investigate the impacts of different risk factors on *Culex quinquefasciatus* population in the central north part of the State of Georgia and particularly in the Atlanta metropolitan area. The main risk factors considered in this study were climate variability, Land use/cover (LULC) types and their impact on water quality and streamflow. To demonstrate which specific components of water chemistry are conducive to breeding *Culex* mosquitoes, a mesocosm experiment was designed. The emergence pattern of *Culex* mosquitoes was found to be strongly related to certain nutrients, and results showed that breeding sites with higher PO_4 or NO_3 concentrations have higher survival rate of larvae. High NO_3 concentrations favor the development of male mosquitoes and suppress the development of female mosquitoes, but those adult females that do emerge, develop faster in containers with high NO_3 levels compared to the reference group. Also, the addition of PO_4 in the absence of nitrogen sources to the larval habitat slowed larval development, however, it took less days for larvae to

reach the pupal stage in containers with combination of NO_3 and PO_4 or NH_4 and PO_4 nutrients. In addition, short term effects of climate conditions on seasonal variation of *Culex* mosquito abundance and their infection rate in the central north part of Georgia from 2002 to 2009 were assessed. The Poisson regression model and Artificial Neural Network (ANN) model were used for the prediction purposes. Statistical analysis revealed that increasing temperature and PET and decreasing surface moisture in preceding late winter and preceding spring increased *Culex quinquefasciatus* female mosquitoes abundance in summer/early fall about 2 times as many and also increased the number of infectious mosquitoes about 3.5 times. Also low precipitation in late winter decreased mosquito abundance in summer. However, above average temperature in late winter and early spring coupled with below average precipitation favors the incidence of WNV in mosquitoes. Both ANN and regression models predicted the seasonal cycle of mosquito abundance fairly accurate. Addition of antecedent mosquito count data or infection rate as predictors improved the prediction power of both models by increasing E_{NASH} values and decreasing R_{BIAS} values. To examine the relationship between LULC and various water quality parameters and to predict water quality in unmonitored watersheds in Atlanta area, an ANN-based model was applied. Streamflow and water quality data from neighboring USGS stations in the Atlanta area with *leave-one-site-out jackknifing* technique were used to build the predictive models for PO_4, NH_4 and NO_3 loading values. NO_3, NH_4 and PO_4 predictive models with best performance had E_{NASH} values of 0.99, 0.89, and 0.66 respectively and R_{BIAS} values of 8%, -6% and -7% respectively. No general trend was observed between percent imperviousness or percent forest cover or

watershed size and the model performances. Also, a lumped model (ANN) and semi-distributed watershed model, Soil & Water Assessment Tool (SWAT), were combined to improve ANN performance for predicting flow during warm and cool. 62% of runs for predicting flow during cool season and 83% of runs for predicting flow during warm season had “good” to “very good” performance ratings. The developed predictive models can be used for a more accurate warning of high-risk periods for WNV and could have important implications for the control of West Nile Virus spread by *Culex* mosquito species. Also, the findings of this study can help reduce the costs and efforts required for effective mosquito vector control by focusing on areas with higher risk.

Acknowledgements

I would like to express the deepest appreciation to my major advisor, Dr. Latif Kalin, who has helped and supported me continuously during my Ph.D. program. Without his guidance and persistent help this dissertation would not have been possible. I would like to thank Dr. Graeme Lockaby, one of my committee members and also the main PI of the project, for his unlimited support during my academic life. I place on record, my sincere gratitude to them for their assistance and guidance and for giving me the opportunity of working with them in a nice friendly environment.

I would like to thank my committee members, Dr. Hanqin Tian and Dr. Puneet Srivastava for their assistance. I also would like to thank Charlene LeBlue for accepting to be my outsider reader. I wish to express my sincere gratitude to Ms. Patti Staudenmaier for the efforts she put to help me during my degree program and to make things work. Ms. Patti brought all the positive energy to me by welcoming me to SFWS with her smile. Without her support, I could not make this happen.

Many people helped make this dissertation possible. I would like to gratefully acknowledge Dr. Krisztian Magori, Dr. Nannan Liu, Dr. Ash Abebe, Dr. Derrick Mathias and Robin Governo who assisted with the mesocosm experiment and with this research. This project was funded by USDA Forest Service, National Urban & Community Forestry Council and Center for Environmental Studies at the Urban-Rural Interface, School of Forestry and Wildlife Sciences,

Auburn University. I would like to thank the Southeast Cooperative Wildlife Disease Study (SCWDS) at the College of Veterinary Medicine at University of Georgia, Athens for providing me the mosquito data.

Off course if I did not have supports of my family and friends, I could not have been here. No doubt, if I did not have the support of a nice caring thoughtful friend like Hamed Majidzadeh, I could not make it through and complete my dissertation. I would like to thank my dearest friends, Luana Ozelim and Golpar Garmestani for their support in my academic and personal life. Many thanks go to my friends and lab mates Dr. Sabahattin Isik, Dr. Amir Sharifi, Mehdi Rezaeianzadeh, Rasika Ramesh and Enis Baltaci for being patient with me and for understanding me. I would like to thank Dr. John Kush for his supports during my program. I also wish to thank my brother, Navid Noori, for his unconditional love and support. I dedicate this work to my parents, in memory of my father, Hossein Noori, and also to my mother, Kobra Sharafaei, for her support and encouragement. My father was my rock and he always believed in me and trusted me.

Table of Contents

List of Tables

List of Figures

Chapter 1. Introduction

Introduction

Transmission of vector-borne diseases in urban environments is an important global health concern and West Nile Virus (WNV) fever has repeatedly been identified as a major epidemiological concern in the developed world (Morens et. al. 2004). Since 1999, more than 39,000 disease cases of WNV had been reported to the Center for Disease Control (CDC) (ArboNET, Arboviral Diseases Branch, Centers for Disease Control and Prevention, 2013). WNV is primarily maintained in nature by transmission cycles between mosquitoes and avian hosts (Deichmeister and Telang, 2010). This virus can infect other hosts including humans and horses. *Culex* species are the major vector of West Nile Virus disease in the United States. In the southeast U.S., over 96% of the West Nile Virus positive mosquito pools reported to the CDC from 1999 to 2010 have been obtained from *Culex* mosquitoes, among which 64.6% were from *Culex quinquefasciatus* (Andreadis, 2012). The state of Georgia, and especially the Atlanta area has been a hotspot of WNV incidence in 2012 with 117 WNV human cases, 6 deaths and 125 WNV positive mosquito pools (among which over 81% were from *Culex quinquefasciatus*) reported by the Georgia Department of Public Health.

Mosquito infection rate changes from year to year spatiotemporally. Multiple environmental drivers can affect WNV amplification and transmission to humans. Assessing the spatial patterns

of environmental determinants associated with vector and host can help recognize the geographic locations of populations at risk. Temporal analysis can also clarify inter-annual and seasonal variation of the vector abundance, and long-term predictions of shifts in mosquito abundance which can help identify high-risk periods for WNV (Rezaeian et al. 2007; Zeger et al. 2004; Wimberly et al. 2013).

Major components of any arboviral surveillance system include a thorough understanding of the population dynamics of vectors and avian amplification hosts, the spatiotemporal distribution of the arboviruses, the interrelationships of vectors, environmental condition of mosquito habitats, and meteorological factors, including rainfall and temperature, that drive arboviral cycles (Day 1991, Day and Lewis 1992). In spite of the large number of studies on vector-borne diseases, most of them assessed the impacts of changes in landscape characteristics on WNV transmission in a general level and solely from remotely sensed data or these contextual factors are often neglected in research related to disease transmission and public health (Brown et al. 2008, LaBeaud et al. 2008, Messina et al. 2011).

In this research, quantitative relationships among *Culex quinquefasciatus* productivity, landscape characteristics, climatic variability and water quality conditions in streams were explored. The ability of predicting WNV carrying *Culex quinquefasciatus* population will be enhanced by applying the identified relationships among landscape characteristics and temporal and spatial patterns of WNV risk. Data from the state of Georgia, specifically Atlanta area, was utilized in developing and testing these relationships. It is critical to improve our capability to

predict WNV risk across rural as well as developed landscapes to prevent the future spread of WNV infection. Detailed assessment of environmental risk factors would help predict spatial patterns of human WNV risk in Atlanta area. Also by directing surveillance activities and environmental monitoring and public health interventions, the early warning of WNV risk outbreaks would be possible.

Proposed Research

The prevalence and transmission of vector-borne pathogens is determined by the distribution and abundance of the primary vector (Reiter and LaPointe, 2007). These parameters affect WNV risk because of their influences on mosquito habitat suitability, avian host communities and human exposure to infected mosquitoes (Chuang et al. 2012). To assess the prevalence of vector-borne diseases within an area and to implement control measures, understanding the spatial and temporal dynamics of mosquito communities is vital (Buckner et al. 2010). In this study, some important risk factors were considered and their relationship with *Culex quinquefasciatus* population was assessed.

1. Water quality and *Culex quinquefasciatus* population

Culex larval habitats remain one of the largest targets for municipal surveillance programs in the United States (Deichmeister and Telang, 2010). Environmental modifications due to urbanization and human activity increase the number of artificial water collection reservoirs which

are common aquatic habitats for *Culex quinquefasciatus*. These species are found in artificial larval habitats such as catch basins, open containers that hold water and organic material long enough for the development of larvae to the adult stage (Jacob et al. 2006, Gardner et al. 2013). Combined sewer overflows (CSOs) are considered point source pollution and major urban breeding sites for *Culex quinquefasciatus* as they provide nutrient rich water which is unfavorable for mosquito predators due to diminished oxygen concentrations (Calhoun et al. 2007). Some studies have assessed the impacts of CSOs on WNV vector mosquito production (Bentley and Day 1989, Calhoun et al. 2007, Chaves et al. 2009). However, even after CSO improvements, elevated levels of WNV cases are observed in urban areas, which reveals that CSOs and catch basins are not the only sources of *Culex* mosquito production. Limited information exists on the effects of nutrient concentrations typically found in field conditions, and dose-response curves in general, for *Culex* species, despite their importance as major vectors of WNV.

To clarify which specific water chemistry is conducive to breeding the mosquitoes associated with the virus, a mesocosm experiment was designed. The water concentrations of NO_3, NH_4 and PO_4 have been selected to reflect the ranges commonly reported in urban streams in the Southeast U.S. Statistical analyses were performed to determine if the treatments significantly affected the number of larvae, pupae and adult mosquitoes. This study enabled us to develop dose–response relationships between larval development and NO_3, NH_4, and PO_4 concentrations in the stream water. This experiment can determine the mosquito reactions under different water quality conditions, specifically in lower nutrient concentrations which are more widespread in the

landscape. This will be more significant when it comes to human health especially in residential areas with standing waters in flower pots, buckets, tires and barrels in back yards which are good mosquito breeding sites with different nutrient levels.

2. Climatic variability and *Culex quinquefasciatus* abundance and their infection rate

Climatic variability is one of the most important drivers of inter-annual WNV transmission risk. Climate directly affects the vector population, pathogens and hosts distribution, and their abundances (Roiz et al., 2014). Changes in meteorological conditions such as temperature, relative humidity and wind speed can impact mosquito populations (Curriero et al., 2005). Drought followed by wetting of the land surface is significantly associated with the spatial-temporal variability of WNV human cases (Shaman et al. 2005). The extreme weather conditions accompanying long-term climate change may be contributing to the spread of WNV in the United States and Europe (Epstein, 2001; Platonov et. al., 2008). Changes in weather patterns with global climate change make it especially important to improve our ability to predict how inter-related local weather and environmental factors affect vectors and vector-borne disease risk (Ruiz et. al., 2010).

However, in most previous studies, the impact of meteorological conditions on mosquito abundance was limited to single point lags which consider the conditions at a certain time point prior to trapping. In this study, to investigate the correlation between climate forces and inter-annual and seasonal variation of *Culex mosquito* population carrying WNV as well as their

infection rate, cross-correlation maps (CCMs), introduced by Curriero et al. (2005), were developed for mosquito data from the central north part of the State of Georgia (GA). The main goal was to develop an improved predictive model of *Culex quinquefasciatus* population and their infection rate, which would advance our understanding of the transmission of mosquito-borne arboviruses (Walsh et al., 2008), using the lagged climate data and by extending effects of climate conditions over a range of time rather than a single point in time. Two modeling approaches were applied in this study, multi-regression and Artificial Neural Network (ANN); lagged climate data were fed into these models for prediction purposes at four weeks moving average scale.

3. Linkage between LULC and water quality

A growing human population accelerates urbanization, forest disturbance and other types of LULC changes. Such land use changes modify the hydrological processes and water balance of river basins. Environmental disturbances such as urbanization and deforestation play a key role in the emergence of many infectious diseases (Patz et al. 2004; Saleeza et al. 2011) through changing hydrological processes and water balance of river basins. Urban/suburban land use can enhance environmental conditions for enzootic and bridge transmission of WNV to humans (Brown et al., 2008). Concentrations of many water quality constituents changes due to altered sediment transport rate, chemical loads, and watershed hydrology. Nutrient concentrations and conductivity increase in urbanized streams due to water quality degradation (Paul and Meyer 2001; Walsh et al. 2005, Chadwick et. al.; 2012). As nutrients are limiting resources for bacteria and mosquitoes

feed on bacteria, stream pollution is a major determinant of the abundance of mosquito vectors (Chaves et al. 2010; Calhoun et al. 2007).

However, there are not enough water quality data available in trap sites with high number of WNV positive mosquito pools around Atlanta area. To examine the relationship between LULC and various water quality parameters and to predict water quality in unmonitored watersheds with similar characteristics, Kalin et al. (2010) developed an ANN-based model. To predict water quality as a function of LULC in ungauged sites close to the mosquito trap sites in the Atlanta area, GA, Kalin et al. (2010) methodology was extended in this study. Data from neighboring USGS stations in the Atlanta area, GA was used to build the model. Streamflow was one of the input data to the model and since no streamflow data was available, a quasi-distributed model, Soil and water assessment tool (SWAT), was applied to simulate streamflow.

4. Combined impact of environmental predictors of *Culex quinquefasciatus* abundance

Environmental conditions prompt mosquito population dynamics and consequently affect disease spread. To control mosquito populations and to prevent the disease, understanding this vector‑environment relationship is essential. Biotic and abiotic conditions affect mosquito behaviors and consequently the risk of WNV epidemics (Paz et al. 2013). This virus occurrence is impacted by many risk factors such as the presence of susceptible avian hosts, infected birds, mosquito abundance that feed on birds and human or horses, and the interaction of the vector with the biotic and abiotic environment. The most important environmental factors influencing the

maintenance of WNV are climate variability, land use characteristics, water quality conditions of mosquito breeding sites and socio-economic conditions. The impacts of spatially heterogeneous environmental and ecological factors on mosquito population dynamics are complex and understanding the inter-relationships between vectors, hosts, and their environment can provide valuable information for identifying conditions suitable for pathogen transmission (Bisanzio et al. 2011).

In this part of study, to characterize the water quality conditions of streams around Atlanta and to link it to distribution of WNV transmission risk, mosquito trap sites that have been used at least 10 times in Fulton, DeKalb and Cobb counties and were located near a stream network with the distance of 1 km or less were selected. Daily streamflow and nutrient loadings were predicted using the developed ANN models from previous chapter and the results were linked to the developed regression models from the mesocosm experiment to estimate *Culex quinquefasciatus* population under water quality conditions in Atlanta area.

General outline

This research is organized according to the following framework: Chapter 1 delivers an introductory overview of the topic, presents the research purposes and objectives, and also a review of the methodology proposed for each objectives in chapters 2 to 5. Chapter 2 documents the relationship between larval development and different nutrient concentrations in stream water by

conducting a mesocosm experiment. This chapter has been accepted for publication in Journal of Vector Ecology (Noori et al. 2015).

Chapter 3 explains the inter-annual and seasonal variation of *Culex quinquefasciatus* and its infection rate based on the climate variability in the central north part of the State of Georgia, United States. Two modeling approaches: multi-regression and ANN were applied in this chapter to develop an improved predictive model of *Culex quinquefasciatus* population and their infection rate using the lagged climate data. This chapter is in the process of being submitted to a journal.

Chapter 4 examines the relationship between different LULC types and water quality parameters to develop a predictive model in unmonitored watersheds in the Atlanta area using an ANN-based model. Also, streamflow was predicted for ungauged watersheds using both ANN and SWAT models. Chapter 5 presents the predicted water quality constituents in the Atlanta area nearby mosquito trap sites and the predicted values in trap sites were linked to the mosquito population and larval development using the findings from chapter 2. This chapter also discusses the combined impacts of environmental factors on mosquito abundance in Atlanta area. Chapter 6 is a summary of major findings to the preceding chapters. Suggestions for the future studies are also discussed in this chapter.

References

Andreadis, Th.G., 2012. The contribution of *Culex pipens* complex mosquitoes to transmission and persistence of West Nile Virus in North America. The American Mosquito Control Association, Inc. Vol. 28, No. 4, page: 137-151.

Bently, M.D. and Day, J.F. 1989. Chemical ecology and behavioral aspects of mosquito oviposition. Ann. Rev. Entomol. 34: 401-421.

Bisanzio, D., Giacobini, M., Bertolotti, L., Mosca, A., Balbo, L., Kitron, U., Vazquez-Prokopec, G.M., 2011. Spatio-temporal patterns of distribution of West Nile virus vectors in eastern Piedmont Region, Italy. Parasites & Vectors. 4:230.Brown, H.E., Childs, J.E., Diuk-Wsser, M.A., Fish, D. 2008. Ecological factors associated with West Nile virus transmission, Northeastern United State. Emerg. Infect. Dis. 14: 1539-1545.

Brown, H.E., Childs, J.E., Diuk-Wsser, M.A., Fish, D. 2008. Ecological factors associated with West Nile virus transmission, Northeastern United State. Emerg. Infect. Dis. 14: 1539-1545.

Buckner, E.A., Blackmore, M.S., Golladay, S.W., Covich, A.P. 2010. Weather and landscape factors associated with adult mosquito abundance in southwestern Georgia, U.S.A. J. Vector Ecol. Vol. 36, No.2. 269-278.

Calhoun, L.M., Avery, M., Jones, L., Gunarto, K., King, R., Roberts, J., Burkot, T.R. 2007. Combined Sewage Overflows (CSO) Are Major Urban Breeding Sites for *Culex quinquefasciatus* in Atlanta, Georgia. Am. J. Trop. Med. Hyg. 77: 478–484.

Center for Disease Control and Prevention, division of Vector-Borne Dieases., 2013. West Nile Virus in the United States: Guidelines for Surveillance, Prevention, and Control. U.S. Department of Health and Human Services. Public Health Service.

Chadwick, M.A., Thiele, J.E., Huryn, A.D., Benke, A.C., Dobberfuhl, D.R. 2012. Effects of urbanization on macroinvertebrates in tributaries of the St. Johns River, Florida, USA. Urban Ecosyst, Springer. 15:347-365.

Chaves, L.F., Keogh, C., Vazquez-Prokopec, G.M., Kitron, U.D. 2009. Combined Sewage Overflow Enhances Oviposition of *Culex quinquefasciatus* (Diptera: Culicidae) in Urban Areas. J. Med. Entomol. 46: 220-226.

Chuang, T.W., Ionides, E.L., Knepper, R.G., Stanuszek, W.W., Walker, E.D., Wilson, M.L., 2012. Cross-Correlation Map analyses show weather variation influences on mosquito abundance patterns in Saginaw County, Michigan, 1989–2005. J Med Entomol. 49(4):851-858.

Curriero, F.C., Shone, S.M., Glass, G.E., 2005. Cross Correlation Maps: A tool for visualizing and modeling time lagged associations. Vector Borne Zoonotic Dis. Vol. 5, Number 3, 267-275.

Day, J. F. 1991. A review of the 1990 St. Louis encephalitis virus epidemic in Indian River County, Florida. Proc. New Jersey Mosquito Control Association. 78: 32-39.

Day, J. F., and A. L. Lewis. 1992. An integrated approach to St. Louis encephalitis surveillance in Indian River County, Florida. Fla. J. Public Health 4: 12-16.

Deichmeister, J.M. and Telang, A. 2010. Abundance of West Nile virus mosquito vectors in relation to climate and landscape variables. J. Vector Ecol. Vol. 36, no. 1: 75-85.

Epstein, P. R., 2001. West Nile Virus and the Climate. J Urban Health: Bulletin of the New York Academy of Medicine. Vo. 78, No, 2.

Gardner, A.M., Anderson, T.K., Hamer, G.L., Johnson, D.E., Varela, K.E., Walker, E.D., Ruiz, M.O. 2013. Terrestrial vegetation and aquatic chemistry influence larval mosquito abundance in catch basins, Chicago, USA. Parasit Vectors. 6:1-11.

Jacob, B.G., Shililu, J., Muturi, E.J., Mwangangi, J.M., Muriu, S.M., Funes, J., Githure, J., Regens, J.L., Novak, R.J. 2006. Spatially targeting *Culex quinquefasciatus* aquatic habitats on modified land cover for implementing an Integrated Vector Management (IVM) program in three villages within the Mwea Rice Scheme, Kenya. Int J Health Geogr. 5: 1-9.

Kalin, L., Isik, S., Schoonover, J.E., Lockaby, B.G. 2010. Predicting Water Quality in Unmonitored Watersheds Using Artificial Neural Networks. J Environ Qual. 39(4):1429-1440.

LaBeaud, A.D., Gorman, A., Koonce, J., Kippes, Ch., McLeod, J., Lynch, J., Gallagher, T., King, Ch. H., Mandalakas, A.M. 2008. Rapid GIS-based profiling of West Nile virus transmission: defining environmental factors associated with an urban-suburban outbreak in Northeast Ohio, USA. Geospat. Health. 2: 215-225.

Messina, J.P., Brown, W., Amore, G., Kitron, U.D., Ruiz, M.O. 2011. West Nile Virus in the greater Chicago area, a geographic Examination of Human Illness and risk from 2002 to 2006. URISA. 23, 5-18.

Morens, D. M., Folkers, G.K., Fauci, A.S. 2004. The challenge of emerging and re-emerging infectious diseases. Nature. 4390: 242-249.

Noori, N., Lockaby, G.B., Kalin, L. 2015. Larval development of *Culex quinquefasciatus* in water with low to moderate pollution levels. J. Vector Ecol. Vol. 40 (2).

Patz, J.A., Daszak, P., Tabor, G.M., Aguirre, A.A., Pearl, M., Epstein, J., Wolfe, N.D., Kilpatrick, A.M., Foufopoulos, J., Molyneux, M., Bradley, D.J. 2004. Unhealthy landscape: policy recommendations on land use change and infectious disease emergence. Environ. Health Perspect. 112: 1092-2098.

Paul, M.J. and Meyer, J.L. 2001. Streams in the urban landscape. Annu. Rev. Ecol. Syst. 32: 333-365.

Paz, Sh., Semenza, J.C. 2013. Environmental Drivers of West Nile Fever Epidemiology in Europe and Western Asia—A Review. Int. J. Environ. Res. Public Health. 10, 3543-3562.

Platonov. A.E., Fedorova. M.V., Karan. L.S., Shopenskaya, T.A., Platonova, O.V., Zhuravlev, V.I. 2008. Epidemiology of West Nile infection in Volgograd, Russia, in relation to climate change and mosquito (Diptera: Culicidae) bionomics. Parasitol Res. 103: S45-S53.

Reiter, M. and LaPointe, D.A. 2007. Landscape factors influencing the spatial distribution and abundance of Mosquito Vector *Culex quinquefasciatus* (Diptera: Culicidae) in a mixed residential–agricultural community in Hawai‘i. J. Med. Entomol. 44(5): 861-868.

Rezaeian, M.; Dunn, G.; St Leger, S.; Appleby, L. 2007. Geographical epidemiology, spatial analysis and geographical information systems: a multidisciplinary glossary. J. Epidemiol. Commun. Health, 61, 98–102.

Roiz, D., Ruiz, S., Soriguer, R., Figuerola, J., 2014. Climatic effects on mosquito abundance in Mediterranean wetlands. Parasites & Vectors. 7:333.

Ruiz, M.O., Chaves. L.F., Hamer, G.L., Sun, T., Brown, W.M., Walker, E.D., Haramis, L., Goldberg, T.L., Kitron, U.D. 2010. Local impact of temperature and precipitation on West Nile virus infection in *Culex* species mosquitoes in northeast Illinois, USA. Parasites & Vectors. 3:19.

Saleeza, S.N.R., Norma-Rashid, Y., Azirun, M.S. 2011. Mosquitoes larval breeding habitat in urban and suburban areas, Peninsular Malaysia. WASET. 58: 569-573.

Shaman, J., Day, J.F., Stieglitz, M., 2005. Drought-Induced Amplification and Epidemic Transmission of West Nile Virus in Southern Florida. J Med Entomol. 42(2): 134-141.

Walsh, A.S., Glass, G.E., Lesser, C.R., Curriero, F.C., 2008. Predicting seasonal abundance of mosquitoes based on off-season meteorological conditions. Environ Ecol Stat, 15:279–291.

Wimberly, M.C., Giacomo, P., Kightlinger, L., Hildreth, M.B. 2013. Spatio-temporal epidemiology of human West Nile Virus disease in South Dakota. Int. J. Environ. Res. Public Health, 10, 5584-5602.

Zeger, S.L.; Irizarry, R.A.; Peng, R.D. 2004. On time series analysis of public health and biomedical data. Annu. Rev. Public Health, 27, 57–69.

Chapter 2. Larval development of *Culex quinquefasciatus* in water with low to moderate pollution levels

Abstract

Population growth and urbanization have increased the potential habitats, and consequently the abundance of *Culex quinquefasciatus*, the southern house mosquito, a vector for West Nile Virus in urban areas. Water quality is critical in larval habitat distribution and in providing microbial food resources for larvae. To demonstrate which specific components of water chemistry are conducive to breeding *Culex* mosquitoes, a mesocosm experiment was designed. Dose–response relationships between larval development and NO_3, NH_4, and PO_4 concentrations in stream water were developed through this experiment to describe the isolated effects of each nutrient on pre-adult development. The emergence pattern of *Culex* mosquitoes was found to be strongly related to certain nutrients, and results showed that breeding sites with higher PO_4 or NO_3 concentrations have higher survival rate of larvae. High NO_3 concentrations favor the development of male mosquitoes and suppresses the development of female mosquitoes, but those adult females that do emerge, develop faster in containers with high NO_3 levels compared to the reference group. Also, the addition of PO_4 in the absence of nitrogen sources to the larval habitat slowed larval development, however, it took less days for larvae to reach the pupal stage in containers with combination of NO_3 and PO_4 or NH_4 and PO_4 nutrients. Results from this study may bolster efforts

to control WNV in urban landscapes by exploring water quality conditions of *Culex* larval habitats that produce adult mosquitoes.

Keywords*:* West Nile Virus, water quality, urbanization, *Culex* species, mosquito habitat, mesocosm.

Introduction

Infectious diseases continue to pose major challenges to global economies and public health (Morens et al. 2004, Jones et al. 2008). The transmission of vector-borne diseases in urban environments, particularly West Nile Virus (WNV), has repeatedly been identified as a major epidemiological concern in the developed world (Morens et al. 2004). Since WNV was recognized in New York City in 1999, it has spread rapidly across the United States (Center for Disease Control and Prevention (CDC) 2011). As a result of rapid land development in the Southeast, habitats for *Culex quinquefasciatus* have become enhanced. The primary drivers of arbovirus disease outbreaks are human-induced land use/cover (LULC) changes (Patz et al. 2004). Environmental modifications due to road, drainage, canal, and residential developments have created new artificial breeding habitats for mosquitoes (Saleeza et al. 2011). Urbanization and human activity increase the number of artificial water collection reservoirs which are common aquatic habitats for *Culex quinquefasciatus*. These species are found in artificial larval habitats such as catch basins, open containers that hold water and organic material long enough for the

development of larvae to the adult stage (Jacob et al. 2006, Gardner et al. 2013). Small, flooded depressions in the soil, tire tracks, and shallow ditches are also suitable habitats for *Culex quinquefasciatus* (Jacob et al. 2006).

Although many studies have been carried out to link environmental conditions to WNV risk, most of them assessed the impacts of changes in landscape characteristics on WNV transmission at a general level and solely from remotely sensed data (Brown et al. 2008, LaBeaud et al. 2008, Messina et al. 2011). Number of factors that have been suggested to influence WNV risk poorly understood. A key factor in determining the local abundance of insect populations is the choice of habitat for pre-adult development (Chaves et al. 2009). The selection of mosquito breeding sites is the result of the recognition of key physical and chemical factors. Sites with higher nutrient concentrations provide greater microbial food resources and mitigate resource competition (Dowling et al. 2013). The major food resources for *Culex* species are microorganisms and detritus, and the water column is their feeding microhabitat. Bacteria are the most abundant microorganisms present in larval food, and mosquito growth can occur with bacteria as the only food source (Merritt et al. 1992). Bacteria use nitrogen as a source of energy through NO_3 dissimilation and as an essential element for growth through fixation of gaseous nitrogen. NH_4 is also used by nitrifying bacteria as a primary energy source in aquatic systems. NH_4 oxidation produces nitrite that is then quickly oxidized to NO_3 by bacteria (Rheinheimer 1980, Bock et al. 1986, Paul and Meyer 2001). The nitrifying and denitrifying bacterial communities represent readily available potential food resources to developing mosquito larvae. The dissolved phosphorus can also be utilized for growth

by algae and bacteria (Cembella et al. 1984). These nutrients are introduced from different point and non-point sources. Two-thirds of phosphorus loads to lakes and rivers originate from non-point sources, such as runoff from pastures and croplands, atmospheric deposition, and stream bank erosion. Other non-point sources include urban runoff, non-agricultural rural runoff and seepage from individual sewage treatment systems. Nitrogen is also introduced through sewage and fertilizers. Heavy rains can produce runoff carrying these materials into nearby streams and lakes. NO_3 can also be formed in water bodies through the oxidation of other forms of nitrogen. Ammonia and organic nitrogen can enter water through sewage effluent and runoff from land where manure has been applied or stored. The extent of the increase in nutrient levels depends on wastewater treatment technology, the degree of illicit discharge and leaky sewer lines, as well as fertilizer use (Paul and Meyer 2001). Nutrients coming from these sources may be replenished in temporary pools by runoff or during flooding which represent potential mosquito breeding habitats.

The heterogeneity of urban areas in their extent, degree, and distribution of environmental modifications, affects the dynamic transmission systems through which the pathogen propagates (Magori et al. 2011). Watersheds with high impervious cover have higher nutrient concentrations and loads and lower dissolved organic carbon (DOC), indicative of the influence of urbanization on biogeochemical inputs to streams (Nagy et al. 2012, Tu 2001, Crim 2007). Combined sewer overflows (CSOs) are considered point source pollution and major urban breeding sites for *Culex quinquefasciatus* as they provide nutrient rich water which is unfavorable for mosquito predators

due to diminished oxygen concentrations (Calhoun et al. 2007). Habitats created by CSOs are similar to other urban mosquito habitats such as catch basins (Lund et al. 2014), where ammonia concentrations were found to be positively correlated to larval mosquito abundance (Gardner et al. 2013). Some studies have assessed the impacts of CSOs on WNV vector mosquito production (Bentley and Day 1989, Calhoun et al. 2007, Chaves et al. 2009). It was found that polluted water pulses coming from CSOs enhance oviposition and mosquito densities. Also, mosquitoes from sewage overflow water emerge faster, are bigger, and have an increased ratio of females to males (Chaves et al. 2010). Ammonia and PO_4 concentrations and mosquito populations are higher in CSOs than in non-CSO creeks. However, even after CSO improvements, elevated levels of WNV cases are observed in urban areas, which reveals that CSOs and catch basins are not the only sources of *Culex* mosquito production. For instance, although CSOs in the Atlanta area were remediated in 2008 and water quality indices improved (Lund et al. 2014), an outbreak in 2012 with a high number of positive mosquitoes occurred. This potentially indicates that mosquitoes carrying WNV do not necessarily require very high nutrient levels to thrive, and studies that only focused on mosquito development in sewage water are limited and confounded. Limited information exists on the effects of nutrient concentrations typically found in field conditions, and dose-response curves in general, for *Culex* species, despite their importance as major vectors of WNV.

The nutrient influences on mosquito larvae development at low to moderate levels have not been clarified, and the quantitative relationships between specific nutrient concentrations in water

and larvae have not been studied. In most previous studies artificial pools were treated with dog food, yeast or liver powder to feed mosquito larvae during the experiment and to make the breeding habitat nutrient rich (Telang et al. 2006, Chaves et al. 2009, Cardoso et al. 2010, Nguyen et al. 2012, Ariani et al. 2015). This creates a critical problem, specifically in lower nutrient concentrations which are much more widespread in the landscape than those of CSOs. This study helps to clarify that CSOs and catch basins are not the only habitats for *Culex* mosquitoes that could transmit WNV in urban areas. Understanding breeding habitats with low nutrient concentrations, and their impacts on *Culex* mosquito development, may help reduce WNV prevalence by identifying and eliminating such hitherto unrecognized sources of mosquito production. This may be more significant when it comes to human health in residential areas with standing water in flower pots, buckets, tires and barrels in back yards which are good mosquito breeding sites for various species with different nutrient levels (CDC 2012). For improved risk prediction in urbanized areas, relationships between water quality and mosquito reproductive potential need to be better understood.

To explore the breeding of *Culex* mosquitoes under different water quality conditions, especially in habitat with medium to low levels of components of water chemistry, a mesocosm experiment was designed. Through this experiment, dose–response relationships between larval development and NO_3, NH_4, and PO_4 concentrations in stream water were developed. It was hypothesized that addition of PO_4 to the breeding water favors mosquito development. Results

from clarification of nutrients-mosquito relationships can be critical in developing tools for predicting WNV risk across developed landscapes.

Materials and methods

The water quality data from several highly urbanized streams within the Atlanta metropolitan area, Georgia U.S.A., collected and analyzed by USGS and USEPA, indicate concentrations range of 0.05-18 mg/L for NO_3, 0-14 mg/L for NH_4, and 0.01-9 mg/L for PO_4 (http://ga.water.usgs.gov/) (http://www.epa.gov/storet/dbtop.html). The maximum nutrient concentrations in a CSO site in Atlanta area were reported as 1.50 mg/L for NO_3, 30.0 mg/L for ammonia and 8.0 mg/L for PO_4 in Lund et al. (2014). Therefore, in this experiment, water concentrations of NO_3, NH_4 and PO_4 have been selected to reflect the ranges commonly reported in urban streams in the Southeast U.S.

Ninety 1.25 liter plastic containers were filled with 1 liter of stream water from a reference stream (i.e. a stream associated with a watershed with minimal development near Auburn, AL), ensuring that naturally-occurring communities of microflora were present in the containers. Eighteen treatments (Table 2.1), each replicated five times, were assigned to containers in a completely randomized design. Among these eighteen treatments, five of them contained low to high NO_3 concentrations (Trt3 to Trt7), five had low to high NH_4 concentrations (Trt8 to Trt12), four treatments covered low to high PO_4 levels (Trt13 to Trt16), 1 treatment had NO_3 and PO_4 constituents combined (Trt17) and 1 treatment had PO_4 and NH_4 constituents combined (Trt18). The stock solutions were made in the lab using sodium nitrate for NO_3, ammonium chloride for

NH_4 and monopotassium phosphate for PO_4 and containers were spiked one week prior to the addition of larvae. All containers, except Trt1, were seeded with 0.1 g of ground senesced foliage from a flowering dogwood (Cornus Florida), a species with low lignin content and high decomposition rate which served as a source of carbon. After determining the NO_3, NH_4, and PO_4 concentrations in the reference stream water which were below detection limits, appropriate amounts of nutrients were added in order to achieve the target concentrations for treatments shown in Table 2.1. The treatment selection allowed for isolation of the influence of nitrogen source (NO_3, NH_4), PO_4, as well as level of N and P in a setting where major sources of variation are controlled. One hundred *Culex quinquefasciatus* larvae as 1st instars were obtained from the laboratory colonies and were added to each container. All containers were placed in an indoor facility where a constant temperature of 25 ^oC (± 2 ^oC) was maintained (Rueda et al. 1990). Containers were checked daily for pupae, which were isolated after pupation. Larvae were individually counted in each container after day 30 of the experiment, when it was possible to count them manually. Each pupa that successfully emerged into an adult was sexed and the number of days to pupation was recorded. The Thermo Scientific Dionex ICS-1500 ion chromatography system (Waltham, Massachusetts) was used to analyze water for each container at the end of experiment for anions (chloride, nitrite, nitrate, phosphate, and sulfate) and cations (sodium, ammonium, potassium, magnesium, calcium). About every two weeks, approximately 300 ml of water was added to containers to maintain a water level sufficient for larval and pupal development. The nutrient levels were not kept constant during the experiment to simulate a more natural system as nutrient

concentrations vary tremendously in the field. Figure 2.1 shows the initial and final nutrients concentrations and also the water volume remaining in each container after larval development. NH_4 content decreased as adult mosquitoes emerged. PO_4 was also utilized by algal cells for growth. In some containers especially those with very high PO_4 levels or very high NO_3 levels, the nutrient concentrations increased due to low water volume left at the end of experiment.

Statistical analysis

Statistical analyses were performed to determine if the treatments significantly affected the number of larvae, pupae and adult mosquitoes and to ascertain whether concentrations of different nutrients affect each response variable. Because of the discrete nature of the responses, count-data models, such as Poisson and negative binomial regression models (MuCullagh and Nelder 1989) were used. Due to excess zeroes in data, maximum likelihood fits of these models did not provide satisfactory fits to the data. Thus the models were modified to accommodate the excess zeros. There are two common statistical approaches for modifying count-data models to accommodate excess zeroes: inflating (Lambert 1992) and hurdling (Mullahy 1986). Inflating is appropriate when excess zeroes are due to inability to observe in addition to the actual absence or absence due to a source that is unaccounted for in the study. Zero-inflated Poisson (ZIP) or zero-inflated negative Binomial (ZINB) are two such models. Hurdling is used when all zero data are from one "structural" source (Hu et al. 2011). The source of zeroes in this study is mortality of larvae due to lack of food (very low nutrient and carbon source). There were no flaws in the containers and

hence we are unable to justify two separate sources for the zeroes as required by ZIP and ZINB models. Thus, all zero data were assumed to come from one "structural" source and hurdle models were applied. The standard errors of the regression coefficients were estimated using robust sandwich estimators (Huber 1967, Zeileis 2004, 2006) that can deal with slight deviations from normality, heteroscedasticity, and some observations that exhibit large residuals or influence. These standard errors were used to construct Wald test statistics to test the significance of regression coefficients (Zeileis et al. 2008). Also, pairwise contrasts of the treatment groups while adjusting for multiple comparisons using the Tukey's method, was performed based on the fitted Poisson hurdle model for the count response variables which were number of pupae and number of adult males or females. The contrasts were estimated for both count and zero hurdle models. The effect of nutrient levels on the time required for a mosquito to develop from a larva to a pupa was analyzed using a linear model. The concentrations of NO_3, NH_4 and PO_4 were covariates in the model. An analysis of variance (ANOVA) was also used to compare the time to pupation among the treatment groups. Following statistical significance at the $p < 0.05$ level, a Tukey's Honest Significant Difference (HSD) test was used to separate treatment means. To see the effect of each specific nutrient alone on the response variable, all analyzes were also done within groups of treatments, including Trt2 as reference. All analyses were performed in R statistical software (version 3.0.2.) (R Core Team 2013).

In addition, the dose-response relationship between each nutrient and response variable (number of larvae, pupae and adult mosquitoes and time to pupation) was developed by creating a

simulated dataset. Each statistically significant nutrient concentration was varied from its minimum to maximum value and the nonsignificant nutrient concentrations were fixed at their mean value of all the experiments. The response variable was predicted based on the simulated dataset.

Time series of number of larvae

To describe the variation in the number of surviving larvae as a function of time and nutrient concentration, larvae were counted starting on the day 30^{th} of the experiment and continued until the experiment ended. The time series of larvae number was analyzed using a Poisson generalized linear mixed model (GLMM), (Breslow and Clayton 1993). The package *nlme* (Pinheiro et al. 2012) from the R software was applied for the number of larvae time series. The concentrations of NH_4, NO_3, PO_4, and time were considered as fixed effects; and containers as a random effect. The interactions of nutrients with each other and with time were also considered in the model.

Results

Impact of nutrient concentrations on larval mortality

Summary statistics of number of larvae were plotted for each treatment as shown in Figure 2.2. A linear mixed-effect model was applied to the time series of the number of larvae. NH_4 and the interaction of time and NH_4 were removed from the regression model as they were statistically non-significant. In all containers, larvae declined on average by 0.11 larvae per day (±0.004, ±95%

C.I.) ($p<0.0001$) (Table 2.2). The decline is due to mortality. Those larvae that pupated were counted as survivors thereafter. This decline in surviving larvae can be explained by the reduction in available food over time for larvae. In addition, PO_4 and NO_3 showed significant positive relationships with the number of surviving larvae over this period. The number of surviving larvae increased by 0.43 (±0.14, ±95% C.I.), ($p <0.0001$) following each 1 mg/L increase of PO_4. Also, for each 1 mg/L increase of NO_3, number of larvae increased by 0.09 (±0.06, ±95% C.I.), ($p=0.003$). Therefore, in containers with higher PO_4 or NO_3 concentration, the larval survival rate is larger due to an increase in food sources available for larvae. The same analysis was performed also within each group of treatments, including Trt2 as reference to see the effect of each nutrient on larval mortality separately. Results were in agreement with the findings from Table 2.2.

We also observed statistically significant interactions between different nutrients and time but the impact size on the number of larvae is low (between 0.001 and 0.005, estimate value column in Table 2.2). To clarify the interactions, predicted time series of minimum, average and maximum number of larvae were graphed and shown in Figure 2.3 a, b and c. In addition, the average number of larvae was predicted at days 30, 40, 50 and 60 of experiments and was graphed (Figure 2.3 d). The negative relationship between time and number of larvae is shown in this figure. As time proceeds from day 30 to day 60, for fixed values of NO_3 and PO_4, the number of larvae decreases. Also, for a fixed time, by increasing the PO_4 or NO_3 level, the number of larvae increases. There was no significant interaction between PO_4 and NO_3 (Figure 2.3 c). In conclusion, breeding sites with higher PO_4 or NO_3 concentrations have higher survival rate of larvae.

Impact of nutrient concentrations on number of larvae pupating

The number of pupae obtained at the end of the experiment for each treatment is shown in Figure 2.4. Containers without leaves (treatment 1) has low productivity compared to treatment 2. Average number of pupae in treatments 1 and 2 were 0.2 and 1.4 respectively (Figure 2.4). On average, 1.22 larvae out of 100 per container pupated successfully (0.31-4.14, 95% C.L.). Since about 33% of the containers failed to produce pupae, a hurdle model was fitted to the data. According to the zero hurdle model, a significant positive relationship was found between the concentrations of both NH_4 and PO_4 and the probability of any larvae pupating. The odds of any larvae pupating increased by 29% (1.29, 1.02-1.63 95% C.L.), (p=0.04) and 25% (1.25, 1.00-1.56 95% C.L.), (p=0.04) for each mg/L increase in NH_4 and PO_4 level in containers, respectively. No significant correlation was found between NO_3 and number of pupae (Table 2.3). To develop the dose-response curve of number of pupae versus PO_4 and NH_4 concentrations, a simulated dataset was created that has PO_4 concentrations varying from 0 to 12 mg/l, NH_4 concentrations varying from 0 to 8 mg/l and NO_3 fixed at its mean value of all the experiments. The fitted hurdle model to the actual data was used to predict the number of pupae based on the simulated dataset. Figure 2.5 describes the effects of PO_4 and NH_4 on the number of larvae successfully pupating. The same analysis was performed within each group of treatments including Trt2 as the reference treatment to show impact of each nutrient on the response variable separately. No significant correlation was found between the nutrient and number of larvae pupating within each group. In addition, pairwise

contrasts on the fitted Poisson hurdle model using the Tukey's test did not show any significant differences for the number of pupae among treatment groups (results not shown).

Impact of nutrient concentrations on time to pupation

In addition to monitoring pupae, larvae, and adult densities during the experiment, the average time required for mosquitoes to develop into a pupa was also recorded (Figure 2.6). On average, larvae pupated in 40.95 days per container (30.22-54.41, 95% C.I.). A linear model considering NO_3, PO_4 and NH_4 concentrations as predictors was fitted to the data. NO_3 has a significant negative relationship with time to pupation (Table 2.4): for each 1 mg/L increase in NO_3 concentration, the pupation time decreased by 0.55 (± 0.35, ±95% C.I.) day, ($p = 0.003$). Therefore, increased NO_3 levels increased the rate of larval development and pupation.

Time to pupation was separated for males and females and the linear model was run for each sex separately. For females, a 1 mg/L increase in NO_3 also shortened the time to pupation by 0.79 (± 0.44, ±95% C.I) day, ($p=0.002$) (Table 2.4). As the impact of NO_3 on time to pupation for females was statistically significant, a simulated dataset was created with NO_3 concentrations varying from 0 to 28 mg/l, and PO_4 and NH_4 concentrations fixed at their mean value of all the experiments. The dose-response curve of time to pupation of females per container versus NO_3 concentration was developed based on the fitted linear model, as shown in Figure 2.7. For males, increased NH_4 concentrations decreased pupation time, while increased PO_4 concentrations increased pupation time. Increasing the concentration of NH_4 by 1 mg/L, resulted in decreased

time to pupation for male mosquitoes by 1.32 (± 1.08, ±95% C.I.) day, (p=0.02). Also, by each 1 mg/L increase in PO_4, it takes 1.41 (± 1.23, ±95% C.I.) day longer for larvae to become pupae and emerge as males (p=0.03), (Table 2.4). The dose-response curve of time to pupation per container for males versus NH_4 and PO_4 concentrations was developed using the simulated dataset. Figure 2.8 describes the isolated effects of PO_4 and NH_4 on male pupation time. PO_4 slows the development of male mosquitoes while NH_4 enhances the rate of development of male mosquitoes. The same analysis was performed within each treatment group to assess the impacts of each nutrient alone on time to pupation. Similar result was obtained for NH4 group. No significant correlation was found between NO_3 or PO_4 and pupation time.

To compare mean pupation time among groups defined in Table 2.1, an ANOVA contrast matrix was used. Time to pupation for the combined group (Trt17 & Trt18) was the shortest (24.6 days) in comparison to other groups and it was significantly shorter compared to the reference (by 19.26 days, p=0.001), NH_4 (by 20.05 days, p<0.0001) and PO_4 (by 24.8 days, p<0.0001) groups. The NO_3 group had the shortest pupation time (34.5 days) after the combined group and was significantly shorter relative to that of PO_4 (by 14.84 days, p=0.0002) and NH_4 (by 10.09 days, p=0.008) groups (Table 2.5). The same analysis was repeated for female and male pupation time separately. Similarly, fewer days were required for both females and males to pupate when breeding pools contained both NO_3 or NH_4 and PO_4 compared to other treatment groups (results not shown). Generally, mosquitoes took longer to pupate in the PO_4 group, while the combination of PO_4 and NO_3 or NH_4 decreased the average time required for mosquitoes to develop into pupae.

The ANOVA contrast analysis showed significant differences in average pupation time between treatments with 1 mg/L NO_3 level (Trt3) and treatments combined with no NO_3 and also between treatments with 10 mg/L NO_3 level (Trt17) and treatments combined with no NO_3 (Table 2.6). Trt17 is a combined treatment with the NO_3 level of 10 mg/L and PO_4 level of 1 mg/L. Time for larvae to reach the pupal stage in the combined treatment was 24.24 days shorter than the time with no NO_3 treatment ($p=0.0004$). Also, by increasing the PO_4 level from 1 mg/L (Trt13, Trt17 and Trt18) to 2 mg/L (Trt14), the time to pupation increased by about 16 days.

The same analysis was done for male and female pupation time. No significant differences were identified among groups for females. For males, average pupation time for treatments with the PO_4 level of 2 mg/L (Trt13) and 12 mg/L (Trt16) was significantly different from the treatments without PO_4 ($p=0.01$ and $p=0.03$, respectively) (Table 2.6). Also average pupation time of males in these two levels was significantly different from the PO_4 level of 1 mg/L ($p=0.001$ and $p=0.01$, respectively). Increased PO_4 level caused the time male mosquitoes need to develop from larvae to pupae to increase. In addition, the pupation time of males in treatment with NO_3 levels of 10 mg/L (Trt17) was significantly shorter than treatments with no NO_3 or NO_3 levels of 3.5 mg/L ($p=0.004$ and $p=0.01$, respectively). As a result, addition of PO_4 in breeding waters increases the time to pupation, but addition of a combination of NO_3 and PO_4 to the container makes mosquitoes develop faster.

Impact of nutrient concentrations on number of adult mosquitoes

At the end of the experiment, the number of adult mosquitoes, their sex, and the container of origin were recorded. As shown in Figure 2.9, 43% of treatment containers (Trt3 to Trt19, 5 replicates) and 40% of control containers (Trt1 & Trt2, 5 replicates) successfully produced adults. 29% of treatment containers and 10% of control containers produced adult males, and 21% of treatment containers and 30% of control containers produced adult females. The mean number of adults produced per container, along all 90 containers, was 0.6 (0.13-2.77, 95% C.L.); the mean number of adult males produced per container was 0.34 (0.08-2.04, 95% C.L,); and the mean number of females produced was 0.26 (0.06-1.75, 95% C.L.). As 78% of the containers did not produce any females, and 73% of the containers did not produce any males, the data was analyzed using a hurdle model. NO_3 was negatively correlated to the number of adult females (Table 2.7). The count-data hurdle model found that for each 1 mg/L decrease in NO_3 concentration, the number of adult females increased by 72%, (1-0.28), (0.15-0.52, 95% C.L.) (p=0.0001). Therefore, higher NO_3 levels reduced the adult female populations (Table 2.7). At high NO_3 levels, fewer females were produced but those that did emerge developed faster. Conversely, at low NO_3 levels, more females emerged but took longer to develop. A dose-response curve of the predicted number of females versus NO_3 concentration was developed based on a simulated dataset that has NO_3 concentrations varying from 0 to 28 mg/l and PO_4 and NH_4 fixed at their mean value of all the experiments. Using the developed hurdle model including both count model and zero hurdle model, average count data of adult females per container was predicted. Figure 2.10 describes the

isolated effect of NO_3 on the number of females. The same analysis was done for adult male mosquitoes and no statistically significant relationship was found between nutrients and male mosquitoes (Table 2.8). Also, the hurdle model analysis was performed within each treatment group to assess the impact of each nutrient separately on the number of adult mosquitoes. However, due to excess zeroes in the dataset and a low number of data points within each group of treatments, the results are not reported here.

Pairwise contrasts of the treatment groups using the Tukey's test, was performed based on the fitted Poisson hurdle model for the number of adult males or females. The contrasts were estimated for both count and zero hurdle models. No significant contrasts were estimated for the zero hurdle model of adult males or females (results not shown). For the count model, the results indicated that containers treated with NO_3 alone and PO_4 in combination with either NO_3 (Trt17) or NH_4 (Trt18) produced a significantly lower number of adult females compared to NH_4, PO_4 and reference treatment groups (Table 2.9). The expected difference in log count of adult females between NO_3 group and NH_4 group was 10.29 (8.05-12.53, 95% C.L.) ($p<0.0001$), between NO_3 group and PO_4 was 10.14 (7.87-12.41, 95% C.L.) ($p<0.0001$), and between reference group and NO_3 group was -10.94 (-13.00- -8.88, 95% C.L.) ($p<0.0001$). Also, the expected log count for combined group decreased by 10.87, 10.22 and 10.08 compared to reference group, NH_4 group and PO_4 group respectively.

For the adult males, pairwise contrasts based on the count part of the hurdle model showed opposite results than adult females. Containers treated with NO_3 alone and PO_4 in combination

with either NO_3 (Trt17) or NH_4 (Trt18) produced a significantly greater number of males compared to the NH_4, PO_4, and reference treatment groups (Table 2.9). The expected increase in log count adult males for containers treated with NO_3 alone was 12.12, 12.72 and 10.86 compared to NH_4, PO_4 and reference groups respectively. For the combined treatments (Trt17 and Trt18), the log count adult males also increased by 10.29, 11.56 and 12.15 compared to the reference, NH_4 and PO_4 groups (Table 2.9). This indicates that mosquito breeding sites containing NO_3 or either a combination of NO_3 and PO_4 or a combination of NH_4 and PO_4 produce higher numbers of male mosquitoes. It can be concluded that NO_3 favors the adult male mosquitoes and suppresses the development of adult females.

Discussion

The mesocosm experiment results have demonstrated that higher PO_4 or NH_4 concentrations increase the number of surviving mosquito larvae and the number of larvae successfully pupating (Table 2.2). These results are in agreement with Carpenter (1982) and Sunish and Reuben (2001) who found that PO_4 concentration exerts a positive influence on late aquatic stages of mosquito larvae. This can be due to acceleration in leaf litter breakdown. Faster breakdown rates are associated with significantly higher phosphorus concentrations in agricultural streams (Paul et al. 2006). Therefore, microbial activity increases in association with faster breakdown rate, which affects organic matter availability as a food source for mosquito larvae. Organic carbon source plays an important role in mosquito growth as we found that productivity was very low in containers without

leaves compared to other containers (Walker et al. 1991). In addition, more adult females emerged in containers with lower NO_3 concentrations (Table 2.7). Therefore, the addition of NO_3 to the breeding water decreased the number of adult females that emerged. Pairwise contrasts of the number of adult females and males among treatment groups showed that containers with NO_3 constituent or a combination of either NO_3 and PO_4, or NH_4 and PO_4 constituents, have more adult males and fewer adult females than treatments with elevated PO_4 or NH_4 alone and reference treatments (Table 2.9).

Previous studies found that addition of nutrients into water accelerates mosquito larval development as well as increases the survival of larvae, and the proportion of larvae that pupate (Reiskind et al. 2004). However, our study showed that the response depends on the type and amount of the added nutrients. As the experiment progressed, the food source available for the larvae was reduced and larval mortality increased and population size decreased (Table 2.2). Larval growth and development of mosquitoes to reproductive maturity are dependent on nutrient availability. Larval nutrition scarcity can increase development time, decrease pupation and emergence rates, and result in smaller adult female body size, as demonstrated for *Culex tarsalis* (Dodson et al. 2011). In this study, containers with elevated NO_3 levels reduced the pupation time for females and enhanced the development of larvae in general (Table 2.4). In contrast, addition of NO_3 to the containers appears to have a detrimental effect on adult females. For males, containers with elevated PO_4 concentration had longer pupation times and containers with elevated NH_4 had faster larval development (Table 2.4). PO_4 plays a significant role in keeping larvae alive

longer (Table 2.2) but inhibits pupation in absence of NO_3 or NH_4. Moreover, comparison of mean pupation time of larvae among treatment groups indicated that for containers with combinations of either PO_4 and NO_3 or PO_4 and NH_4, fewer days were required for both females and males to emerge than other groups.

The major findings of this study were: 1) increased NO_3 levels alone in the larval habitat favors the development of male mosquitoes and suppresses the development of female mosquitoes. However, those adult females that do emerge, develop faster in containers with the NO_3 constituent compared to the reference group. Female mosquitoes are larger than males and also their development time is longer than males (Bradshaw et al. 1997), therefore, they need more food than males. Also, as larvae feed on microorganisms in the water column, the algal growth promoted by nitrogen contained in leaves may support *Culex* production (Chaves et al. 2010). In addition, decreasing number of females by increasing NO_3 level is probably due to differences in the effect of this limitation between the genders (i.e. females might need more PO_4 than males for development and are therefore more limited in growth despite the increased levels of nitrogen). 2) Addition of PO_4 alone to the larval habitat increases the larval development time. PO_4 generally increases the proportion of females that emerge and they are larger at emergence (Decker, 2010). Therefore, the emergence time will be longer for females of larger size. However, in this experiment the time to pupation was significantly longer for males with increasing PO_4 levels. The increase in the developmental time occurs in the absence of nitrogen. Nitrogen is required for chitin development and severely limiting for larval growth and development. Therefore, the combination

of NO_3 and PO_4 or NH_4 and PO_4 nutrients in the container favors mosquito development and shortens pupation time.

This study demonstrated the importance of understanding how nutrients influence mosquito pre-adult development and the quantitative relationships between specific nutrient concentrations in water and developmental parameters. This experiment enabled us to develop dose–response relationships between larval development and NO_3, NH_4, and PO_4 concentrations in stream water (Figure 2.3, 2.5, 2.7, 2.8 and 2.10). These dose-response curves provide guidelines on the conditions required for *Culex quinquefasciatus* to survive and develop at low nutrient and carbon levels especially in non-CSO sites, and potentially maintain a population at a background level. The continued maintenance of *Culex* populations, even if at low levels, is important, because it allows mosquito populations to expand dramatically when high-nutrient habitats appear in the landscape. This reveals that WNV risk can remain even in the presence of larval habitats with low to moderate nutrient levels which are more common in the landscape than the levels characteristic of CSOs. Specifically around residential areas, the number of *Culex* mosquitoes and WNV prevalence might be maintained with standing water in containers such as flower pots, wheelbarrows, gutters, buckets, old tires, pool covers, pet water dishes, discarded tires, bird baths, (CDC, 2012). These findings should promote the development of targeted larviciding interventions, thus reducing the costs and efforts required for effective mosquito vector control. The results of this experiment may also help identify specific larval habitats for *Culex* mosquitoes by predicting which water quality conditions in urban landscapes are most likely to support

mosquito development, which could lead to improved control of WNV transmission. However, incidence of WNV varies spatially and temporally and is influenced by a wide range of environmental factors. The interrelationships of vectors, environmental condition of mosquito habitats, and meteorological factors need to be investigated more thoroughly. In addition, other risk factors including socioeconomic factors, land use / cover changes and urbanization, which affect water quality and quantity and therefore the transmission of WNV, should be considered for future studies.

References

Ariani, C.V., P. Juneja, S. Smith, M.C. Tinsley, and F.M. Jiggins. 2015. Vector competence of *Aedes aegypti* mosquitoes for filarial nematodes is affected by age and nutrient limitation. Exp Gerontol. 61: 47-53.

Bently, M.D. and J.F. Day. 1989. Chemical ecology and behavioral aspects of mosquito oviposition. Ann. Rev. Entomol. 34: 401-421.

Bock, E., H. Koops, and H. Harms. 1986. Cell biology of nitrifying bacteria. In J. I. Prosser (ed.), Nitrification. Vol. 20. IRL Oxford; Washington, DC.

Bradshaw, W.E., Ch.M. Holzapfel, Ch.A. Kleckner, and J.J. Hard. 1997. Heritability of development time and protandry in the pitcher-plant mosquito, Wyeomyia Smithii. Ecology. 78: 969-976.

Brown, H.E., J.E. Childs, M.A. Diuk-Wsser, and D. Fish. 2008. Ecological factors associated with West Nile virus transmission, Northeastern United State. Emerg. Infect. Dis. 14: 1539-1545.

Breslow, N. E. and D. G. Clayton. 1993. Approximate Inference in Generalized Linear Mixed Models. JASA. 88: 9-25.

Calhoun, L.M., M. Avery, L. Jones, K. Gunarto, R. King, J. Roberts, and T.R. Burkot. 2007. Combined Sewage Overflows (CSO) Are Major Urban Breeding Sites for *Culex quinquefasciatus* in Atlanta, Georgia. Am. J. Trop. Med. Hyg. 77: 478–484.

Cardoso, A.F., R.L. Cres, A.S. Moura, F. de Almeida, and A.T. Bijovsky. 2010. *Culex quinquefasciatus* vitellogenesis: morphological and biochemical aspects. Mem Inst Oswaldo Cruz. 105: 254-262.

Carpenter, S.R. 1982. Stemflow chemistry: effects on population dynamics of detritivorous mosquitoes in tree-hole ecosystems. Oecologia (Berlin). 53:1-6.

Cembella, A.D., N.J. Antia, P.J. Harrison, and G-Y. Rhee. 1984. The Utilization of Inorganic and Organic Phosphorous Compounds as Nutrients by Eukaryotic Microalgae: A Multidisciplinary Perspective: Part 2. Crit Rev Microbiol. 11: 13-81.

Center for Disease Control and Prevention. 2012. West Nile Virus (WNV) fact sheet. National center for emerging and zoonotic infectious diseases, division of vector-borne diseases.

Center for Disease Control and Prevention. 2011. Surveillance for human West Nile Virus disease-United States, 1999-2008. Surveillance summaries, Morbidity and Mortality Weekly Report (MMWR). 59: SS-2.

Chaves, L.F., C. Keogh, G.M. Vazquez-Prokopec, and U.D. Kitron. 2009. Combined Sewage Overflow Enhances Oviposition of *Culex quinquefasciatus* (Diptera: Culicidae) in Urban Areas. J. Med. Entomol. 46: 220-226.

Chaves, L.F., C.L. Keogh, A.M. Nguyen, G.M. Decker, G.M. Vazquez-Prokopec, and U.D. Kitron. 2010. Combined sewage overflow accelerates immature development and increases body size in the urban mosquito *Culex quinquefasciatus*. J Appl. Entomol. 135: 611–620.

Crim, J.F. 2007. Water quality changes across an urban-rural land use gradient in streams of the west Georgia piedmont. M.Sc. thesis, Auburn University, School of forestry and Wildlife Sciences.

Decker, G.M. 2010. The influence of immature density and nutrient addition on adult *Culex quinquefasciatus* weight, emergence, and sex ratio in Atlanta, GA. Thesis submitted to Emory College of Art and Sciences of Emory University, Department of Environmental Studies.

Dodson, B.L., L.D. Kramer, and J.L. Rasgon. 2011. Larval Nutritional Stress Does Not Affect Vector Competence for West Nile Virus (WNV) in *Culex tarsalis*. Vector Borne Zoonotic Dis. 11: 1493-1497.

Dowling, Z., Sh.L. Ladeau, P. Armbruster, D. Biehler, and P.T. Leisnham. 2013. Socioeconomic Status Affects Mosquito (Diptera: Culicidae) Larval Habitat Type Availability and Infestation Level. J Med Entomol. 50:764-772

Gardner, A.M., T.K. Anderson, G.L. Hamer, D.E. Johnson, K.E. Varela, E.D. Walker, and M.O. Ruiz. 2013. Terrestrial vegetation and aquatic chemistry influence larval mosquito abundance in catch basins, Chicago, USA. Parasit Vectors. 6:1-11.

Hu, M.Ch., M. Pavlicova, and E.V. Nunes. 2011. Zero-inflated and Hurdle Models of Count Data with Extra Zeros: Examples from an HIV-Risk Reduction Intervention Trial. Am J Drug Alcohol Abuse. 37: 367–375.

Huber, P.J. 1967. The behavior of maximum likelihood estimates under nonstandard conditions. Fifth Berkeley Symposium on Mathematical Statistics and Probability. 1: 221-233.

Jacob, B. G., J. Shililu, E.J. Muturi, J.M. Mwangangi, S.M. Muriu, J. Funes, J. Githure, J.L. Regens, and R.J. Novak. 2006. Spatially targeting *Culex quinquefasciatus* aquatic habitats on modified land cover for implementing an Integrated Vector Management (IVM) program in three villages within the Mwea Rice Scheme, Kenya. Int J Health Geogr. 5: 1-9.

Jones, K.E., N.G. Pate, M.A. Levy, A. Storeygard, D. Balk, J.L. Gittleman, and P. Daszak. 2008. Global trends in emerging infectious diseases. Nature. 451: 990-994.

LaBeaud, A.D., A. Gorman, J. Koonce, Ch. Kippes, J. McLeod, J. Lynch, T. Gallagher, Ch. H. King, and A.M. Mandalakas. 2008. Rapid GIS-based profiling of West Nile virus transmission: defining environmental factors associated with an urban-suburban outbreak in Northeast Ohio, USA. Geospat. Health. 2: 215-225.

Lambert, D. 1992. Zero-inflated poisson regression, with an application to defects in manufacturing. Technometrics. 34: 1-14.

Lund, A., J. McMillan, R. Kelly, Sh. Jabbarzadeh, D.G. Mead, Th.R. Burkot, U.D. Kitron, and G.M. Vazquez-Prokopec. 2014. Long term impacts of combined sewer overflow remediation on water quality and population dynamics of *Culex quinquefasciatus*, the main urban West Nile virus vector in Atlanta, GA. Environ. Res. 129: 20-26.

Magori, K., W.I. Bajwa, S. Bowden, and J.M. Drake. 2011. Decelerating Spread of West Nile Virus by Percolation in a Heterogeneous Urban Landscape. PLOS Comput. Biol. 7: 1-13.

McCullagh, P. and J.A. Nelder. 1989. *Generalized Linear Models*. Second ed. London: Chapman and Hall.

Mullahy, J. 1986. Specification and testing of some modified count data models. J Econometrics. 33: 341‑365.

Merritt, R.W., R.H. Dadd, and E.D. Walker. 1992. Feeding behavior, natural food, and nutritional relationships of larval mosquitoes. Ann. Rev. Entomol. 37:349-376.

Messina, J.P., W. Brown, G. Amore, U.D. Kitron, and M.O. Ruiz. 2011. West Nile Virus in the greater Chicago area, a geographic Examination of Human Illness and risk from 2002 to 2006. URISA. 23, 5-18.

Morens, D. M., G.K. Folkers, and A.S. Fauci. 2004. The challenge of emerging and re-emerging infectious diseases. Nature. 4390: 242-249.

Nagy, C., B.G. Lockaby, L. Kalin, and C. Anderson. 2011. Effects of Urbanization on Stream Hydrology and Water Quality: The Florida gulf Coast. Hydrological Processes. 26: 2019-2030.

Nguyen, A. T. and A.J. Williams. 2012. Seasonal Weather, Nutrients, and Conspecific Presence Impacts on the Southern House Mosquito Oviposition Dynamics in Combined Sewage Overflows. J Med. Entomol. 49: 1328-1338.

Patz, J.A., P. Daszak, G.M. Tabor, A.A. Aguirre, M. Pearl, J. Epstein, N.D. Wolfe, A.M. Kilpatrick, J. Foufopoulos, M. Molyneux, and D.J. Bradley. 2004. Unhealthy landscape:

policy recommendations on land use change and infectious disease emergence. Environ. Health Perspect. 112: 1092-2098.

Paul, M.J. and J.L. Meyer. 2001. Streams in the urban landscape. Annu. Rev. Ecol. Syst. 32: 333-365.

Paul, M.J., J.L. Meyer, and C.A. Couch. 2006. Leaf breakdown in streams differing in catchment land use. Freshwater Biol. 51: 1684-1695.

Pinheiro, J., D. Bates, S. DebRoy, D. Sarkar and the R Development Core Team. 2012. nlme: Linear and Nonlinear Mixed Effects Models. R package version 3.1–103.

R Core Team. 2013. R: a language and environment for statistical computing. Reference Index. R Foundation for Statistical Computing, Vienna, Austria. Version 3.0.1.

Reiskind, M.H., E.T. Walton, and M.L. Wilson. 2004. Nutrient-dependent reduced growth and survival of larval *Culex restuans* (Dipetra: Culicidae): laboratory and field experiments in Michigan. J Med. Entomol. 41: 650-656.

Rheinheimer, G. 1980. *Aquatic microbiology*, 2nd ed. Wiley, New York.

Rueda, L.M., K.J. Patel, R.C. Axtell, and R.E. Stinner. 1990. Temperature-dependent development and survival rates of *Culex quinquefasciatus* and *Aedes aegypti* (Dipetra: Culicidae). J Med. Entomol. 27: 892-898.

Saleeza, S.N.R., Y. Norma-Rashid, and M.S. Azirun. 2011. Mosquitoes larval breeding habitat in urban and suburban areas, Peninsular Malaysia. WASET. 58: 569-573.

Sunish, I.P. and R. Reuben. 2001. Factors influencing the abundance of Japanese encephalitis vectors in ricefields in India-I. abiotic. Med. Vet. Entomol. 15: 381-392.

Telang, A., Y. Li, F.G. Noriega, and M.R. Brown. 2006. Effects of larval nutrition on the endocrinology of mosquito egg development. J Exp Biol. 209: 645-655.

Tu, J. 2011. Spatial and temporal relationships between water quality and land use in northern Georgia, USA. J Integr. Environ. Sci. 8: 151-170.

Walker, E.D., D.L. Lawson, R.W. Merritt, W.T. Morgan, and M.J. Klug. 1991. Nutrient dynamics, bacterial populations, and mosquito productivity in tree hole ecosystems and microcosms. Ecology. 72: 1529-1546.

Zeileis A. 2004. Econometric Computing with HC and HAC Covariance Matrix Estimators. J Stat. Softw. 11: 1-17.

Zeileis A. 2006. Object-oriented Computation of Sandwich Estimators. J Stat. Softw. 16: 1-16.

Zeileis, Z., Ch. Kleiber, and S. Jackman. 2008. Regression model for count data in R. J Stat. Softw. 27: 1-25.

Table 2.1. Mesocosm treatments with different nutrient levels.

Treatments	Description	Groups
Trt1	Reference stream conditions (RSC)*	Reference
Trt2	Addition of 0.1 g of leaf litter to RSC	
Trt3	trt 2 + NO_3=1 mg/l	Nitrate
Trt4	trt 2 + NO_3=3.5 mg/l	
Trt5	trt 2 + NO_3=9 mg/l	
Trt6	trt 2 + NO_3=14 mg/l	
Trt7	trt 2 + NO_3=28 mg/l	
Trt8	trt 2 + NH_4=0.29 mg/l	Ammonium
Trt9	trt 2 + NH_4=1 mg/l	
Trt10	trt 2 + NH_4=2.57 mg/l	
Trt11	trt 2 + NH_4=4 mg/l	
Trt12	trt 2 + NH_4=8 mg/l	
Trt13	trt 2 + PO_4=1 mg/l	Phosphate
Trt14	trt 2 + PO_4=2 mg/l	
Trt15	trt 2 + PO_4=6 mg/l	
Trt16	trt 2 + PO_4=12 mg/l	
Trt17	trt 2 + NO_3=10 mg/l & PO_4=1 mg/l	Combined
Trt18	trt 2 + NH_4=2.86 mg/l & PO_4=1 mg/l	

* NO_3, PO_4, NH_4 were all below the detection limits.

Table 2.2. Results of a mixed effects model for time series of number of larvae.

Parameter	Estimate	Std.Error	p-value
(Intercept)	7.64	0.26	<0.0001
Time	-0.11	0.002	<0.0001
NO_3	0.09	0.03	0.003
PO_4	0.43	0.07	<0.0001
Time:NO_3	-0.001	0.0003	<0.0001
Time:PO_4	-0.005	0.001	<0.0001

Table 2.3. Results of a Hurdle model analysis of number of pupae.

Parameter	Estimate*	95% CL		p-value
Count model coefficients				
Intercept	1.51*	1.03	2.23	0.03
NO_3	0.98	0.95	1.02	0.43
NH_4	0.96	0.84	1.08	0.48
PO_4	1.00	0.93	1.08	1.00
Zero hurdle model coefficients				
zero_Intercept	1.09	0.57	2.06	0.80
zero_NO_3	1.04	0.97	1.12	0.21
zero_NH_4	1.29	1.02	1.63	0.04
zero_PO_4	1.25	1.00	1.56	0.04

* Odds ratios were derived using the link function $e^{(coefficient)}$ and coefficient estimates of the Hurdle model to determine the likelihood of any larvae pupating .

Table 2.4. Results of a linear model fitted to the time to pupation.

	Time to pupation			Time to pupation (females)			Time to pupation (males)		
Parameter	Estimate	Std. Error	p-value	Estimate	Std. Error	p-value	Estimate	Std. Error	p-value
Intercept	43.19	2.46	<0.0001	46.90	2.55	<0.0001	32.02	3.69	<0.0001
PO_4	0.29	0.38	0.45	0.54	0.73	0.47	1.32	0.54	0.02
NH_4	-0.48	0.77	0.53	0.59	0.74	0.44	-1.41	0.61	0.03
NO_3	-0.55	0.18	0.003	-0.79	0.22	0.002	-0.52	0.27	0.07

Table 2.5. Comparison of the mean pupation time of different groups.

Parameter	Diff Between Means	Std. Error	p-value
Reference - NO_3	9.3	4.94	0.06
Reference - NH_4	-0.79	4.89	0.87
Reference - PO_4	-5.54	4.89	0.26
Reference - Combined	19.26	5.69	0.001
NO_3 - NH_4	-10.09	3.67	0.01
NO_3 - PO_4	-14.84	3.67	0.0002
NO_3 - Combined	9.96	4.68	0.04
NH_4 - PO_4	-4.75	3.61	0.19
NH_4 - Combined	20.05	4.63	<0.0001
PO_4 - Combined	24.8	4.63	<0.0001

Mean pupation time				
Ref	NH_4	Combined	NO_3	PO_4
43.8	44.6	24.6	34.5	49.4

Table 2.6. Tukey's HSD test results for pupation time.

Adults pupation time				
NO_3 (mg/L)	Diff between means	lower	upper	p-value
1-0	-20.91	-38.87	-2.95	0.01
10-0	-24.24	-39.98	-8.51	0.0004
PO_4 (mg/L)	Diff between means	lower	upper	p value
2-1	16.55	0.40	32.69	0.04
Adult males pupation time				
PO_4 (mg/L)	Diff between means	lower	upper	p-value
2-0	17.90	4.84	30.95	0.01
2-1	24.92	10.61	39.22	0.001
12-1	29.92	8.07	51.77	0.01
12-0	22.90	1.84	43.95	0.03
NO_3 (mg/L)	Diff between means	lower	upper	p-value
10-0	-19.76	-33.41	-6.10	0.004
10-3.5	-33.08	-57.70	-8.47	0.01

Table 2.7. Results of a Hurdle model analysis of number of adult females.

Parameter	Estimate	95% CI		p-value
Count model coefficients				
Intercept	0.70	0.26	1.86	0.46
NO_3	0.28	0.15	0.52	0.0001
NH_4	0.53	0.25	1.12	0.09
PO_4	0.77	0.55	1.08	0.13
Zero hurdle model coefficients				
zero_Intercept	0.30	0.14	0.66	0.00
zero_NO_3	0.96	0.84	1.08	0.48
zero_NH_4	1.00	0.77	1.29	0.97
zero_PO_4	1.06	0.91	1.25	0.44

Table 2.8. Results of a Hurdle model analysis of number of adult males.

Parameters	Estimate	95% CI		p-value
Count model coefficients				
Intercept	1.00	0.25	4.02	1.00
NO_3	1.00	0.92	1.08	0.91
NH_4	0.77	0.50	1.20	0.25
PO_4	0.49	0.19	1.27	0.14
Zero hurdle model coefficients				
zero_Intercept	0.28	0.14	0.56	0.0005
zero_NO_3	1.03	0.97	1.10	0.36
zero_NH_4	1.07	0.84	1.37	0.56
zero_PO_4	1.06	0.91	1.23	0.45

Table 2.9. Pairwise contrasts of the treatment groups using the Tukey's test based on the fitted Poisson hurdle model for the number of adult males or females.

	Adult Females					Adult Males			
Parameter	Estimate*	95% CL		p-value		Estimate	95% CL		p-value
NO_3-Reference	-10.94	-13.00	-8.88	<0.0001		10.86	8.63	13.08	<0.0001
NH_4-Reference	-0.65	-2.94	1.65	0.98		-1.26	-3.57	1.05	0.80
PO_4-Reference	-0.80	-3.12	1.53	0.96		-1.86	-4.02	0.30	0.41
Combined-Reference	-10.87	-12.93	-8.81	<0.0001		10.29	8.03	12.56	<0.0001
NH_4-NO_3	10.29	8.05	12.53	<0.0001		-12.12	-13.64	-10.60	<0.0001
PO_4-NO_3	10.14	7.87	12.41	<0.0001		-12.72	-13.99	-11.44	<0.0001
Combined-NO_3	0.06	-1.94	2.06	1.00		-0.56	-2.01	0.88	0.93
PO_4-NH_4	-0.15	-2.63	2.34	1.00		-0.60	-2.01	0.82	0.91
Combined-NH_4	-10.22	-12.47	-7.98	<0.0001		11.56	9.99	13.12	<0.0001
Combined-PO_4	-10.08	-12.35	-7.81	<0.0001		12.15	10.81	13.49	<0.0001

*The coefficient estimates of the hurdle model was not converted in this table to Odds ratios due to large number which will be obtained using the link function $e^{(Estimate)}$.

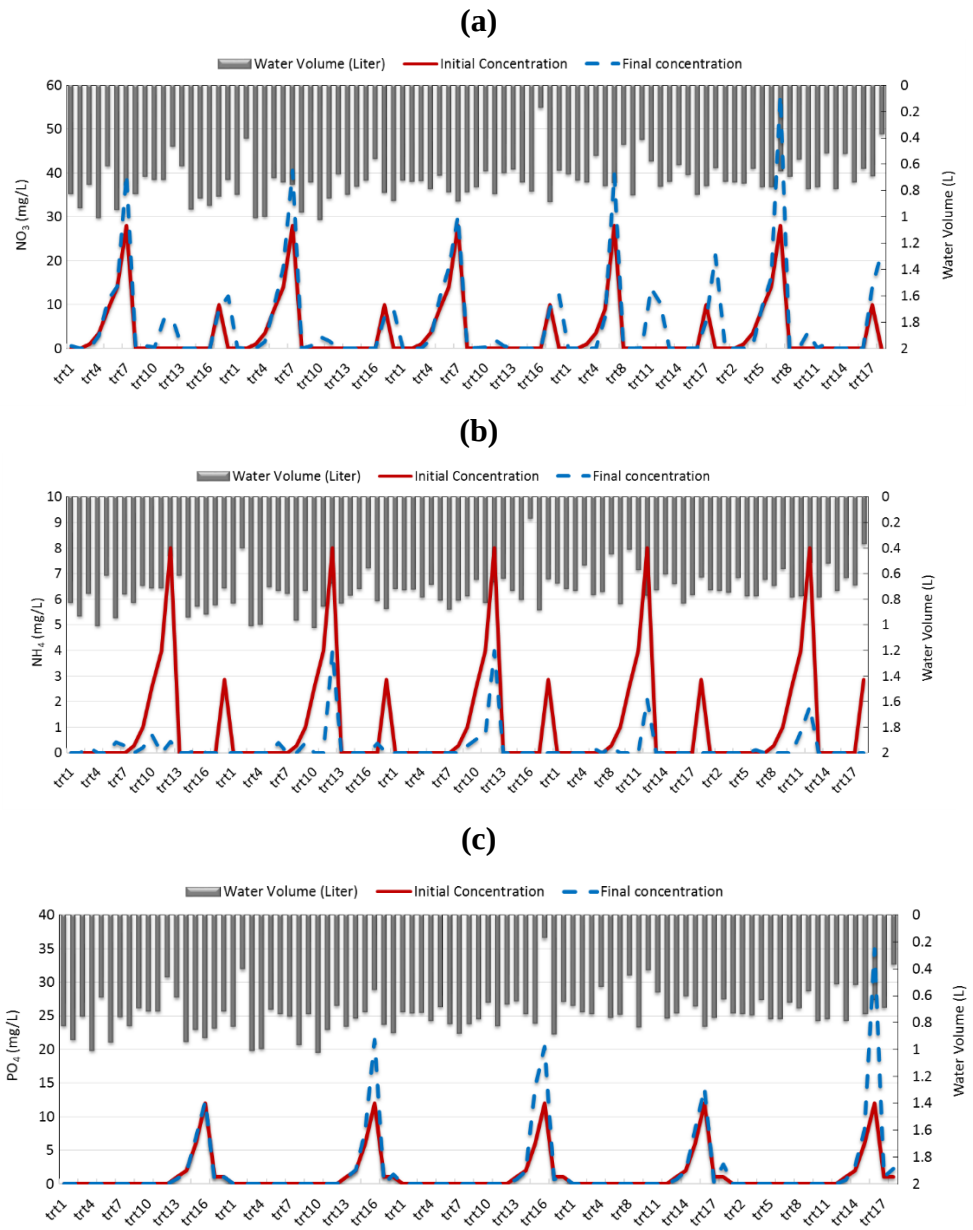

Figure 2.1. Nutrient levels at the beginning and end of the experiment and the final water volume for each container. (a) NO_3 concentrations, (b) NH_4 concentrations, (c) PO_4 concentrations. The treatments along the x-axis are organized as replicates.

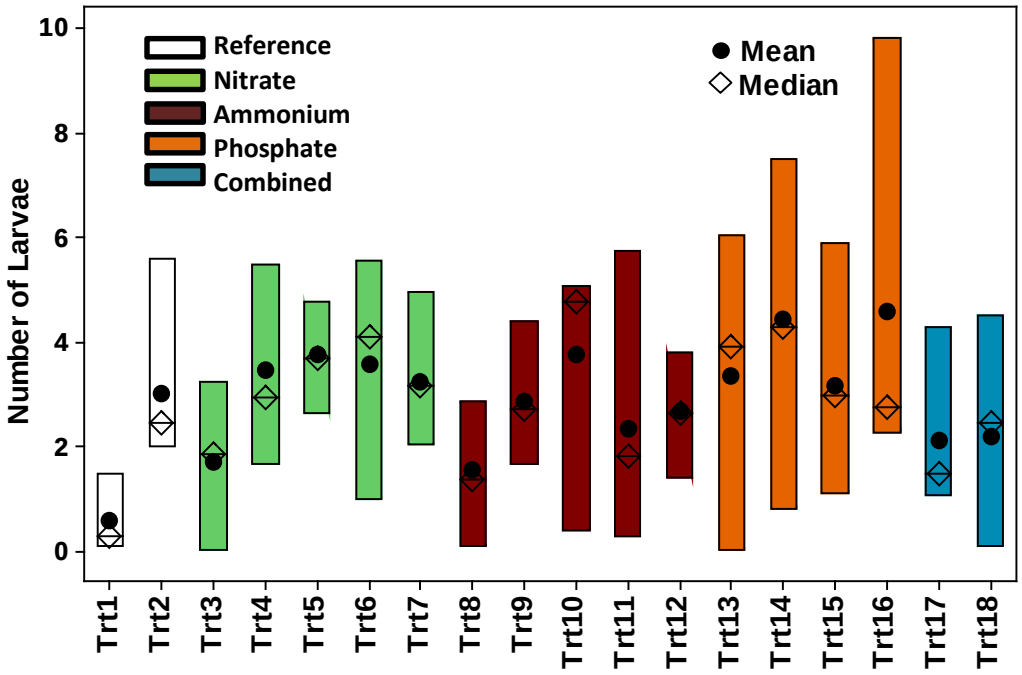

Figure 2.2. Mean, median and range of the number of larvae that either survived or pupated over the 40 day period for different treatments.

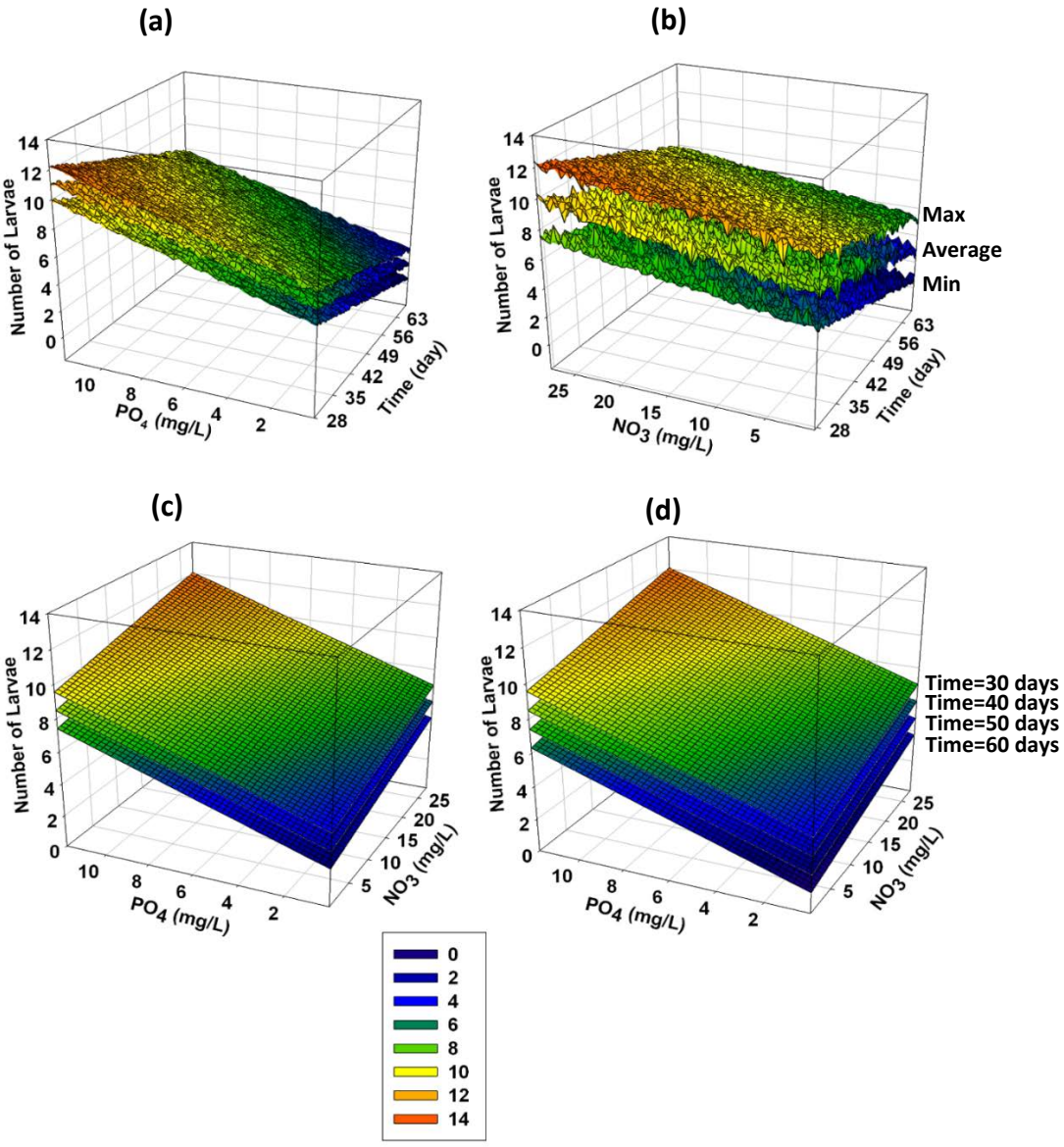

Figure 2.3. Predicted number of larvae by fitted mixed effects model versus time and nutrients. Graphs a, b and c show predicted time series of minimum, average and maximum number of larvae. Graph d shows average number of larvae predicted at days 30, 40, 50 and 60 of experiments.

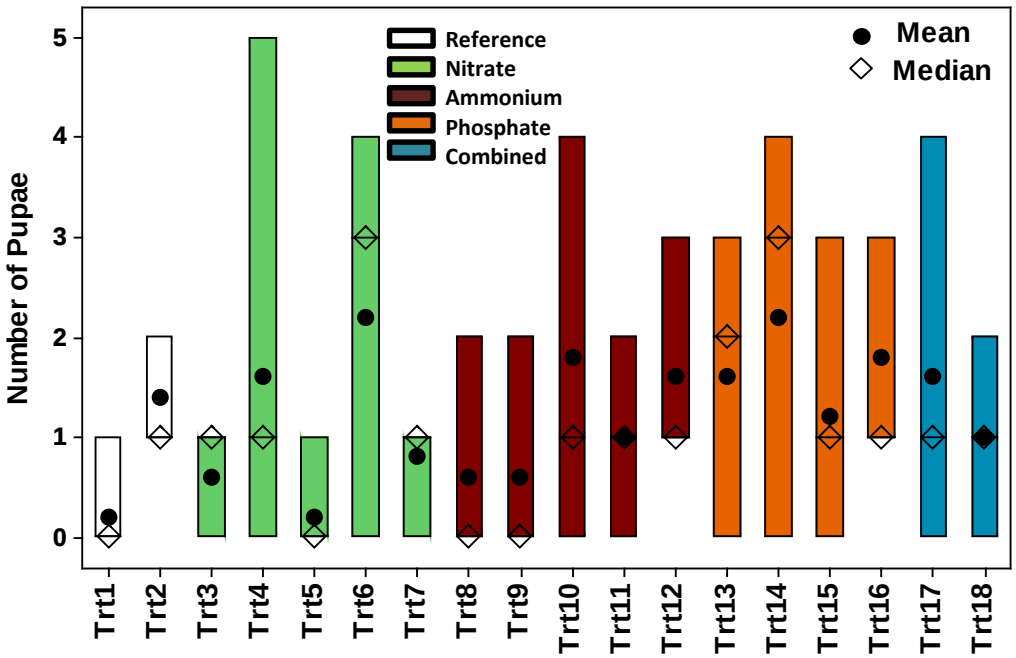

Figure 2.4. Mean, median and range of the number of pupae for different treatments.

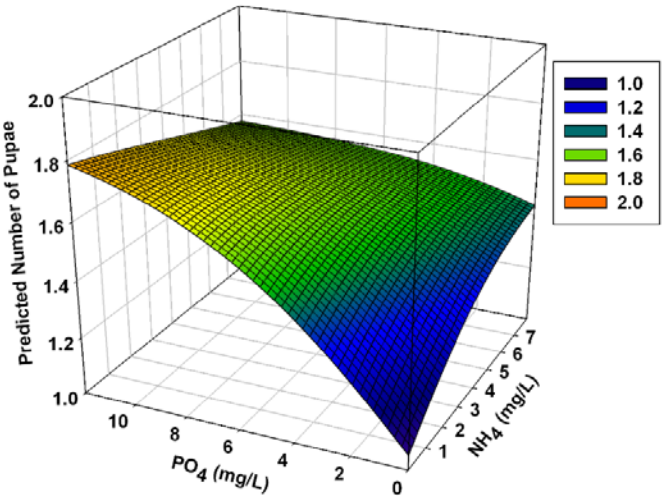

Figure 2.5. Predicted number of pupae per container by fitted Hurdle model versus NH_4 or PO_4 levels. Increasing NH_4 or PO_4 had positive impacts on probability of any larvae pupating.

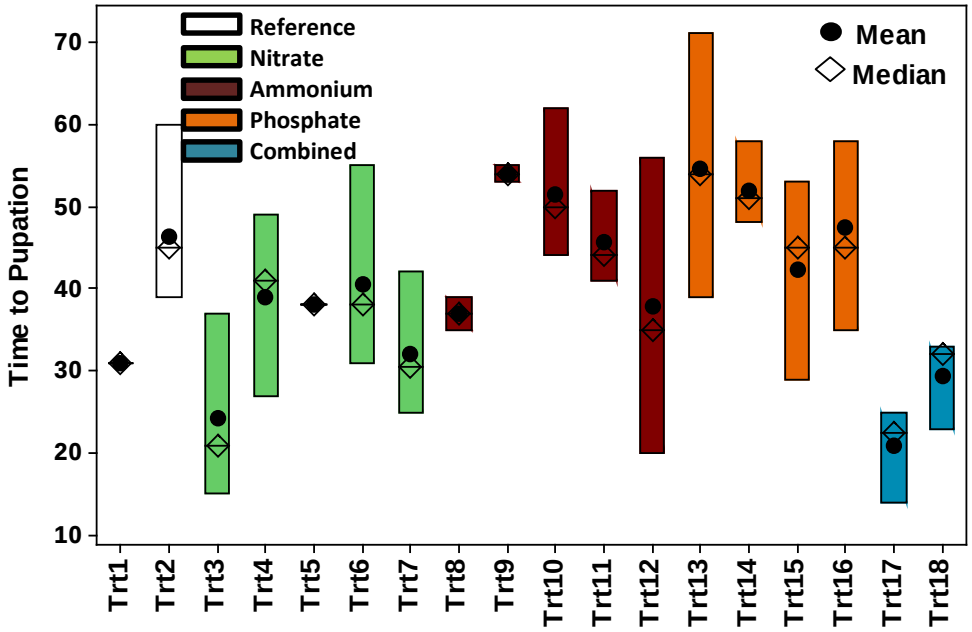

Figure 2.6. Mean, median and range of time to pupation for different treatments.

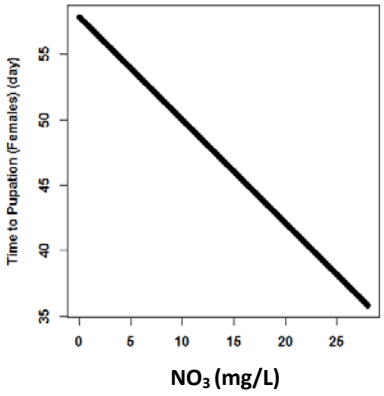

Figure 2.7. Predicted pupation time of females per container by fitted linear model versus NO_3 levels. By increasing NO_3 level, time to pupation of adult females decreased.

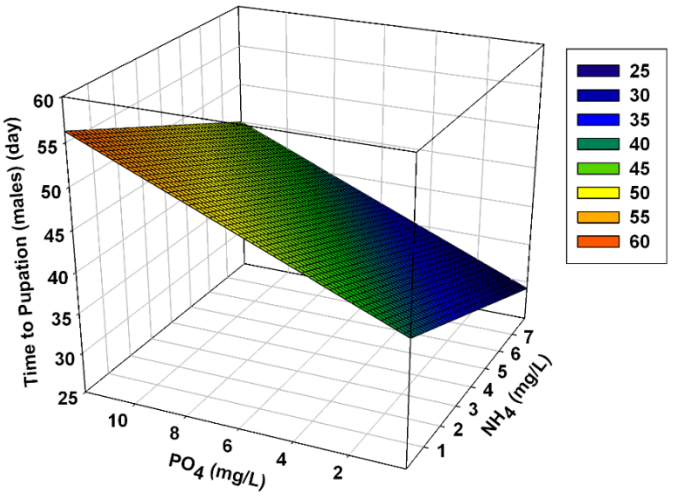

Figure 2.8. Predicted pupation time of males per container by fitted linear model versus PO_4 and NH_4 levels. By increasing NH_4, time to pupation decreased and by increasing PO_4, it took longer for larvae to pupate and emerge as males.

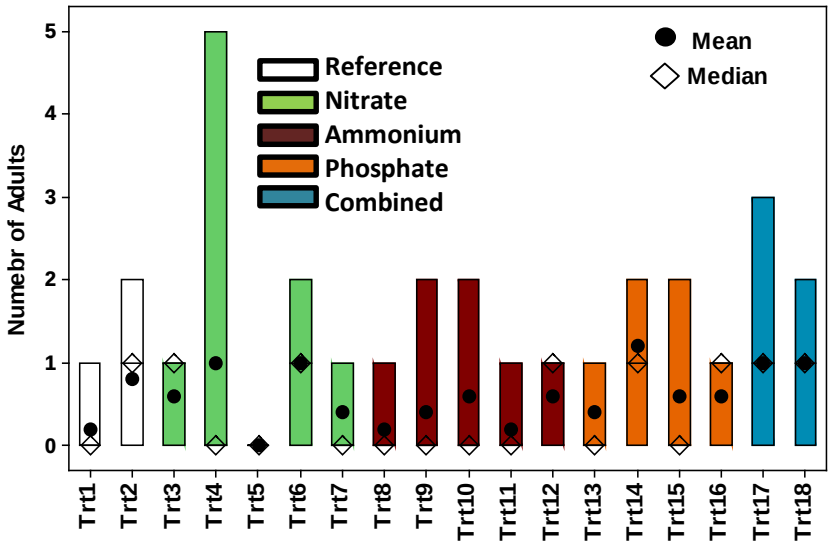

Figure 2.9. Mean, median and range of the number of adults for different treatments.

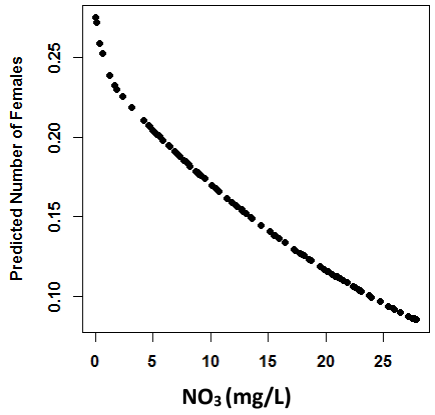

Figure 2.10. Predicted number of females per container by fitted Hurdle model versus NO_3 levels. Increasing NO_3 concentration is predicted to decrease the number of adult females that emerge.

Chapter 3. Short term prediction of *Culex quinquefasciatus* abundance carrying West Nile Virus and their infection rate in Central North Georgia, U.S.A based on the climate variability

Abstract

Mosquito population density plays a key role in determining outbreaks and transmission of vector-borne infectious risk such as West Nile Virus (WNV). *Culex quinquefasciatus* is the main vector of WNV in the southeast United States and inter-annual and seasonal variation of this vector abundance is mainly related to climate variability. In this study, short term effects of climate conditions on seasonal variation of *Culex* mosquito abundance and their infection rate in the central north part of the State of Georgia, United States, from 2002 to 2009 were assessed. Weekly and four weeks moving average temperature, precipitation, potential evapotranspiration (PET), and available moisture in surface layer were considered as risk factors. Cross-correlation maps (CCMs) were developed to investigate influence of preceding environmental conditions during a time lagged interval on mosquito count data as well as estimated infection rate. The Poisson regression model and Artificial Neural Network (ANN) model were used for the prediction purposes. Two sets of predictors were used for these models: 1) the interval lagged climate data with the highest correlation, 2) single time lag antecedent *Culex* mosquito abundance or infection rate up to 10 weeks prior to the events combined with lagged climate data. Statistical analysis revealed that increasing temperature and PET and decreasing surface moisture in preceding late winter and

preceding spring increased *Culex quinquefasciatus* female mosquitoes abundance in summer/early fall about 2 times as many and also increased the number of infectious mosquitoes about 3.5 times. Also low precipitation in late winter decreased mosquito abundance in summer. However, when temperature in late winter and early spring is above average coupled with low precipitation favors the incidence of WNV in mosquitoes. Both ANN and regression models predicted the seasonal cycle of mosquito abundance fairly accurate. Addition of antecedent mosquito count data or infection rate improved the prediction power of both models by increasing E_{NASH} values and decreasing R_{BIAS} values. Our results highlight the impacts of preceding climate conditions over a range of time on *Culex* vector species which can be modeled under climate change scenarios so that long-term predictions of shifts in mosquito abundance can be estimated. Also, using the developed predictive model, warning of high-risk periods for WNV can become more accurate.

Keywords: *Culex* mosquito population, West Nile Virus, prediction, seasonal variation, climate variables.

Introduction

Culex species are the major vector of West Nile Virus disease in the United States. This virus was first identified in North America in New York City in 1999. By the end of 2013, more than 39,000 disease cases of West Nile Virus (WNV) had been reported to the CDC (Centers for Disease Control and Prevention, 2013). Just recently in 2012, 5674 human cases and 286 deaths were reported to the CDC. In the southeast U.S., over 96% of the West Nile Virus positive

mosquito pools reported to the CDC from 1999 to 2010 have been obtained from *Culex* mosquitoes, among which 64.6% were from *Culex quinquefasciatus* (Andreadis, 2012). The state of Georgia, and especially the Atlanta area has been a hotspot of WNV incidence in 2012 with 117 WNV human cases, 6 deaths and 125 WNV positive mosquito pools (among which over 81% were from *Culexquinquefasciatus*) reported by the Georgia Department of Public Health (2012).

Transmission of vector-borne diseases is influenced by a wide range of environmental factors. Among these, climatic variability is one of the most important drivers of inter-annual WNV transmission risk. Climate directly affects the vector population, pathogens and hosts distribution, and their abundances (Roiz et al., 2014). *Culex* species display a seasonal behavior. Their activity reaches its minimal level in the winter, then rises in the spring to the peak levels of summer and continues until mid-fall (Strickman, 1988). Females which emerge in late summer search for sheltered areas where they hibernate until spring. They become inactive when the temperature drops below 15°C (Rey, 2011), while warm weather brings them out in search of water on which to lay their eggs (AMCA, 2014). Changes in meteorological conditions such as temperature, relative humidity and wind speed can impact mosquito populations (Curriero et al., 2005). The greatest WNV transmissions during the epidemic summers of 2002 to 2004 in the U.S. were linked to above normal temperatures. Analysis of temperature deviations from the 30-yr mean (1971-2000) during summer in the United States showed that during years with above normal temperatures, WNV always dispersed into new areas and the amplification occurred during

summers with above or normal temperatures. Subsequent cool summers were associated with decreased or delayed virus activity, especially at northern latitudes (Reisen et al., 2006).

Temperature influences the development rate and fitness of immature mosquitoes and the biting rate and survival of adult female mosquitoes (Dohm et. al., 2002). Drought can lead to a decline in the number of mosquito predators and it may encourage birds to gather near standing water, where the virus can circulate more easily. High temperatures also speed the development of viruses within the mosquito carriers (Epstein, 2001; Patz et. al., 2008; Wang et. al., 2010). During periods of drought between rainfall events, blood-fed and potentially infected mosquitoes digest blood meals and wait for a heavy rainfall that floods the temporary pools to oviposit (Day, 2001). Rainfall and the surface moisture first create temporary freshwater habitats and also maintain permanent aquatic habitats that are used as egg-laying sites by female mosquitoes. Subsequently, rainfall saturates the ground and increases near-surface humidity levels (Shaman et al., 2002).

The increase in the relative rate of WNV human cases from 2001 to 2005 in the U.S. has been linked to warmer temperatures, elevated humidity, and heavy precipitation independent of season using conditional logistic regression (Soverow et. al., 2009). WNV mosquito infection changes from year to year spatiotemporally. For the temporal scale, higher temperature and less rainfall are associated with more human cases and also with the highest WNV prevalence in the mosquitoes. WNV infection can also be negatively correlated with the previous year's precipitation (Ruiz et. al., 2010). For the spatial analysis, temperature plays a bigger role than precipitation in comparison to the temporal patterns (Ruiz et. al., 2010). The spatiotemporal variability of human West Nile

cases is associated with the spatiotemporal variability of drought followed by wetting of the land surface (Shaman et. al, 2005). Spring drought induces the amplification of WNV by concentrating vector mosquitoes in humid vegetated areas where nesting birds are present. This makes the virus transmission easier as birds are the natural host of WNV and this virus is maintained in nature in a mosquito-bird-mosquito transmission cycle. Subsequent summer rainfall and wetting of the land surface enable the dispersal of infected mosquitoes into the open, sparsely vegetated areas they had avoided during the drought (Day and Shaman, 2008).

To control mosquito populations and to prevent disease, understanding this vector-environment relationship is essential. It is also helpful to understand the responses of WNV transmission risk to climate variability to adapt the public health policies based on the consequent impacts (Wang et al., 2011). Predictive models can be helpful in this regard to enhance warning of high-risk periods for WNV and to describe the variations in mosquito abundance over time. Numerous studies have been conducted to develop mosquito abundance prediction models which mostly rely on meteorological and environmental data from the days and weeks preceding the capture of mosquitoes (Walsh et al., 2008). Such models can be designed to provide continuous daily or weekly estimates of mosquito populations under the impacts of different environmental conditions. Ahumada et al. (2004) proposed a discrete-time population model to simulate the temporal dynamics of *Culex quinquefasciatus* abundance. The model incorporated temperature and rainfall dependence and breeding site density dependent competition. This model simulated the mosquito population growth through time and at different elevations in Hawaii. Temperature

was the major driving force behind mosquito population growth and abundance in Hawaii but precipitation dependence also constrained population size which was evident during dry years.

A climate based model was developed by Gong et al. (2007) to predict mosquito abundance of WNV *Culex* species. Temperature, rainfall, evaporation and photoperiod were used as inputs to the model. A moisture index was also created based on 7 days cumulative rainfall and evaporation. The model was developed on temperature-dependent functions including development rate and survival rate, a moisture index dependent function, and daily egg laying rate.

The Dynamic Mosquito Simulation model (DyMSiM) developed by Morin and Comrie (2010) was used in simulating *Culex quinquefasciatus* population dynamics in Florida and California. This model breaks up the larval phases into separate instar stages. The model used daily temperature and precipitation to drive population simulations throughout the year. This model revealed that dry conditions in California reduced mosquito populations due to loss of immature mosquito habitats, while drier late summer conditions in Florida decreased late-season adult mosquito populations.

In most of the previously mentioned analyses, the impact of meteorological conditions on mosquito abundance was limited to single point lags which consider the conditions at a certain time point prior to trapping. Curriero et al. (2005) introduced cross-correlation maps (CCMs) as a graphical method for visualizing the influence of preceding environmental conditions during a time lagged interval on the abundance of *Ochlerotatus sollicitans* species. Since then, this tool has been used to identify the timing and duration of potential meteorological effects on mosquito

populations (Shone et al., 2006; Walsh et al., 2008; Chuang et al., 2012; Lebl et al., 2013). In this study, to investigate the correlation between climate forces and inter-annual and seasonal variation of *Culex mosquito* population carrying WNV as well as their infection rate, CCMs were developed for mosquito data from the central north part of the State of Georgia (GA). The main goal was to develop an improved predictive model of *Culex quinquefasciatus* population and their infection rate, which would advance our understanding of the transmission of mosquito-borne arboviruses (Walsh et al., 2008). Using the lagged climate data extend effects of climate conditions over a range of time rather than a single point in time. Two modeling approaches were applied in this study, multi-regression and Artificial Neural Network (ANN); lagged climate data were fed into these models for prediction purposes. In addition, as there is correlation between any two observations of the time series of the response variable (mosquito count data or infection rate), antecedent conditions of response variable up to 10 weeks prior to the event were added to the models as predictors. It was hypothesized that addition of past values of mosquito count data or the infection rate to the model improves the model performance and increases the prediction accuracy.

Methodology

Mosquito and meteorological data

In this study, effects of meteorological variation on female *Culexquinquefasciatus* abundance per trap night and Vector Index were explored for the central north part of the State of Georgia.

Vector Index is an estimate of the average number of infectious mosquitoes per trap night and reflects risk of human diseases (CDC, 2013). The weekly meteorological data including mean weekly precipitation, temperature, potential evapotranspiration (PET) and available moisture in surface layer from 2002 to 2009 were downloaded from the National Weather Service, Climate Prediction Center (CPC) (http://www.cpc.ncep.noaa.gov/products/monitoring_and_data/drought.shtml). Climatic divisions were defined for the state of GA by CPC and as Atlanta metropolitan area is located in division 2, the central north part of GA, weekly climatic data were obtained for this division (Figure 3.1). Soil moisture is estimated by a one-layer hydrological model (Huang et al., 1996; Van den Dool et al, 2003). The model takes observed precipitation and temperature and calculates soil moisture, evaporation and runoff. Potential evapotranspiration is computed from observed temperature and using Thornthwaite method (Thornthwaite, 1948). Mosquito data were obtained from 2002 to 2009 for the counties located in division 2. As adult *Culex* species hibernate during winter, no traps were set up for winter time and mosquito counts were assumed to be zero for this period. Figure 3.1 shows the average weekly precipitation, temperature and female *Culexquinquefasciatus* abundance over the period 2002 to 2009 for counties located in the central north of GA.

Statistical analysis

The potential relationship between female *Culex quinquefasciatus* mosquito abundance and various meteorological forcings was analyzed using cross correlation maps (CCMs). This

graphical approach characterizes the temporal structure of mosquito population size or Vector Index in association with meteorological variables. Using this method, the key antecedent environmental conditions, their timings, and durations were identified which can improve the ability of developing predictive models of vector abundances. Assume *Y(t)* and *X(t)* represent two time series with time index *t*, CCMs illustrate the correlation coefficients (*r*) between *Y(t)*, here number of captured female *Culex mosquito*s or Vector Index at time *t*, and a meteorological variable *X*, averaged over a time period starting at time *t*−*j* and ending at time *t*-*k* with *j*≥*k*:

$$r(Y, X_{j,k}) = cor(Y(t), \overline{X(t-j, t-k)})$$

Here, *t* changes from 1 to 52 for a given year (i.e. weekly time interval). Spearman's rank order correlation was applied to calculate the correlation as it makes no assumption about the distribution of the data and does not consider a linear relationship between mosquito abundance and climate data. The CCMs were developed for weekly, and four weeks moving average scales. As preceding climate condition up to 5 months prior to summer plays a significant role on the life cycle of mosquitoes, the maximum time lag was set to 20 weeks. In addition, the sample autocorrelation function (ACF) was defined for time series of each response variable to identify the time interval over which a correlation in the data series exists. All analyses were performed in R statistical software (version 3.0.2.) (R Core Team, 2013).

Predictive model

As the response variables are count data, Poisson regression model was selected for prediction purposes. To capture the potential complex nonlinear relationships between climate variables and mosquito abundance or the infection rate, the ANN model was also used. Some climatic variables are highly correlated with each other (e.g. evaporation and temperature), which will cause high variance inflation in the Poisson regression model. To handle such collinearities, Principle Component Analysis (PCA) was used. PCA is a variable reduction technique that uses orthogonal transformation to convert a set of observations of correlated variables into a set of values of linearly uncorrelated variables called principle components. PCA was applied to two sets of predictors, the first set included the interval lags of climate variables with highest correlation; temperature, precipitation, PET and available moisture in surface layer, the second set included the interval lags of climate variables and also antecedent conditions of response variables. Components that explained the variability of observed data were fed into ANN and Poisson regression models.

ANN is a black box type lumped model that has the ability to identify a relationship from given patterns which makes it possible to solve nonlinear models. ANNs can be categorized based on the direction of information flow and processing. In a feed-forward network, the connections between nodes is from an input layer, through one or more hidden layers, to an output layer (Dawson and Wilby, 2001) (Figure 3.2). The most common method used to find the number of hidden layers and nodes is a trial-and-error approach (Kalin et al., 2010). In this study, the number of hidden neurons changed from 4 to 6, and the number of hidden layer was set to 1 to build a

parsimonious model and to avoid data overtraining. A neural network was constructed using MATLAB version 7.10.0 (2010) and was trained by adjusting the weights that link its neurons. Separate models were developed for predicting weekly and four weeks moving average mosquito abundance and Vector Index. The ANN model was trained and tested using the Principal Components (PCs) and the response variable. 70% of the time series data, selected randomly from the whole data set (Rezaeian Zadeh et al., 2010), was used for training and 30% of data was used for testing purposes into the ANN and regression models. Model performances were assessed with the coefficient of determination (R^2), Nash–Sutcliffe efficiency (E_{NASH}) (Nash and Sutcliffe, 1970), and bias ratio (R_{BIAS}) (Salas et al., 2000).

In addition, female *Culex* mosquito abundance as well as Vector Index were predicted based on Principle Components (PCs) and the Poisson regression models and were graphed against real dataset of climate variable for the purpose of sensitivity analysis and to visualize the potential relationship between predictors and the response variables.

Results

Weekly analysis

Culex quinquefasciatus is the main vector of WNV in the southeast United States and studying the effect of climate on the population dynamics of this species would help predict the virus risk more accurately. To do so, for each climate variable, Cross Correlation Maps (CCMs) were generated for weekly time scale by varying the temporal lag and the period over which the variable

was averaged. As shown in Figure 3.3, each map indicates the correlation between preceding climate condition and *Culex* mosquito abundance (female *Culex quinquefasciatus* species) as well as Vector Index with all combinations of interval time lags.

Female *Culex quinquefasciatus* abundance

Weekly *Culex* mosquito abundances (*M*) were highly correlated with the mean temperature of the 16 to 9 weeks prior a capture event, $r(M, T_{16,9}) = 0.82$. PET averaged over the interval of (t-15) to (t-12) weeks also had a strong positive correlation with mosquito abundance at time t, $r(M, PET_{15,12}) = 0.82$. Surface moisture averaged over 17 to 7 weeks prior the capture event had the highest negative correlation with mosquito population $r(M, \theta_{17,7}) = -0.72$. Precipitation averaged over 20 to 16 weeks preceding time frame showed the weakest negative correlation with mosquito abundance in comparison to other climate variables $r(M, P_{20,16}) = -0.08$. As mosquito population density peaks in summer/early fall (Figure 3.1 C), counting back the lags with the highest correlation identifies the preceding late winter and spring as most relevant time-period.

These selected interval lags were fed into PCA to eliminate the collinearity. PC1, and PC2 together explain 96% of variance in observed data (Table 3.1). PC1 had strong positive loadings for temperature and PET and strong negative loading for surface moisture which considering summer/early fall as peak *Culex* species population, reflects warmer and drier late winter and spring. About 27% increase in weekly temperature or 30% decrease in weekly surface moisture with respect to their average value over the period of 2002 to 2009 leads to 1 unit increase in PC1

(Figures 3.4 a & b). PC2 had a strong negative loading for precipitation which reflects low rain in late winter/early spring. About 50% decrease in total weekly precipitation from with respect to its average value over the 2002-2009 period corresponds to 1 unit increase in PC2 (Figure 3.4).

These components were fed into ANN and Poisson regression models for prediction purposes. 70% of randomly selected input data were used for training and the rest for testing. Table 3.2 shows the regression model summary. For 1 unit increase in PC1, female *Culex mosquito* abundance increased by a factor of 2.24 (2.15-2.33, 95% C.L.), ($p<0.0001$). Also, for 1 unit decrease in PC2, mosquito abundance is decreased by 14% (0.86, 0.82-0.91, 95% C.L.), ($p<0.0001$). To visualize the relationship between climate variables and mosquito abundance, mosquito data was predicted using the Poisson regression model and PCs and was plotted against climate dataset (Figure 3.5). When average weekly temperature goes above 24 °C in mid-March through May coupled with low moisture conditions, below 0.5 cm per week, the population of *Culex* vectors in mid-July increases up to 35 (Figure 3.5 b & Table 3.2). During the late winter and spring, Adult females overwinter and hide under buildings or storm drains and sewers. Mild winter and early spring increase the survival rate of these species throughout winter resulting in a rapid buildup of mosquito populations in the spring and summer. Weekly precipitation about 2 cm averaged in March, increases mosquito abundance in mid-July up to 40 per week (Figure 3.5 a & d). As shown in Figure 3.5 d, there is no clear trend between mosquito abundance and precipitation. In general, the graph displays high mosquito population when precipitation is about 2 cm followed by a small secondary peak in mosquito counts when precipitation is around 6 cm. Precipitation

influences the mosquito population dynamics through increasing near-surface humidity associated with rainfall and consequently enhancing mosquito flight activity and also through changing the abundance and type of aquatic habitats available for mosquito breeding. Higher precipitation in late winter provides pools as potential mosquito breeding sites. Warm spring and warm later winter cause mosquitoes to start their season earlier and increase the *Culex* mosquito population and infection rate in summer.

Two PCs were randomized and fed into ANN as well for prediction purposes. Time series of observed vs predicted data for the whole data set were plotted after sorting the randomized data (Figure 3.6). ANN predicted slightly better than regression model with the E_{NASH} value of 0.54 and R_{BIAS} value of 6%. Both models underestimated the peak values, especially weekly mosquito counts of 40 and higher.

To improve the developed predictive model and for a short term prediction, antecedent values of *Culex mosquito* count data extending back 10 weeks were fed into the PCA in addition to climate variables. There is a significant correlation between mosquito abundance at time *t* and mosquito abundance at time *t-h* for h= 1 to 12 (Figure 3.7). Three components which explained 97% of the variance of observed data were selected and used as inputs to the ANN and Poisson regression models (Table 3.3). Figure 3.8 shows time series of predicted values using both models versus observed data for the whole period after sorting the randomized data set. In addition, a graph showing the performance of ANN and regression model based on the E_{NASH} values versus single time lags extending back 10 weeks prior sampling was plotted for *Culex* mosquito abundance data

for testing and training periods (Figures 3.9). As the lag interval increases, model performance gradually decreases, however the model built based on lagged climate data and antecedent mosquito count data 10 weeks preceding time frame for the testing period still had an acceptable accuracy level with E_{NASH} value of 0.56 and 0.50 for ANN and regression model respectively. ANN models worked better than regression model in general. Figure 3.9 indicates that by using climate data of preceding time frame, for instance late winter and spring, and using estimated weekly mosquito abundance in the past up to 10 weeks prior to the point of interest, both models are able to predict *Culex mosquito* population in upcoming summer with a good level of accuracy.

Vector Index

For the weekly Vector Index (*VI*), the highest correlation was found for temperature and PET averaged from 20 weeks prior to trapping and extended into 8 or 6 weeks prior to sampling, $r(VI, T_{20,6}) = r(VI, PET_{20,8})$=0.65. Also, surface moisture averaged over 20 to 5 weeks prior the capture event was negatively correlated with weekly Vector Index, $r(VI, \theta_{5,20})$=-0.56. Precipitation Averaged over (t-20) to (t-16) weeks were negatively and weakly correlated with Vector Index at week *t*, $r(VI, P_{20,16})$ =-0.09. Considering summer as peak mosquito activity, the selected interval lags indicate the climate variability in preceding late winter and spring.

The climate data of interval lags with the highest positive or negative correlation were fed into PCA. Table 3.4 shows the proportion of variance of each component and how much each variable contributed to that principle component. PC1 and PC2 describe about 97% of the variance in

observed data and reflect the same definition as PCs for mosquito data shown in Table 3.1. Considering the seasonal behavior of mosquito abundance and their peak activity in summer/early fall (Figure 3.1 C), PC1 reflects warmer and drier spring, and 25% increase in weekly temperature or 27% decrease in weekly surface moisture with respect to their average values from the period 2002-2009 leads to 1 unit increase in PC1 (Figures 3.10 a & b). PC2 has a strong negative loading for precipitation, this reflects less rain in late winter. About 50% decrease in total weekly precipitation from its average value over the 2002-2009 period corresponds to 1 unit increase in PC2 (Figure 3.10). These PCs were fed into ANN and Poisson regression models for prediction purposes. Table 3.5 shows the regression model summary. Two sets of input data were fed into the Poisson model: only PC1, PC1 and PC2. Although PC2 was not statistically significant, the model containing both components worked better in terms of prediction than the model built using just PC1. Therefore, the two components were kept into the model for prediction purposes. For 1 unit increase in PC1, Vector Index increased by a factor of 4.96 (1.37-18.76, 95% C.L.), (p=0.02). Also, 1 unit increase in PC2 leads to decrease in Vector Index by 33% (0.67, 0.26-1.78, 95% C.L.), (p=0.42). To clarify the relationship between climate variables and mosquito infection rate, Vector Index was predicted using PCs and the Poisson regression model and was plotted against climate dataset (Figure 3.11). When average weekly temperature is around 24 °C in March through early June coupled with low moisture conditions, below 0.5 cm per week, infection rate in mid-July will be around 0.2 (Figure 3.11, a). Dry and warm spring increases mosquito population in summer and consequently increases the chance of circulating virus between vector and host. Precipitation vs

Vector Index graph shows a peak Vector Index value of 0.25 in mid-July when the precipitation is less about 2 cm in March followed by a smaller secondary peak in mosquito infection rate when precipitation is about 6 cm (Figure 3.11 c).

Two components were also fed into the ANN model to predict weekly Vector Index. ANN had some negative predictions which were converted to zero. Both model performances were very close to each other with a slightly higher E_{NASH} value for the Poisson regression model and smaller R_{BIAS} value for the ANN model for the testing period (Figure 3.12). Both models underestimated the peak values especially values above 0.2. To improve the developed predictive model and for the short term prediction, antecedent values of Vector Index up to 10 weeks prior to the event were fed into the PCA in addition to climate variables. Significant correlation exists in the Vector Index (*VI)* data series between VI_t and VI_{t-h} for h= 1 to 5 (Figure 3.7). For the new set of PCs, five components were defined and three of them which explained about 97% of the variance of observed data were fed into the ANN and Poisson regression model (Table 3.6). Time series of predicted Vector Index by both models versus observed data for the whole period (training + testing) after sorting the randomized data were given in Figure 3.13. In addition, a graph showing the performance of ANN and regression model based on the E_{NASH} values versus lag intervals over 10 weeks preceding time frame was developed and plotted for Vector Index (Figure 3.14). For the training period, ANN with higher E_{NASH} predicted Vector Index more accurately than regression model. As the lag interval increases, model performance accuracy decreases especially from lag 1 through lag 3, although even using single time lags Vector Index extending back 10 weeks prior

to sampling, model accuracy for the testing period was acceptable with E_{NASH} value of 0.54 and 0.58 for ANN and regression model respectively. By estimating infection rate 10 weeks prior to summer season and having climate data of preceding late winter and spring seasons, *Culex mosquito* infection rate can be predicted in following summer with an acceptable level of accuracy.

Four weeks moving average analysis

In order to perform the analysis in monthly scale having sufficient number of data, four weeks moving average of mosquito and its infection rate and climate data were obtained for each week of the period studied. CCMs were generated for each climate variable and *Culex* mosquito abundance data as well as Vector Index as shown in Figure 3.15.

Female *Culex quinquefasciatus* abundance

Four weeks moving average *Culex* mosquito data showed stronger correlation with climate data in comparison to weekly data. *Culex* vector abundance was positively correlated with temperature and PET respectively over 20 to 5 weeks prior to sampling, $r(M, T_{20,5})$=0.82, and 19 to 7 weeks prior to sampling, $r(M, PET_{19,7})$=0.82 and negatively correlated with four weeks moving average available moisture in surface layer over 16 to 8 weeks prior the capture event, $r(M, \theta_{16,8})$=-0.75. Four weeks moving average precipitation over 20 to 13 weeks was positively correlated with mosquito abundance at week *t*, $r(M, P_{20,13})$=0.1, also precipitation one week prior to mosquito capture event was weakly and negatively correlated with vector abundance,

$r(M, P_{1,1})$=-0.09. As mosquito population density peaks in summer/early fall (Figure 3.1 C), counting back the lag with the highest correlation identifies the preceding late winter and spring as most relevant time-period. The climate data of interval lags with the highest positive or negative correlation were fed into PCA. Table 3.7 shows the proportion of variance of each component and how much each variable contributed to that principle component. PCs 1, 2 and 3 together explain 97% of the variance in observed data. PC1 has negative loadings for temperature and PET and positive loadings for surface moisture which considering summer/early fall as peak *Culex* species population, corresponds to cold and moist late winter and spring. About 24% decrease in weekly moving average temperature or 30% increase in four weeks moving average surface moisture with respect to their average values from the period 2002 to 2009 leads to 1 unit increase in PC1 (Figures 3.16 a & b). PC2 has strong negative loading for precipitation which reflects low precipitation in early spring and PC3 is positively related to precipitation one week prior the trapping event. About 40% decrease in weekly moving average precipitation in early spring from its average value over the period of 2002 to 2009 increases PC2 by 1 unit (Figure 3.16). Also, 55% increase in four weeks moving average precipitation over (t-1, t-1) from its average value leads to 1 unit increase in PC3 (Figure 3.16).

After feeding these components to the Poisson model, it was found that all three PCs have a negative relationship with *Culex* mosquito count data. One unit increase in PC1, decreased mosquito abundance by 50% (0.50, 0.48-0.52, 95% C.L.), ($p<0.0001$), so half as many female *Culex* mosquitoes. PC2 is negatively related to mosquito data, and 1 unit increase in PC2 decreases

mosquito abundance by 22% (0.78, 0.75-0.82, 95% C.L.) ($p<0.0001$) (Table 3.8). In addition, PC3 has a statistically significant negative relationship with mosquito data (0.94, 0.91-0.97, 95% C.L.) ($p=0.0004$). To visualize the relationship between climate variables and mosquito abundance, using PCs and the developed Poisson regression model, mosquito data were predicted and plotted against the climate dataset (Figure 3.17). When four weeks moving average temperature goes above 24 °C in March through June coupled with a surface moisture below 0.5 cm, this condition exacerbates mosquito development leading to high mosquito abundance in summer around mid-July. (Figure 3.17 b). During mild winter and warm spring, the survival rate of those adult females that overwinter and hide under buildings or storm drains and sewers increases. *Culex quinquefasciatus* does not enter a true diapause but rather overwinters in a temperature induced-quiescence (Reisen et al. 1986). Adult females spend the winter for the most part resting in cellars, under dwellings and other protected places and become inactive during cold periods (Tesh et al. 2004). During warm periods, they become active again and renew blood feeding. Survival of considerable numbers of *Culex quinquefasciatus* throughout the winter results in a rapid buildup of mosquito populations early in the spring and summer.

Figure 3.17a shows that when temperature in spring goes above 20 °C up to 24 °C, if there is high precipitation in late winter and early spring, about 6 cm, number of female *Culex* mosquitoes rises to about 40 per trap night in weekly scale. Precipitation-mosquito graphs do not show a strong relationship. In general, highest mosquito abundance in mid-July is seen when precipitation from March to April is about 2 cm followed by a smaller secondary peak in mosquito counts when

precipitation is about 5 cm (Figure 3.17 f). Precipitation influences the mosquito population dynamics by increasing near-surface humidity associated with rainfall and consequently enhancing mosquito flight activity and also by changing the abundance and type of aquatic habitats available for mosquito breeding. Higher precipitation in early spring provides pools as potential mosquito breeding sites. Warm springs and warm winters cause mosquitoes to start their season earlier by looking for standing pools to lay their eggs, thus increasing the *Culex* mosquito population and infection rate in summer. In addition, the chance of getting about 30 female *Culex mosquito*es per trap night will increase especially in summer if the precipitation one week prior to sampling is 2-4 cm or 8 cm and higher combined with temperature of 20-24 °C in spring (Figure 3.17 c and e). One week after a rain event, especially in summer which is the peak mosquito activity season, rainwater stands in pools through the landscape, providing more habitat available for the larvae and therefore accelerates their development rate. Also, late summer and fall rains result in a longer mosquito season. These findings are in agreement with Soverow et al. (2009) that 1-2 weeks after the rainfall, the incidence of reported human WNV infection increased, this condition may expand the mosquito population and influence mosquito host-seeking. However, depending on habitat characteristics and ecology of each mosquito species, the interaction between mosquito population and rainfall is very complex and inconsistent (Roiz et al., 2014).

Three PCs were also randomized and fed to ANN model as input for prediction purposes. Figure 3.18 compares ANN and the regression model performance versus the observed data. ANN predicted the four weeks moving average mosquito abundance more accurately with E_{NASH}=0.62

and R_{BIAS}=9% relative to the regression model with E_{NASH}=0.52 and R_{BIAS}=18%. To improve the model prediction accuracy, the antecedent four weeks moving average *Culex* mosquito abundance data up to 10 weeks prior to sampling, was added to the PCA as a predictor. Table 3.9 shows the proportion of variance of components for each set of PCs. PCs 1 & 2 & 3 & 4 explained about 98% of variance in observed data. Components 1 & 2 & 3 had same interpretation as explained for Table 3.7. Component 4 corresponds to antecedent mosquito abundance condition. These components were fed into ANN and regression model for prediction purposes. Figure 3.19 compares the predicted vs observed data. For all the data sets, ANN performed better, with higher E_{NASH} values and less R_{BIAS} values compared to the regression model and as the lag interval increases, model performances gradually decrease (Figure 3.20). This indicates that by combining interval lagged climate data and single time lag antecedent *Culex* mosquito abundance at the four weeks moving average scale, a stronger model with higher accuracy performance can be built for prediction purposes.

Vector Index

According to CCMs (Figure 3.15), Vector Index had the highest correlation with temperature and PET averaged from 15 weeks prior to sampling and extended into 10 or 12 weeks prior to sampling with $r(VI, T_{15,10}) = r(VI, PET_{15,12})$ =0.79. Also, surface moisture averaged over 18 to 7 weeks prior the capture event was negatively correlated with four weeks moving average Vector Index $r(VI, \theta_{18,7}) = -0.70$. Averaged precipitation over (t-20) to (t-11) weeks were negatively

correlated with Vector Index at week t, $r(VI, P_{20,11})$ =-0.14. These interval lagged climate data were fed into PCA to eliminate the collinearity. Table 3.10 shows the proportion of variance of each component and how much each variable contributed to that principle component. PC1, PC2 and PC3 together explain about 100% of the variance in observed data. PCs 1 and 2 reflect the same definition as PCs in Table 3.4 but in four weeks moving average scale. 25% increase in weekly moving average temperature or about 28% decrease in four weeks moving average surface moisture with respect to their average values from the period 2002 to 2009 leads to 1 unit increase in PC1 (Figures 3.21 a & b). Also, about 37% decrease in weekly moving average precipitation in early spring from with respect to its average value over the period of 2002 to 2009 increases PC2 by 1 unit (Figure 3.21). According to Table 3.10, PC3 had positive loading for four weeks moving average moisture condition but the moisture vs PC3 graph does not show a clear relationship (Figure 3.21). After feeding these PCs to the Poisson regression model, it was found although PCs 2 and 3 were not statistically significant, the regression model including three components predicted the Vector Index more accurately (E_{NASH}=0.69, R_{BIAS}=-19%) than the regression model contained just PC1 (E_{NASH}=0.61, R_{BIAS}=-22%) for testing period. Therefore, all three PCs were kept into the model (Table 3.11). PCs 1 and 3 have positive relationship with Vector Index and PC2 has negative relationship with Vector Index. To visualize the relationship between climate variables and mosquito infection rate, using PCs and the developed Poisson regression model, Vector Index was predicted and was plotted against climate dataset (Figure 3.22). In four weeks moving average scale, temperature about 26 °C and surface moisture around 0.5 cm in late March

through early May increase mosquito infection rate in summer around mid-July up to 0.4. Also, rain events of 2 cm and less in late winter and early spring followed by temperature about 26 °C in spring, favor transmission of WNV within mosquitoes leading to the infection rate as high as 0.25 in mid-July (Figure 3.22 a and b). Precipitation-vector Index graph does not show a strong relationship. In general, highest mosquito infection rate in mid-July is seen when precipitation from March to April is about 2 cm followed by a smaller secondary peak in infection rate when precipitation is about 5 cm (Figure 3.22 e).

PCs 1 and 2 and 3 were fed also into the ANN model for prediction purposes. Figure 3.23 shows time series of predicted versus observed four weeks moving Vector Index for each model for the whole data set. Both models could capture the data trend and ANN performance was slightly better than regression model with E_{NASH}=0.72 and R_{BIAS}=-7%. Although, Vector Index prediction model in four weeks moving average scale is better than weekly scale, both models still underestimated the high peak values. To improve the prediction, the second set of predictors consists of antecedent conditions of Vector Index data up to 10 four weeks moving average preceding point of interest and interval lagged climate data were fed into PCA. Table 3.12 shows the proportion of variance of each component and weight of each variable. Out of five new defined PCs, three components were selected and were added to the prediction models. The first two components explain the same conditions as the first data set. PC3 corresponds to antecedent Vector Index value. Figures 3.24 shows time series of predicted vs observed four weeks moving average Vector Index for the whole period after sorting the randomized data. Also a graph of E_{NASH} value

of each model built using single lagged Vector Index and interval lagged climate data was given in Figure 3.25. Accuracy of performance was much better for models that were built by including lagged interval climate data and antecedent Vector Index value up to 3 weeks prior to point of interest and the peak values were captured by these models. Addition of Vector Index value one week preceding time frame to the model, improved ANN prediction accuracy for the testing period from E_{NASH} value of 0.71 to 0.93.

Discussion

In this study, the associations of preceding meteorological conditions and *Culex* mosquito abundance as well as their infection rates were explored to enhance our understanding of mosquito ecology and disease risk for *Culex quinquefasciatus* vectors carrying WNV. To determine the maximum correlations between mosquito data or infection rate and climate variables, cross correlation maps (CCMs) were generated. The association of vector abundance with leading climate variables under specific time interval lags result in more robust inference than analyses that are restricted to single predefined time lags (Chuang et al., 2012). Using CCMs and considering interval lag structures, both the timing and duration of the meteorological effects are displayed (Curriero et al., 2005). The relationships revealed between interval lagged environmental factors and the abundance of mosquitoes carrying WNV can be used as leading indicators of vector abundance. Predicting WNV activity is an essential requirement for vector control, and studying the *Culex* species population dynamics in relation to climate factors like

ambient air temperature, surface moisture and precipitation could help improve the ability of predicting the WNV risk.

Using PCA, the collinearities among the climate variables were removed and the new components obtained at weekly and four weeks moving average scales were fed into the ANN and Poisson regression models as explanatory variables. Considering the timing of peak mosquito abundance which is summer and early fall, results of CCMs and the Poisson regression model reflected that elevated temperature and PET averaged over late winter and spring were associated with increased abundance of *Culex quinquefasciatus* and their related infection rate in summer (considering mid-July as peak mosquito count, Figure 3.1. C). This is consistent with other field studies as larval and pupal development are temperature dependent (Chuang et al., 2012). Also, drier than normal condition during spring with low available moisture in surface layers creates favorable conditions for the development of *Culex* vectors in summer. Prolonged above normal temperature extends the duration of the mosquito season and vector activity. It also accelerates the development rate, influence fitness of immature mosquitoes, the biting rate and survival of adult female mosquitoes (Patz et al., 2008; Morin and Comrie, 2013). Also, vector breeding conditions are facilitated and the frequency of transmission events is increased due to dry condition by gathering hosts and vectors around nutrient-rich water bodies (Shaman et al., 2005).

Results showed that rain events of 6 cm and higher averaged over March to April combined with mild spring with average weekly temperature of 20 to 24 °C, favor mosquito development in mid-July. Also rain event of 2 cm or less in March through May coupled with temperature around

26 °C, increases the chance of getting higher number of infectious mosquitoes in mid-July. Early period precipitation postpones and shortens the activity of host-seeking mosquitoes, but at the same time leads to higher abundance. Increase in formation and persistence of mosquito breeding sites due to early period precipitation, is associated with increase in abundance of *Culex* mosquitoes (Rosa et al., 2014). Extensive breeding habitats of *Culex* mosquitoes can result from the heavy rains and associated flooding especially in late winter and early spring, which is right before the mosquito life cycle starts. Breeding habitats can include temporary ground pools, pools along receding river floodplain or natural or man-made containers. However, the impact of precipitation on mosquito population is controversial (Roiz et al., 2014). Generally, regions with lower seasonal variation in precipitation such as the southeastern United States, have lower probability of WNV mosquito cases (Harrigan et al., 2014). Also, the southeastern United States receives sufficient precipitation to support mosquito populations throughout the year, making temperature the controlling variable affecting *Culex* mosquito population dynamics (Morin and Comrie, 2013). The CCMs obtained for precipitation versus mosquito count data or versus Vector Index support this statement. Due to exponential growth rates and also complex interaction between mosquito abundance and rainfall, even small effects of weather conditions on a mosquito population could result in vast effects in future generations (Lebl et al., 2013; Roiz et al., 2014).

The ANN and Poisson regression model predicted the seasonal cycle of mosquito abundance and Vector Index fairly accurately. The predictions improved significantly when antecedent conditions of response variable up to 10 weeks prior to point of interest were added as predictors

to the models. Addition of 1 week antecedent mosquito count data to the ANN model as a predictor increased the E_{NASH} value from 0.54 to 0.68 and from 0.62 to 0.89 respectively for weekly and four weeks moving average scales for testing period. Also, addition of estimated weekly mosquito abundance 10 weeks prior to the ANN model, improved the model performance for the testing period by increasing E_{NASH} from 0.54 to 0.56 (weekly scale) and from 0.62 to 0.68 (four weeks moving average scale) (Figures 3.6 and 3.13). For the Vector Index, addition of antecedent infection rate one week prior the capture increased the ANN model performance accuracy and the E_{NASH} value changed from 0.54 to 0.69 and from 0.72 to 0.93 respectively for weekly and four weeks moving average scales for testing period. Also, addition of estimated weekly Vector Index 10 weeks prior as a predictor to PCA and then to the ANN model, improved the model performance for the testing period by increasing E_{NASH} from 0.72 to 0.74 for four weeks moving average scale (Figures 3.6 and 3.10). For weekly scale E_{NASH} value did not change. ANN predicted slightly better than the regression model, which could be due to the non-linearity assumption of ANN in comparison to Poisson which is a log-linear model. Generally including the antecedent mosquito count or Vector Index to the model increased the predictive power of both ANN and regression models. This suggests that meteorological conditions and mosquito data from preceding weeks may be better indicators of future population dynamics for *Culex quinquefasciatus* mosquito species and the WNV risk than just the present size of the population.

Conclusion

The findings of this study and the developed ANN and Poisson regression models for predictions could have important implications for the control of West Nile Virus spread by *Culex* mosquito species. Most other studies developed mosquito abundance regression based models with single time lag antecedent climate data up to 2 months as explanatory variables without fixing the collinearities among climate variables and without extending effects of climate conditions over a range of time. Multi-collinearity can increase the variance of the coefficient estimates and reduce the statistical power of the analysis. In addition, single time lag might not capture meteorological effects on mosquito abundance if preceding conditions contributed to breeding and survival over weeks to months (Chuang et al., 2012). By collecting rigorous climate and mosquito data during important seasons, between January to May, and also addition of any antecedent mosquito count data as well as estimated infection rate 1 to 10 weeks prior, the size of vector populations that are likely to be seen in summer can be estimated and the possible abnormalities in the increase of rates of WNV infestation can be monitored. These climate factors can be modeled under future warming conditions so that long-term predictions of shifts in risk can be estimated (Harrigan et al., 2014). These information could be used for planning of mosquito control strategies and to prioritize the distribution of scarce mosquito control resources before the transmission season begins. Also, it can help enable early detection of virus circulation in mosquitoes and to provide early warning for WNV outbreaks. In years with warm spring and mild late winter, control operations such as applying insecticides can be initiated late in the winter to prevent rapid development of mosquitoes

early in the spring and summer as a result of increase in survival rate of *Culex mosquito*es throughout the winter. Although climate is the main driver of WNV risk and climatic factors increase predictive power of determining risk associated with WNV, further studies are needed to explore whether other environmental factors such as socio-economic conditions, and landscape and mosquito habitat characteristics should be accounted for a better understanding of disease risk and for developing a more comprehensive *Culex* mosquito dynamic simulation model.

References

Ahumada, J.A., Lapointe, D., Samuel, M.D., 2004. Modeling the Population Dynamics of *Culex quinquefasciatus* (Diptera: Culicidae), along an elevational gradient in Hawaii. J Med Entomol. 41(6):1157-1170.

American Mosquito Control Association, 2014. http://www.mosquito.org/

Andreadis, Th.G., 2012. The contribution of *Culex pipens* complex mosquitoes to transmission and persistence of West Nile Virus in North America. The American Mosquito Control Association, Inc. Vol. 28, No. 4, page: 137-151.

Center for Disease Control and Prevention, division of Vector-Borne Dieases., 2013. West Nile Virus in the United States: Guidelines for Surveillance, Prevention, and Control. U.S. Department of Health and Human Services. Public Health Service.

Chuang, T.W., Ionides, E.L., Knepper, R.G., Stanuszek, W.W., Walker, E.D., Wilson, M.L., 2012. Cross-Correlation Map analyses show weather variation influences on mosquito abundance patterns in Saginaw County, Michigan, 1989–2005. J Med Entomol. 49(4):851-858.

Curriero, F.C., Shone, S.M., Glass, G.E., 2005. Cross Correlation Maps: A tool for visualizing and modeling time lagged associations. Vector Borne Zoonotic Dis. Vol. 5, Number 3, 267-275.

Day, J.F., 2001. Predicting St. Louis Encephhalitis Virus Epidemics: Lessons from Recent, and Not So Recent, Outbreaks. Annu. Rev. Entomol. 46:111–138.

Day, J and Shaman, J., 2008. Using hydrologic conditions to forecast the risk of focal and epidemic arboviral transmission in Peninsular Florida. J Med Entomol. 45(3): 458-465

Dawson, C.W., and R.L. Wilby., 2001. Hydrologic modeling using artificial neural networks. Prog. Phys. Geogr. 25:80–108

Dohm D.J., O'Guinn, M.L., Turel, M.J., 2002. Effect of environmental temperature on the ability of Culex pipiens (Diptera: Culicidae) to transmit West Nile virus. J Med Entomol. 39(1):221–5.

Epstein, P. R., 2001. West Nile Virus and the Climate. J Urban Health. Vo. 78, No, 2.

Georgia Department of Public Health, Environmental Health. 2012. 2012 Arbovirus final report. Summary of human West Nile Virus and other arboviral Infections, Georgia.

Gong, H., DeGaetano, A., Harrington, L.C., 2007. A climate based mosquito population model. Proceedings of the World Congress on Engineering and Computer Science, October 24-26, San Francisco, USA.

Harrigan, R.J., Thomassen, H.A., Buermann, W., Smith, Th.B., 2014. A continental risk assessment of West Nile virus under climate change. Glob Change Biol. 20, 2417-2425.

Huang, J., van den Dool, H., and Georgakakos, K.P., 1996. Analysis of model-calculated soil moisture over the United States (1931-93) and application to long-range temperature forecasts. J Climate. Vol.9, No.6.

Kalin, L., Isik, S., Schoonover, J.E., Lockaby, B.G., 2010. Predicting Water Quality in Unmonitored Watersheds Using Artificial Neural Networks. JEQ. 39(4):1429-1440.

Lebl, K., Brugger, K., Rubel, F., 2013. Predicting *Culex pipiens/restuans* population dynamics by interval lagged weather data. Parasites & Vectors. 6:129, 1-11.

Morin, C.W. and Comrie, A.C., 2010. Modeled response to the West Nile virus vector *Culex quinquefasciatus* to changing climate using the dynamic mosquito simulation model. Int J Biometeorol. 54:517–529.

Morin, C.W. and Comrie, A.C., 2013 Regional and seasonal response of a West Nile virus vector to climate change. PNAS. Vol. 110, No. 39.

Nash, J.E., and Sutcliffe, J.V., 1970. River flow forecasting through conceptual models: Part I. A discussion of principles. J. Hydrol. 10:282–290.

Patz, J.A., Olson, S.H., Uejio, Ch. K., Gibbs, H.K., 2008. Disease Emergence from Global Climate and Land Use Change. Med Clin N Am. 92, 1473–1491.

R Core Team. 2013. R: a language and environment for statistical computing. Reference Index. R Foundation for Statistical Computing, Vienna, Austria. Version 3.0.1.

Reisen W.K., Meyer, R.P., Milby, M.M., 1986. Overwintering studies on *Culex tarsalis* (Diptera: Culicidae) in Kern County, California: temporal changes in abundance and reproductive status with comparative observations on C. *quinquefasciatus* (Diptera: Culicidae). Ann Entomol Soc Am. 79:677–685.

Reisen, W., Fang, Y., Martinez, V.M., 2006. Effects of Temperature on the Transmission of West Nile Virus by Culex tarsalis (Diptera: Culicidae). J Med Entomol. Vol. 43, no, 2.

Rey, J.R., 2011. The mosquito. ENY-727 (IN652), one of a series of the Entomology and Nematology Department, Florida Cooperative Extension Service, Institute of Food and Agricultural Sciences, University of Florida.

Rezaeian Zadeh, M., Amin, S., Khalili, D., and Singh, V.P., 2010. Daily outflow prediction by multi layer perceptron with logistic sigmoid and tangent sigmoid activation functions. Water Resour Manage. 24:2673–2688.

Roiz, D., Ruiz, S., Soriguer, R., Figuerola, J., 2014. Climatic effects on mosquito abundance in Mediterranean wetlands. Parasites & Vectors. 7:333.

Rosa, R., Marini, G., Bolzoni, L., Neteler, M., Metz, M., Deluuchi, L., Chadwick, E.A., Balbo, L., Mosca, A., Giacobini, M., Bertolotti, L., Rizzoli, A., 2014. Early warning of West Nile virus mosquito vector: climate and land use models successfully explain phenology and abundance of *Culex pipiens* mosquitoes in north-western Italy. Parasites & Vectors. 7:269.

Ruiz, M.O., Chaves. L.F., Hamer, G.L., Sun, T., Brown, W.M., Walker, E.D., Haramis, L., Goldberg, T.L., Kitron, U.D., 2010. Local impact of temperature and precipitation on West Nile virus infection in Culex species mosquitoes in northeast Illinois, USA. Parasites & Vectors. 3:19.

Salas, J.D., M. Markus, and A.S. Tokar., 2000. Streamflow forecasting based on artificial neural networks. p. 23–51. In R.S. Govindaraju and A.R. Rao (ed.) Artificial neural networks in hydrology. Kluwer Academic, Dordrecht, the Netherlands.

Shaman, J., Stieglitz, M., Stark, C., Blancq, S. L., Cane, M., 2002. Using a Dynamic Hydrology Model to Predict Mosquito Abundances in Flood and Swamp Water. Emerg Infect Diseases. Vol. 8, No. 1.

Shaman, J., Day, J.F., Stieglitz, M., 2005. Drought-Induced Amplification and Epidemic Transmission of West Nile Virus in Southern Florida. J Med Entomol. 42(2): 134-141.

Shone, S.M., Curriero, F.C., Lesser, C.R., Glass, G.E., 2006. Characterizing Population Dynamics of Aedes sollicitans (Diptera: Culicidae) Using Meteorological Data. J Med Entomol. 43(2):393-402.

Soverow, J. E., Wellenius, G.A., Fisman, D.E., Mittleman, M.A., 2009. Infectious Disease in a Warming World: How Weather Influenced West Nile Virus in the United States (2001–2005). Environ Health Perspect. Vol. 117, No. 7.

Strickman, D., 1988. Rate of oviposition by *Culex Quinquafasciatus* in San Antonio, Texas, during three years. J AMCA. Vol 4, No. 3. 339-344.

Tesh, R.B., Parsons, R., Siirin, M, Randle, Y., Sargent, C., Guzman, H., Wuithiranyagool T, Higgs S, Vanlandingham, D.L., Bala, A.A., Haas, K., Zerinque, B., 2004. Year-round West Nile virus activity, Gulf Coast region, Texas and Louisiana. Emerg Infect Dis. 10:1649–1652.

Thornthwaite, C. W., 1948. An approach toward a rational classification of climate. Geographical Review 38 (1): 55–94.

Van den Dool, H., Huang, J., and Fan, Y. (2003). “Performance and analysis of the constructed analogue method applied to U.S. soil moisture over 1981–2001.” J Geophys Res. Vol. 108, NO. D16, 8617.

Walsh, A.S., Glass, G.E., Lesser, C.R., Curriero, F.C., 2008. Predicting seasonal abundance of mosquitoes based on off-season meteorological conditions. Environ Ecol Stat. 15:279–291.

Wang, G., Minnis, R.B., Belant, J.R., Wax, Ch.R., 2010. Dry weather induces outbreaks of human West Nile virus infections. BMC Infect Diseases. 10:28.

Wang, J., Ogden, N.H., Zhu, H., 2011. The Impact of weather conditions on *Culex pipiens* and *Culex restuans* (Diptera: Culicidae) abundance: A case Study in Peel Region. J Med Entomol. 48(2):468-475.

Table 3.1. PCA for climate variables highly correlated with weekly *Culex* mosquito abundance.

		Loadings			
	Spearman Correlation	PC1	PC2	PC3	PC4
$T_{16,9}$	0.82	0.58**	-0.17	0.39	0.69
$P_{20,16}$	-0.08	-0.11	-0.96	-0.25	
$PET_{15,12}$	0.82	0.58	-0.16	0.35	-0.72
$\theta_{17,7}$	-0.72	-0.56	-0.15	0.82	
Proportion of variance	-	70%	26%	4%	0%

T= Temperature, *P*= Precipitation, *PET*=Potential evapotranspiration, θ= Soil moisture in surface layer. First column is the Spearman's rank order correlation coefficient between each climate variable and weekly *Culex* mosquito abundance.

Table 3.2. Poisson model analysis of weekly *Culex* mosquito abundance.

	Estimate*	95% CI		p-value
Intercept	2.99*	2.74	3.26	<0.0001
PC1	2.24	2.15	2.33	<0.0001
PC2	0.86	0.82	0.91	<0.0001

* Odds ratios were derived using the link function $e^{(coefficient)}$ and coefficient estimates of the GLM model.

Table 3.3. PCA for climate variables and weekly lagged mosquito abundance data time series. Each set contains antecedent mosquito data changing from 1 to 10 weeks prior.

	PC1	PC2	PC3	PC4		PC1	PC2	PC3	PC4
$T_{16,9}$	0.52	-0.16	-0.28	0.39	$T_{16,9}$	0.52	0.15	-0.28	0.39
$P_{20,16}$		-0.96		-0.25	$P_{20,16}$		0.96		-0.25
$PET_{15,12}$	0.53	-0.15	-0.22	0.35	$PET_{15,12}$	0.53	0.15	-0.23	0.35
$\theta_{17,7}$	-0.51	-0.15	0.24	0.81	$\theta_{17,7}$	-0.51	0.16	0.23	0.82
$\boldsymbol{M_{t-1}}$	0.43		0.90		$\boldsymbol{M_{t-2}}$	0.42		0.90	
%VAR	66%	21%	10%	3%	*%VAR*	66%	21%	10%	3%
	PC1	PC2	PC3	PC4		PC1	PC2	PC3	PC4
$T_{16,9}$	0.53	0.14	-0.29	0.38	$T_{16,9}$	0.53	0.13	-0.28	0.39
$P_{20,16}$		0.96		-0.25	$P_{20,16}$		0.96		-0.25
$PET_{15,12}$	0.53	0.13	-0.24	0.35	$PET_{15,12}$	0.54	0.13	-0.23	0.35
$\theta_{17,7}$	-0.51	0.17	0.20	0.82	$\theta_{17,7}$	-0.51	0.18	0.20	0.82
$\boldsymbol{M_{t-3}}$	0.42		0.90		$\boldsymbol{M_{t-4}}$	0.41		0.91	
%VAR	65%	21%	10%	3%	*%VAR*	65%	21%	11%	3%
	PC1	PC2	PC3	PC4		PC1	PC2	PC3	PC4
$T_{16,9}$	0.53	0.11	-0.29	0.38	$T_{16,9}$	0.54		-0.27	0.39
$P_{20,16}$		0.95	-0.14	-0.25	$P_{20,16}$		0.94	-0.20	-0.25
$PET_{15,12}$	0.54	0.10	-0.23	0.35	$PET_{15,12}$	0.55		-0.22	0.35
$\theta_{17,7}$	-0.51	0.19	0.17	0.82	$\theta_{17,7}$	-0.52	0.20	0.16	0.82
$\boldsymbol{M_{t-5}}$	0.39	0.17	0.90		$\boldsymbol{M_{t-6}}$	0.37	0.22	0.90	
%VAR	64%	21%	12%	3%	*%VAR*	62%	21%	13%	3%
	PC1	PC2	PC3	PC4		PC1	PC2	PC3	PC4
$T_{16,9}$	0.55		-0.26	-0.39	$T_{16,9}$	0.55		-0.24	-0.39
$P_{20,16}$		0.93	-0.25	0.25	$P_{20,16}$		0.92	-0.30	0.25
$PET_{15,12}$	0.55		-0.21	-0.35	$PET_{15,12}$	0.56		-0.20	-0.35
$\theta_{17,7}$	-0.52	0.21	0.13	-0.82	$\theta_{17,7}$	-0.53	0.20	0.10	-0.82
$\boldsymbol{M_{t-7}}$	0.34	0.28	0.90		$\boldsymbol{M_{t-8}}$	0.30	0.33	0.89	
%VAR	61%	21%	14%	3%	*%VAR*	60%	21%	15%	3%
	PC1	PC2	PC3	PC4		PC1	PC2	PC3	PC4
$T_{16,9}$	0.56		0.22	0.39	$T_{16,9}$	0.57		-0.20	-0.39
$P_{20,16}$		0.89	0.37	-0.25	$P_{20,16}$	-0.10	0.90	-0.35	0.25
$PET_{15,12}$	0.56		0.19	0.35	$PET_{15,12}$	0.57		-0.17	-0.35
$\theta_{17,7}$	-0.54	0.20		0.82	$\theta_{17,7}$	-0.55	0.18		-0.82
$\boldsymbol{M_{t-9}}$	0.27	0.39	-0.88		$\boldsymbol{M_{t-10}}$	0.22	0.38	0.90	
%VAR	59%	22%	16%	3%	*%VAR*	58%	21%	17%	3%

%VAR: Proportion of variance

Table 3.4. PCA for climate variables highly correlated with weekly Vector Index.

		Loadings			
	Spearman Correlation	PC1	PC2	PC3	PC4
$T_{20,6}$	0.65	0.58	-0.18	0.40	0.69
$P_{20,16}$	-0.09	-0.12	-0.96	-0.27	
$PET_{20,8}$	0.65	0.58	-0.17	0.34	-0.72
$\theta_{20,5}$	-0.56	-0.56	-0.16	0.81	
Proportion of variance	-	70.5%	26%	3.3%	0%

Table 3.5. Poisson model analysis of weekly Vector Index.

	Estimate*	95% CI		p-value
Intercept	0.002*	0.0001	0.04	<0.0001
PC1	4.96	1.31	18.76	0.02
PC2	0.67	0.26	1.78	0.42

Table 3.6. PCA for climate variables and weekly lagged Vector Index time series. Each set contains antecedent Vector Index changing from 1 to 10 weeks prior.

	PC1	PC2	PC3	PC4		PC1	PC2	PC3	PC4
$T_{20,6}$	0.54	0.18	0.25	0.38	$T_{20,6}$	0.54	0.15	-0.26	0.38
$P_{20,16}$	-0.11	0.96		-0.27	$P_{20,16}$	-0.10	0.96		-0.27
$PET_{20,8}$	0.54	0.17	0.20	0.34	$PET_{20,8}$	0.55	0.15	-0.20	0.34
$\theta_{20,5}$	-0.53	0.16	-0.17	0.82	$\theta_{20,5}$	-0.53	0.18	0.15	0.82
$\boldsymbol{VI_{t-1}}$	0.36		-0.93		$\boldsymbol{VI_{t-2}}$	0.35		0.93	
%VAR	63%	21%	14%	3%	*%VAR*	62%	21%	14%	3%
	PC1	PC2	PC3	PC4		PC1	PC2	PC3	PC4
$T_{20,6}$	0.54	0.16	-0.24	-0.39	$T_{20,6}$	0.55	0.16	-0.23	-0.40
$P_{20,16}$	-0.11	0.96		0.27	$P_{20,16}$	-0.11	0.96		0.27
$PET_{20,8}$	0.55	0.16	-0.18	-0.34	$PET_{20,8}$	0.55	0.15	-0.18	-0.34
$\theta_{20,5}$	-0.53	0.17	0.18	-0.81	$\theta_{20,5}$	-0.53	0.18	0.17	-0.81
$\boldsymbol{VI_{t-3}}$	0.34		0.94		$\boldsymbol{VI_{t-4}}$	0.33		0.94	
%VAR	62%	21%	14%	3%	*%VAR*	61%	21%	15%	3%
	PC1	PC2	PC3	PC4		PC1	PC2	PC3	PC4
$T_{20,6}$	0.55	-0.16	-0.21	0.40	$T_{20,6}$	0.55	-0.18	-0.17	0.40
$P_{20,16}$	-0.11	-0.96		-0.27	$P_{20,16}$	-0.11	-0.96		-0.27
$PET_{20,8}$	0.55	-0.16	-0.17	0.34	$PET_{20,8}$	0.56	-0.17	-0.15	0.34
$\theta_{20,5}$	-0.53	-0.18	0.17	0.81	$\theta_{20,5}$	-0.54	-0.16	0.18	0.81
$\boldsymbol{VI_{t-5}}$	0.31		0.95		$\boldsymbol{VI_{t-6}}$	0.29		0.957	
%VAR	61%	21%	16%	3%	*%VAR*	60%	21%	16%	3%
	PC1	PC2	PC3	PC4		PC1	PC2	PC3	PC4
$T_{20,6}$	0.56	-0.19	-0.13	-0.40	$T_{20,6}$	0.56	-0.19	-0.11	-0.40
$P_{20,16}$	-0.12	-0.95	0.12	0.27	$P_{20,16}$	-0.12	-0.95	0.12	0.27
$PET_{20,8}$	0.56	-0.19	-0.11	-0.34	$PET_{20,8}$	0.57	-0.19		-0.34
$\theta_{20,5}$	-0.54	-0.14	0.19	-0.81	$\theta_{20,5}$	-0.55	-0.14	0.16	-0.81
$\boldsymbol{VI_{t-7}}$	0.26	0.10	0.96		$\boldsymbol{VI_{t-8}}$	0.23		0.97	
%VAR	59%	21%	17%	3%	*%VAR*	58%	21%	18%	3%
	PC1	PC2	PC3	PC4		PC1	PC2	PC3	PC4
$T_{20,6}$	0.57	0.16	-0.13	-0.40	$T_{20,6}$	0.57	0.13	-0.14	-0.40
$P_{20,16}$	-0.12	0.95	-0.14	0.27	$P_{20,16}$	-0.11	0.88	-0.38	0.27
$PET_{20,8}$	0.57	0.15	-0.12	-0.34	$PET_{20,8}$	0.58	0.13	-0.14	-0.34
$\theta_{20,5}$	-0.55	0.18		-0.81	$\theta_{20,5}$	-0.56	0.18		-0.81
$\boldsymbol{VI_{t-9}}$	0.18	0.16	0.97		$\boldsymbol{VI_{t-10}}$	0.13	0.40	0.91	
%VAR	58%	21%	19%	3%	*%VAR*	57%	21%	19%	3%

Table 3.7. PCA for climate variables highly correlated with four weeks moving average *Culex* mosquito abundance.

		Loadings				
	Spearman Correlation	PC1	PC2	PC3	PC4	PC5
$T_{20,5}$	0.82	-0.57	-0.20		-0.39	0.69
$P_{1,1}$	-0.09		-0.20	0.98		
$P_{20,13}$	0.1	0.14	-0.92	-0.18	0.33	
$PET_{19,7}$	0.82	-0.58	-0.19		-0.31	-0.73
$\theta_{16,8}$	-0.75	0.56	-0.20		-0.80	
Proportion of variance	-	56%	21%	20%	2%	0%

Table 3.8. Poisson model analysis of four weeks moving average *Culex* mosquito abundance.

	Estimate	95% CI		p-value
Intercept	4.22	3.93	4.54	<0.0001
PC1	0.50	0.48	0.52	<0.0001
PC2	0.78	0.75	0.82	<0.0001
PC3	0.94	0.91	0.97	0.0004

Table 3.9. PCA for climate variables and lagged four weeks moving average *Culex* mosquito abundance time series.

	PC1	PC2	PC3	PC4	PC5		PC1	PC2	PC3	PC4	PC5
$T_{20,5}$	-0.52	-0.16		-0.31	-0.38	$T_{20,5}$	-0.52	-0.16		-0.32	-0.37
$P_{1,1}$		-0.20	-0.98			$P_{1,1}$		-0.16	-0.99		
$P_{13,20}$	0.11	-0.92	0.18		0.33	$P_{13,20}$	0.11	-0.93	0.15		0.33
$PET_{19,7}$	-0.52	-0.16		-0.27	-0.30	$PET_{19,7}$	-0.52	-0.15		-0.28	-0.30
$\theta_{16,8}$	0.50	-0.23		0.19	-0.81	$\theta_{16,8}$	0.50	-0.24		0.17	-0.81
$\boldsymbol{M_{t-1}}$	-0.44			0.89		$\boldsymbol{M_{t-2}}$	-0.44	-0.10		0.89	
$\%VAR$	57%	18%	16%	7%	2%	$\%VAR$	57%	18%	17%	7%	2%
	PC1	PC2	PC3	PC4	PC5		PC1	PC2	PC3	PC4	PC5
$T_{20,5}$	-0.52	-0.15		-0.33	-0.37	$T_{20,5}$	-0.52	0.14		-0.33	-0.36
$P_{1,1}$		-0.15	-0.99			$P_{1,1}$		0.153	-0.99		
$P_{13,20}$	0.11	-0.93	0.14		0.33	$P_{13,20}$	0.10	0.92	0.14		0.33
$PET_{19,7}$	-0.52	-0.15		-0.28	-0.30	$PET_{19,7}$	-0.53	0.14		-0.29	-0.30
$\theta_{16,8}$	0.50	-0.24		0.15	-0.82	$\theta_{16,8}$	0.51	0.25		0.13	-0.82
$\boldsymbol{M_{t-3}}$	-0.43	-0.13		0.89		$\boldsymbol{M_{t-4}}$	-0.42	0.16		0.89	
$\%VAR$	56%	18%	17%	7%	2%	$\%VAR$	56%	18%	17%	8%	2%
	PC1	PC2	PC3	PC4	PC5		PC1	PC2	PC3	PC4	PC5
$T_{20,5}$	-0.53	0.12		-0.32	-0.36	$T_{20,5}$	-0.53	-0.11	0.13	-0.30	0.37
$P_{1,1}$		0.21	-0.97			$P_{1,1}$		-0.29	-0.94	-0.18	
$P_{13,20}$	0.10	0.91	0.20	-0.12	0.33	$P_{13,20}$	0.10	-0.88	0.29	-0.14	-0.33
$PET_{19,7}$	-0.53	0.12		-0.28	-0.30	$PET_{19,7}$	-0.53	-0.10	0.12	-0.27	0.30
$\theta_{16,8}$	0.51	0.25		0.11	-0.81	$\theta_{16,8}$	0.51	-0.26			0.81
$\boldsymbol{M_{t-5}}$	-0.41	0.20		0.89		$\boldsymbol{M_{t-6}}$	-0.39	-0.24		0.88	
$\%VAR$	55%	18%	16%	9%	2%	$\%VAR$	54%	18%	17%	9%	2%
	PC1	PC2	PC3	PC4	PC5		PC1	PC2	PC3	PC4	PC5
$T_{20,5}$	0.534		0.15	-0.27	-0.38	$T_{20,5}$	-0.54		0.17	-0.24	-0.38
$P_{1,1}$		-0.34	-0.91	-0.24		$P_{1,1}$		-0.40	-0.86	-0.32	
$P_{13,20}$	-0.11	-0.85	0.36	-0.15	0.33	$P_{13,20}$	0.11	-0.82	0.43	-0.16	0.33
$PET_{19,7}$	0.54		0.14	-0.25	-0.30	$PET_{19,7}$	-0.54		0.16	-0.23	-0.30
$\theta_{16,8}$	-0.52	-0.25			-0.81	$\theta_{16,8}$	0.53	-0.25			-0.81
$\boldsymbol{M_{t-7}}$	0.37	-0.27	-0.10	0.88		$\boldsymbol{M_{t-8}}$	-0.34	-0.31	-0.15	0.87	
$\%VAR$	53%	19%	17%	10%	2%	$\%VAR$	52%	19%	17%	11%	2%
	PC1	PC2	PC3	PC4	PC5		PC1	PC2	PC3	PC4	PC5
$T_{20,5}$	-0.55		0.16	-0.22	-0.38	$T_{20,5}$	-0.56	-0.10	0.15	0.20	-0.39
$P_{1,1}$		-0.35	-0.88	-0.31		$P_{1,1}$		-0.31	-0.90	0.30	
$P_{13,20}$	0.12	-0.83	0.39	-0.18	0.33	$P_{13,20}$	0.12	-0.84	0.36	0.22	0.33
$PET_{19,7}$	-0.55		0.15	-0.22	-0.30	$PET_{19,7}$	-0.56		0.14	0.20	-0.30
$\theta_{16,8}$	0.53	-0.24			-0.81	$\theta_{16,8}$	0.54	-0.23			-0.81
$\boldsymbol{M_{t-9}}$	-0.31	-0.33	-0.15	0.88		$\boldsymbol{M_{t-10}}$	-0.26	-0.36	-0.15	-0.88	
$\%VAR$	51%	19%	17%	12%	2%	$\%VAR$	51%	19%	17%	12%	2%

Table 3.10. PCA for climate variables highly correlated with four weeks moving average Vector Index.

		Loadings			
	Spearman Correlation	PC1	PC2	PC3	PC4
$T_{15,10}$	0.79	0.57	-0.23	0.42	0.67
$P_{20,11}$	-0.14	-0.15	-0.92	-0.36	
$PET_{15,12}$	0.79	0.58	-0.22	0.27	-0.74
$\theta_{18,7}$	-0.70	-0.57	-0.22	0.79	
Proportion of variance	-	70%	27%	2%	0%

Table 3.11. Poisson model analysis of four weeks moving average Vector Index.

	Estimate	95% CI		p-value
Intercept	0.001	0.00	0.07	0.001
PC1	6.07	1.04	35.56	0.04
PC2	0.56	0.17	1.80	0.32
PC3	1.76	0.04	78.62	0.77

Table 3.12. PCA for climate variables and lagged four weeks moving average Vector Index time series.

	PC1	PC2	PC3	PC4		PC1	PC2	PC3	PC4
$T_{15,10}$	0.52	-0.23	-0.29	0.39	$T_{15,10}$	0.52	-0.23	-0.29	0.40
$P_{20,11}$	-0.13	-0.92		-0.35	$P_{20,11}$	-0.13	-0.92		-0.35
$PET_{15,12}$	0.53	-0.22	-0.20	0.28	$PET_{15,12}$	0.53	-0.22	-0.20	0.28
$\theta_{18,7}$	-0.52	-0.22	0.20	0.80	$\theta_{18,7}$	-0.52	-0.22	0.20	0.80
$\boldsymbol{VI_{t-1}}$	0.41		0.91		$\boldsymbol{VI_{t-2}}$	0.40		0.91	
$\%VAR$	65%	22%	11%	2%	$\%VAR$	65%	22%	11%	2%
	PC1	PC2	PC3	PC4		PC1	PC2	PC3	PC4
$T_{15,10}$	0.52	-0.22	-0.28	0.41	$T_{15,10}$	0.53	0.20	-0.27	0.41
$P_{20,11}$	-0.13	-0.93		-0.36	$P_{20,11}$	-0.13	0.93		-0.36
$PET_{15,12}$	0.53	-0.21	-0.21	0.27	$PET_{15,12}$	0.54	0.20	-0.21	0.27
$\theta_{18,7}$	-0.52	-0.23	0.19	0.80	$\theta_{18,7}$	-0.52	0.24	0.17	0.80
$\boldsymbol{VI_{t-3}}$	0.39		0.92		$\boldsymbol{VI_{t-4}}$	0.38		0.92	
$\%VAR$	64%	22%	12%	2%	$\%VAR$	63%	22%	13%	2%
	PC1	PC2	PC3	PC4		PC1	PC2	PC3	PC4
$T_{15,10}$	0.54	0.19	-0.26	0.41	$T_{15,10}$	0.54	0.18	-0.25	0.41
$P_{20,11}$	-0.13	0.92		-0.36	$P_{20,11}$	-0.13	0.92	-0.12	-0.36
$PET_{15,12}$	0.54	0.19	-0.22	0.27	$PET_{15,12}$	0.55	0.17	-0.22	0.27
$\theta_{18,7}$	-0.53	0.25	0.15	0.80	$\theta_{18,7}$	-0.53	0.26	0.12	0.79
$\boldsymbol{VI_{t-5}}$	0.36	0.12	0.93		$\boldsymbol{VI_{t-6}}$	0.33	0.18	0.93	
$\%VAR$	62%	22%	14%	2%	$\%VAR$	61%	22%	15%	2%
	PC1	PC2	PC3	PC4		PC1	PC2	PC3	PC4
$T_{15,10}$	0.55	0.17	-0.24	0.42	$T_{15,10}$	0.56	0.16	-0.23	0.42
$P_{20,11}$	-0.13	0.91	-0.19	-0.36	$P_{20,11}$	-0.13	0.88	-0.27	-0.36
$PET_{15,12}$	0.55	0.16	-0.22	0.26	$PET_{15,12}$	0.56	0.15	-0.22	0.26
$\theta_{18,7}$	-0.54	0.26		0.79	$\theta_{18,7}$	-0.55	0.26		0.79
$\boldsymbol{VI_{t-7}}$	0.30	0.25	0.92		$\boldsymbol{VI_{t-8}}$	0.26	0.33	0.91	
$\%VAR$	60%	22%	16%	2%	$\%VAR$	59%	23%	17%	2%
	PC1	PC2	PC3	PC4		PC1	PC2	PC3	PC4
$T_{15,10}$	0.56	0.15	-0.21	0.42	$T_{15,10}$	0.57	-0.15	-0.19	-0.42
$P_{20,11}$	-0.13	0.86	-0.35	-0.36	$P_{20,11}$	-0.14	-0.82	-0.42	0.36
$PET_{15,12}$	0.57	0.14	-0.21	0.26	$PET_{15,12}$	0.57	-0.14	-0.19	-0.26
$\theta_{18,7}$	-0.55	0.24		0.79	$\theta_{18,7}$	-0.56	-0.22		-0.79
$\boldsymbol{VI_{t-9}}$	0.20	0.41	0.89		$\boldsymbol{VI_{t-10}}$	0.14	-0.48	0.86	
$\%VAR$	58%	23%	17%	2%	$\%VAR$	57%	23%	18%	2%

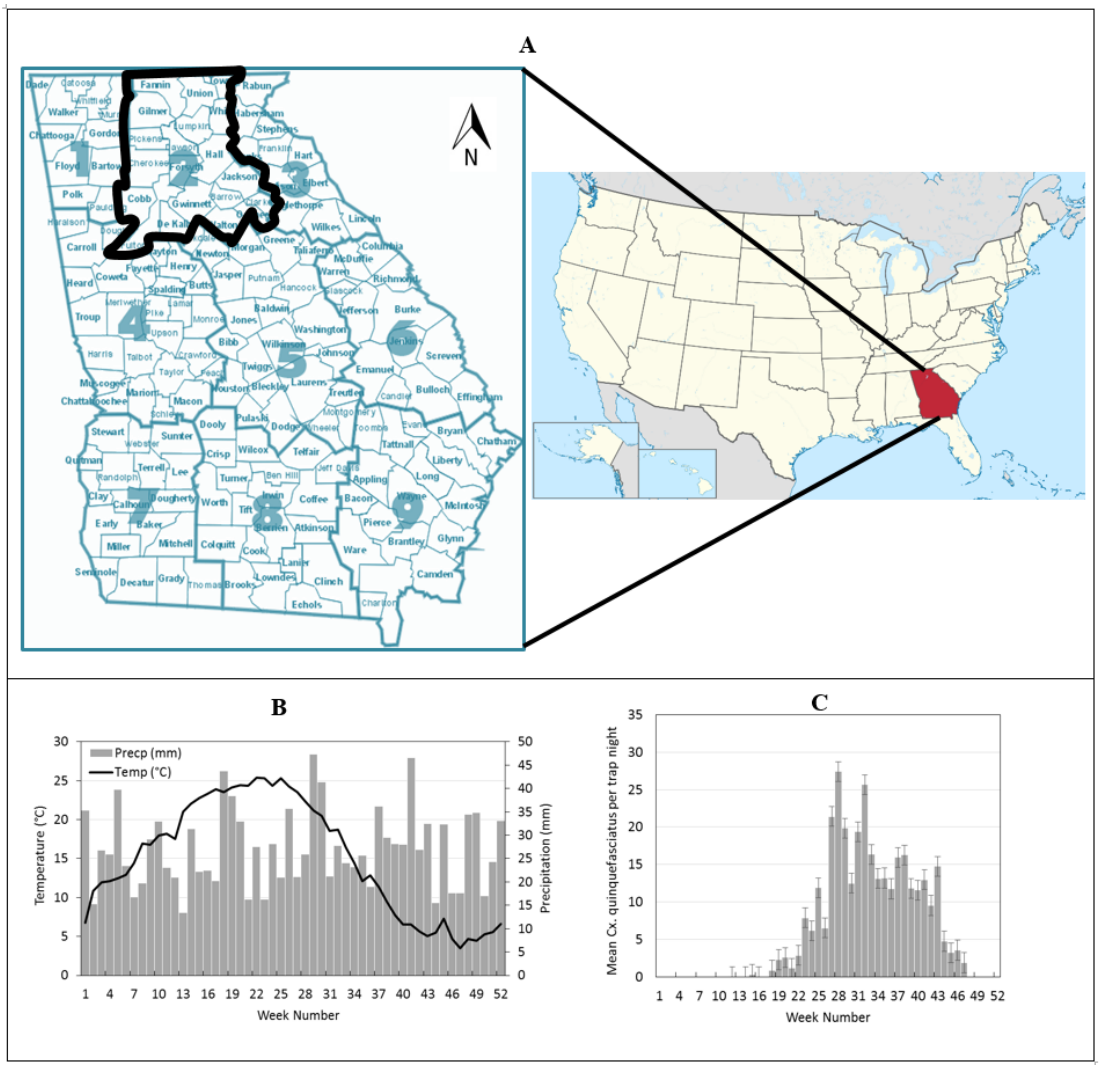

Figure 3.1. A: Climatic divisions for the state of Georgia defined by Climate Prediction Center (http://www.cpc.ncep.noaa.gov/products/monitoring_and_data/drought.shtml). B& C: Average weekly climate and mosquito abundance data over the period 2002 to 2009 for the central north. GA.

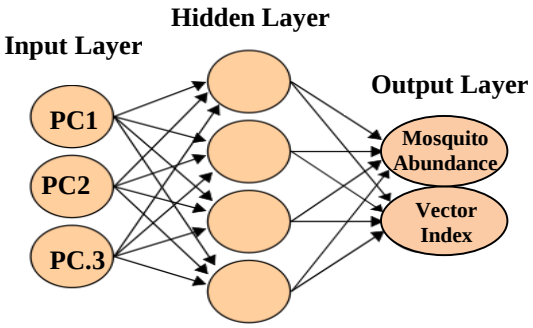

Figure 3.2. An example of feed-forward artificial neural network (ANN) structure with three vectors as inputs, 1 hidden layer with 4 neurons and two output vectors.

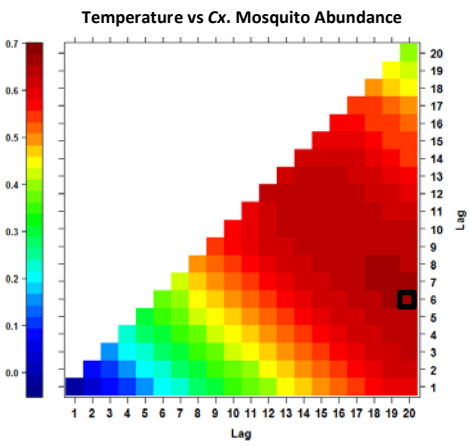

Temperature vs *Cx*. Mosquito Abundance

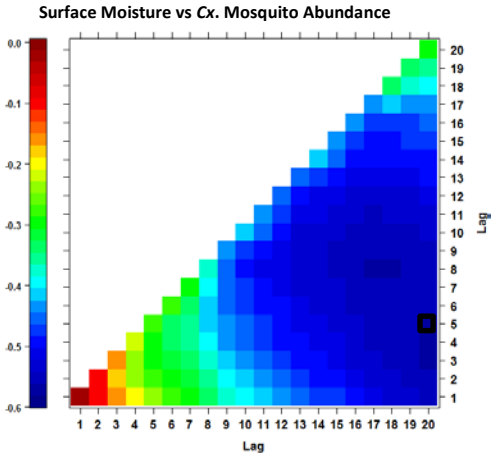

PET vs *Cx*. Mosquito Abundance

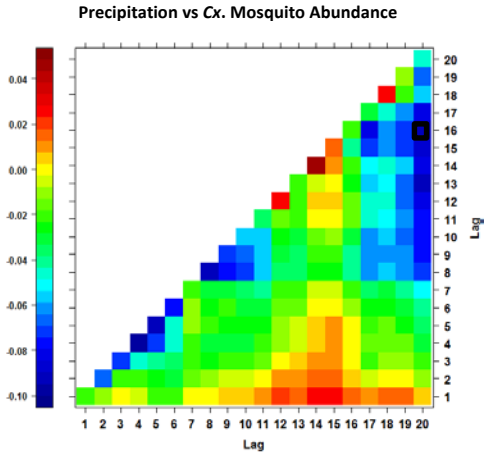

Precipitation vs *Cx*. Mosquito Abundance

"Continued on next page."

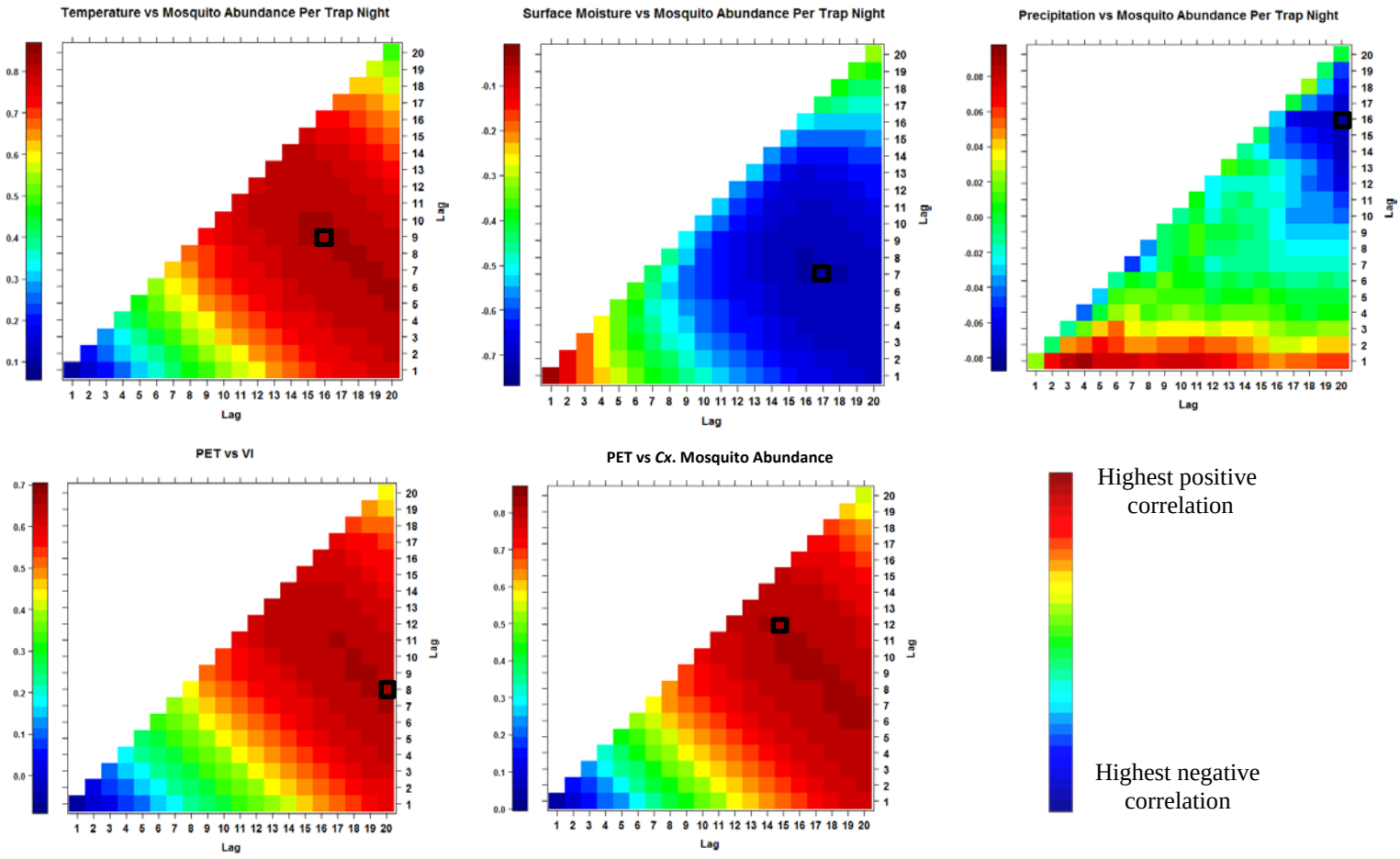

Figure 3.3. Cross correlation maps (CCMs) of weekly *Culex* mosquito abundance and Vector Index (VI) vs climate variables.

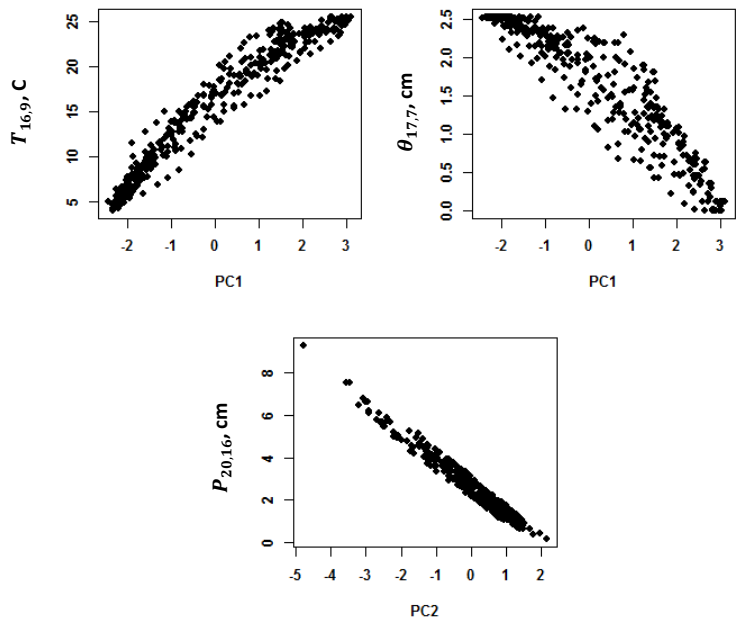

Figure 3.4. Graphs of climate variables versus each PC at weekly scale for *Culex* mosquito data. (P=Precipitation, T=Temperature, θ= Surface moisture.)

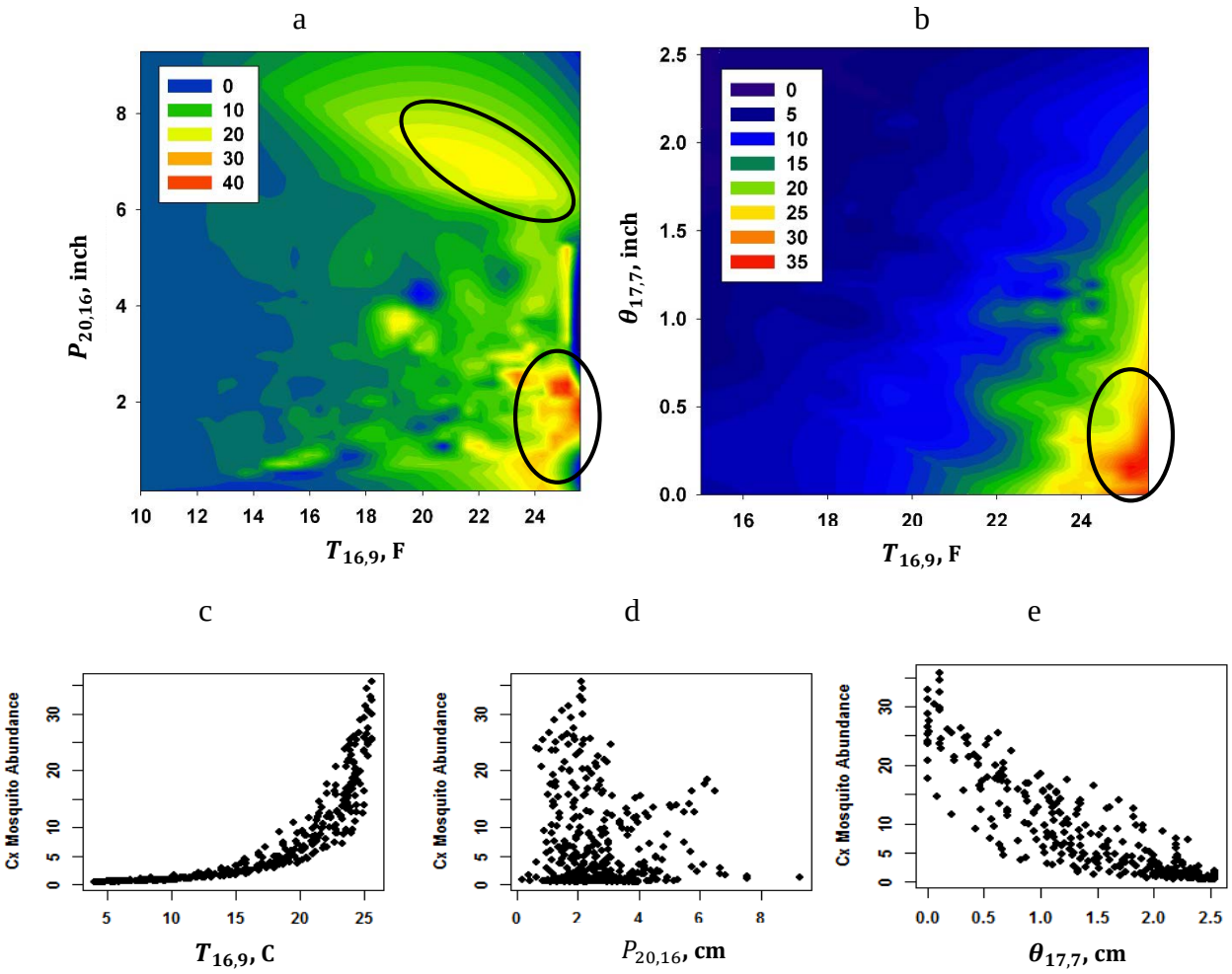

Figure 3.5. Predicted weekly female *Culex mosquito* abundance by fitted Poisson model versus climate variables. Highlighted regions correspond to high mosquito abundances.

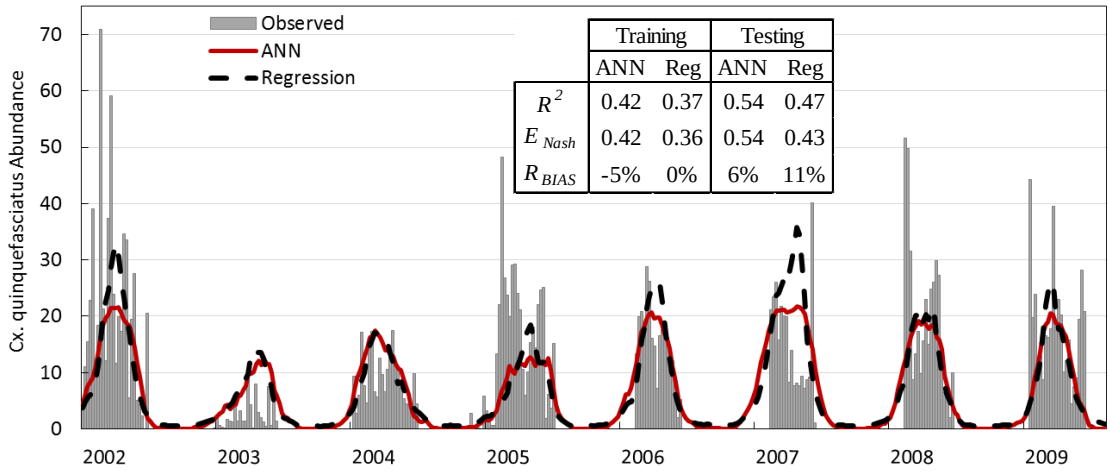

	Training		Testing	
	ANN	Reg	ANN	Reg
R^2	0.42	0.37	0.54	0.47
E_{Nash}	0.42	0.36	0.54	0.43
R_{BIAS}	-5%	0%	6%	11%

Figure 3.6. Comparison of predicted weekly *Culex* mosquito abundance by ANN and regression models vs observed data for the whole period (training + testing).

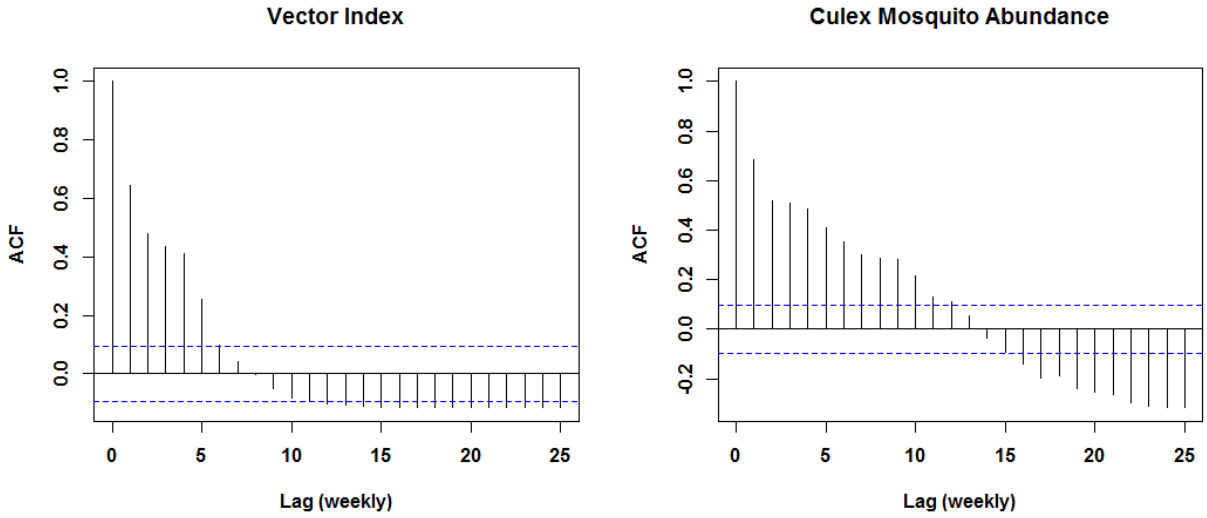

Figure 3.7. Autocorrelation function graphs of weekly *Culex* mosquito abundance and Vector Index

Input: Lagged climate data + $Mosq_{t-1}$

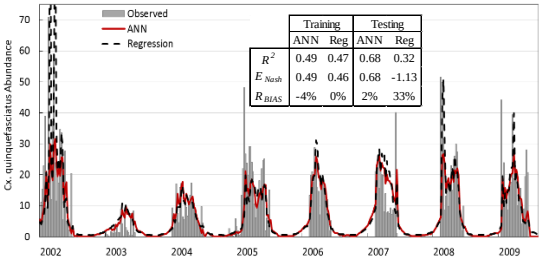

Input: Lagged climate data + $Mosq_{t-2}$

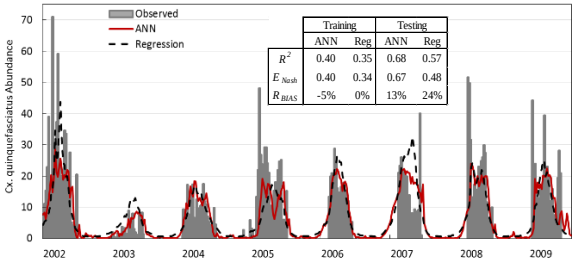

Input: Lagged climate data + $Mosq_{t-3}$

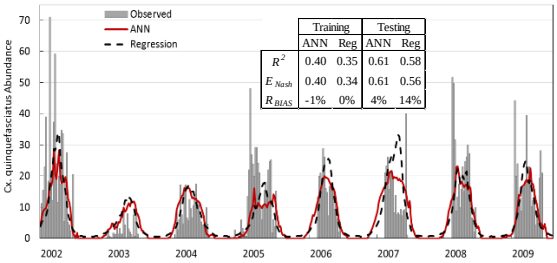

Input: Lagged climate data + $Mosq_{t-4}$

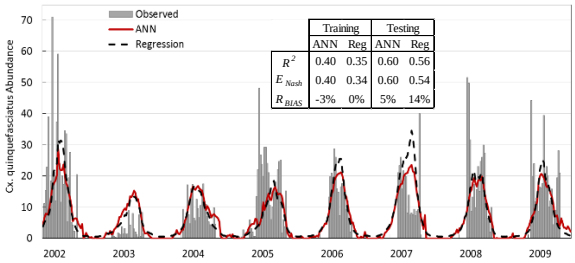

Input: Lagged climate data + $Mosq_{t-5}$

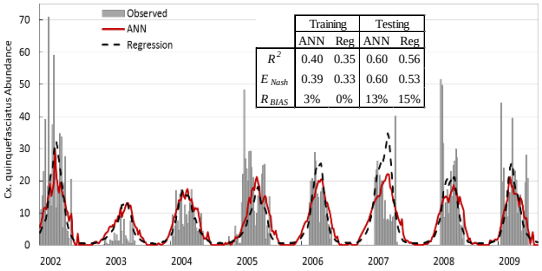

Input: Lagged climate data + $Mosq_{t-6}$

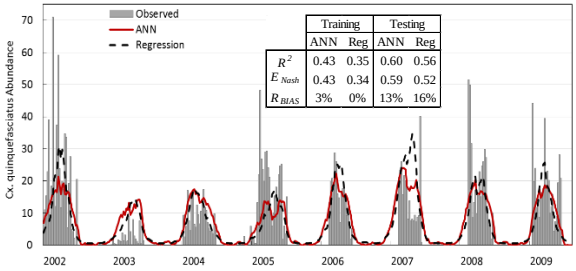

Input: Lagged climate data + $Mosq_{t-7}$

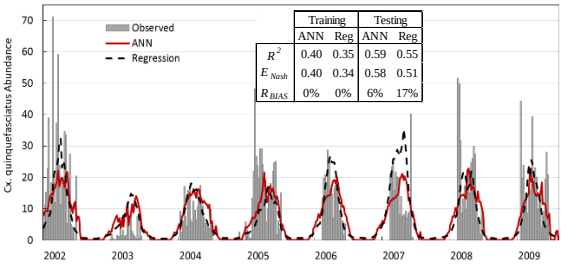

Input: Lagged climate data + $Mosq_{t-8}$

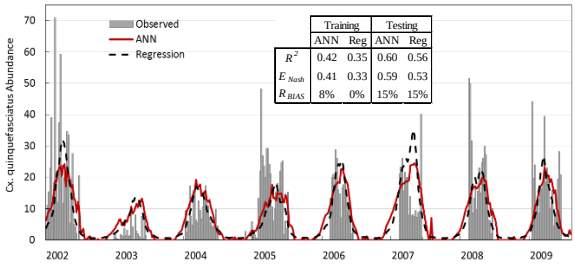

"Continued on next page."

Input: Lagged climate data + $Mosq_{t-9}$

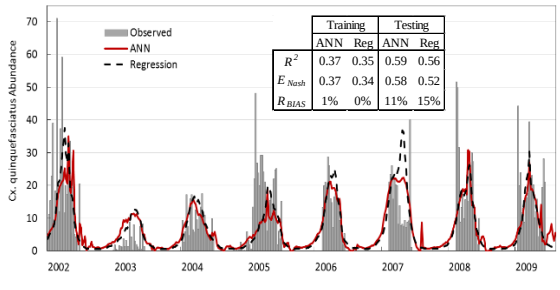

Input: Lagged climate data + $Mosq_{t-10}$

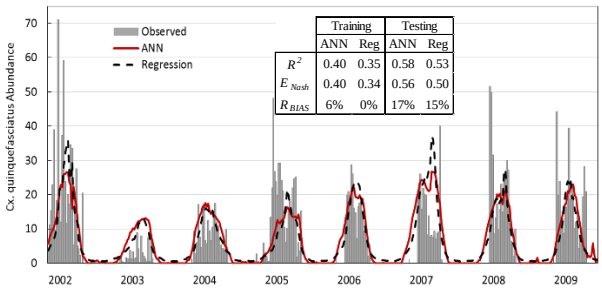

Figure 3.8. Time series of predicted weekly *Culex* mosquito abundance by ANN and regression models vs observed data using different antecedent values of mosquito abundance and lagged climate data as predictors for training and testing periods.

(a) Training period

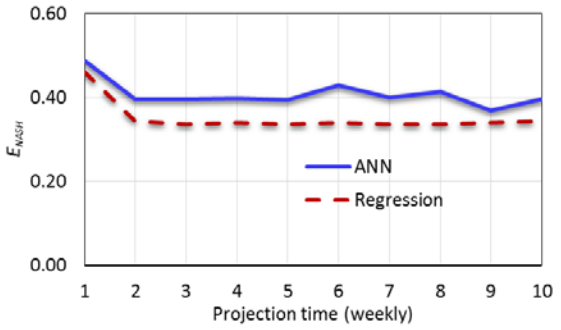

(b) Testing period

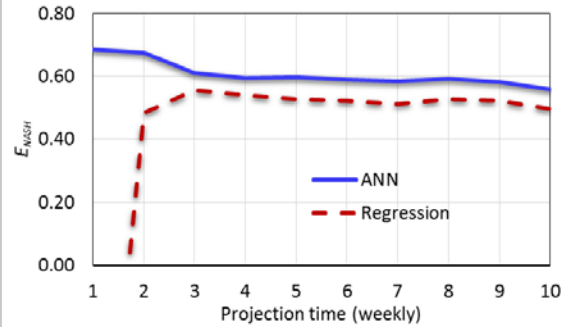

Figure 3.9. ANN and regression model performances built using lagged climate data and antecedent weekly *Culex* mosquito for (a) training period, and (b) testing period.

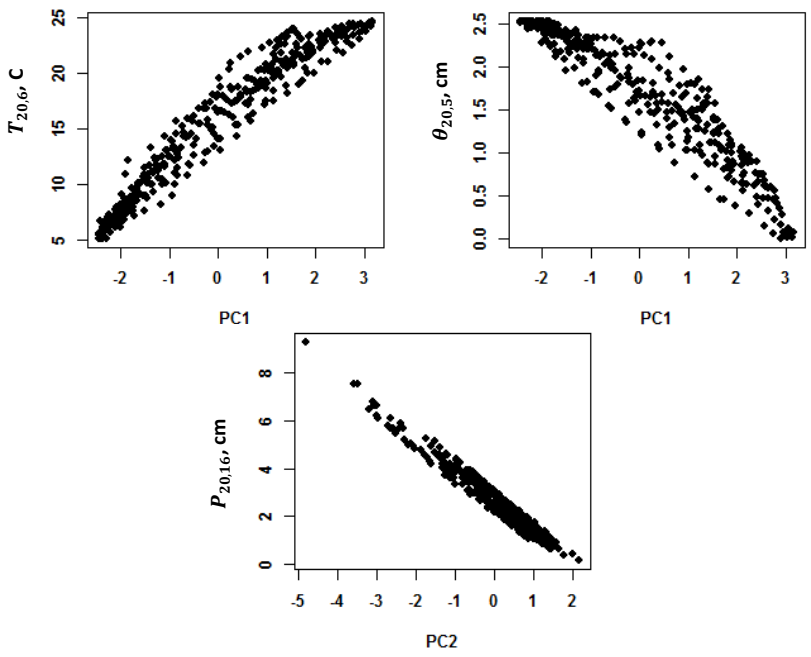

Figure 3.10. Graphs of climate variables versus each PC at weekly scale for Vector Index data.

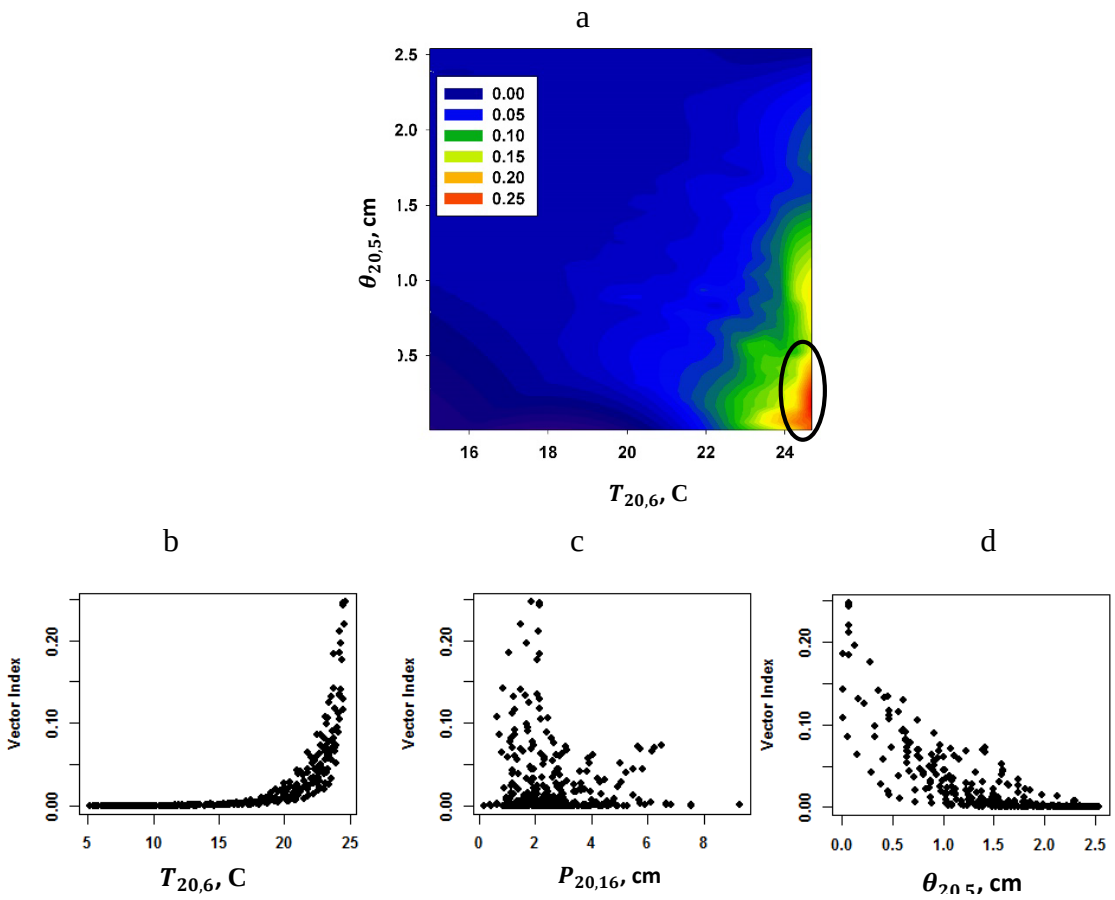

Figure 3.11. Predicted weekly Vector Index by fitted Poisson model versus climate variables. Highlighted region corresponds to high mosquito abundance.

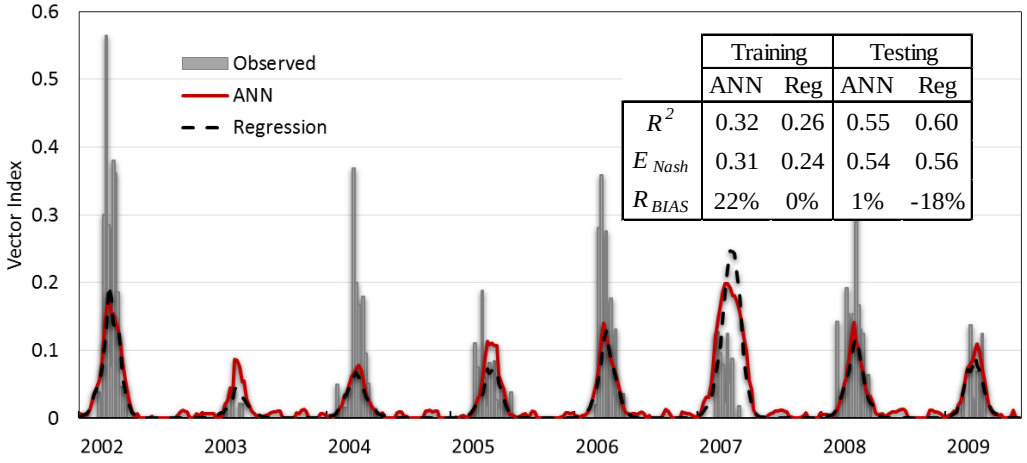

	Training		Testing	
	ANN	Reg	ANN	Reg
R^2	0.32	0.26	0.55	0.60
E_{Nash}	0.31	0.24	0.54	0.56
R_{BIAS}	22%	0%	1%	-18%

Figure 3.12. Comparison of predicted weekly Vector Index by ANN and regression models vs observed data for the whole period (training + testing).

Input: Lagged climate data + VI_{t-1}

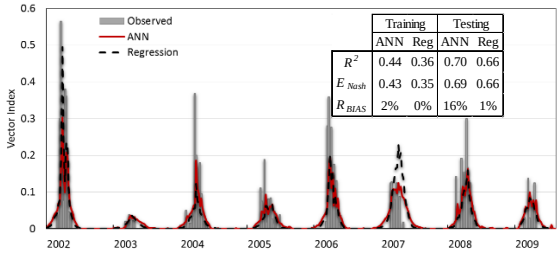

	Training		Testing	
	ANN	Reg	ANN	Reg
R^2	0.44	0.36	0.70	0.66
E_{Nash}	0.43	0.35	0.69	0.66
R_{BIAS}	2%	0%	16%	1%

Input: Lagged climate data + VI_{t-2}

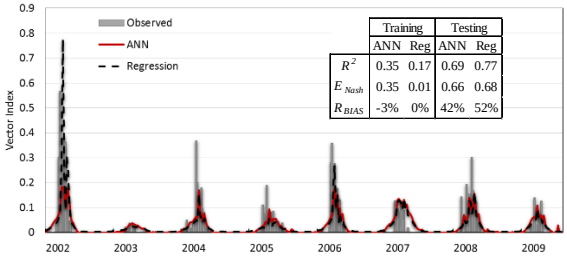

	Training		Testing	
	ANN	Reg	ANN	Reg
R^2	0.35	0.17	0.69	0.77
E_{Nash}	0.35	0.01	0.66	0.68
R_{BIAS}	-3%	0%	42%	52%

Input: Lagged climate data + VI_{t-3}

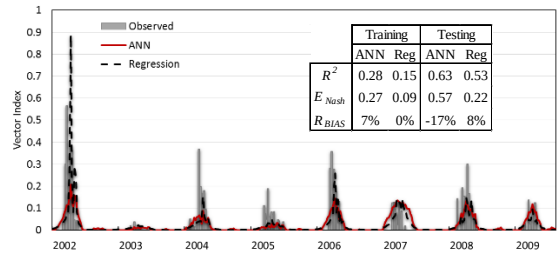

	Training		Testing	
	ANN	Reg	ANN	Reg
R^2	0.28	0.15	0.63	0.53
E_{Nash}	0.27	0.09	0.57	0.22
R_{BIAS}	7%	0%	-17%	8%

Input: Lagged climate data + VI_{t-4}

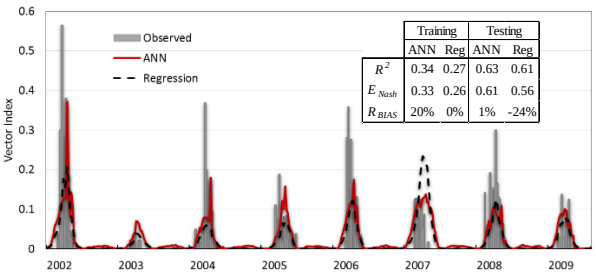

	Training		Testing	
	ANN	Reg	ANN	Reg
R^2	0.34	0.27	0.63	0.61
E_{Nash}	0.33	0.26	0.61	0.56
R_{BIAS}	20%	0%	1%	-24%

"*Continued on next page.*"

Input: Lagged climate data + VI_{t-5}

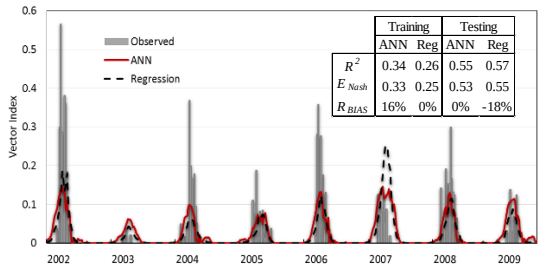

Input: Lagged climate data + VI_{t-6}

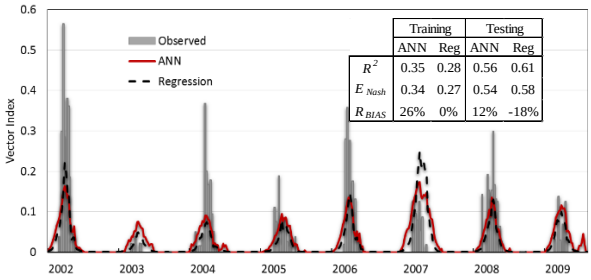

Input: Lagged climate data + VI_{t-7}

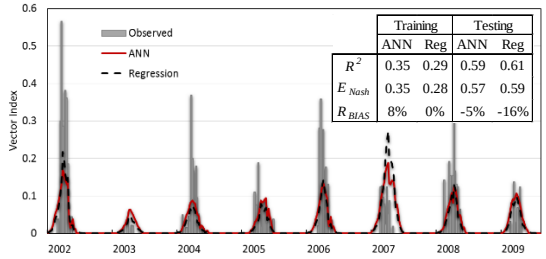

Input: Lagged climate data + VI_{t-8}

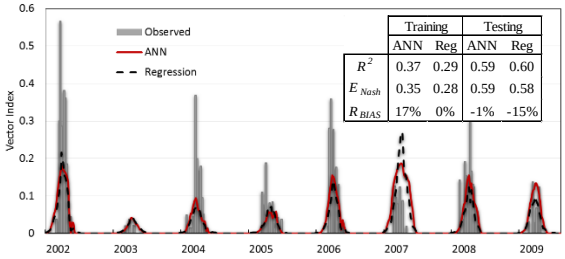

Input: Lagged climate data + VI_{t-9}

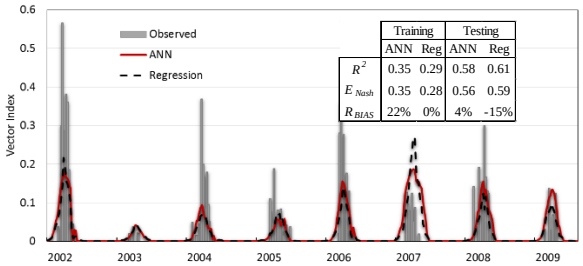

Input: Lagged climate data + VI_{t-10}

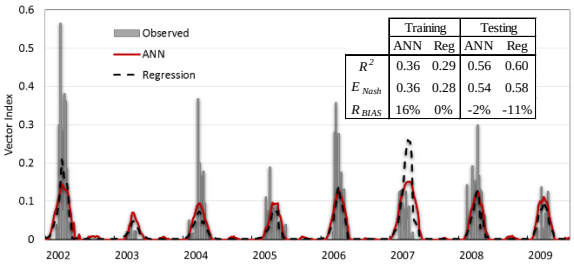

Figure 3.13. Time series of predicted weekly Vector Index by ANN and regression models vs observed data using different antecedent values of Vector Index and lagged climate data as predictors for training and testing periods.

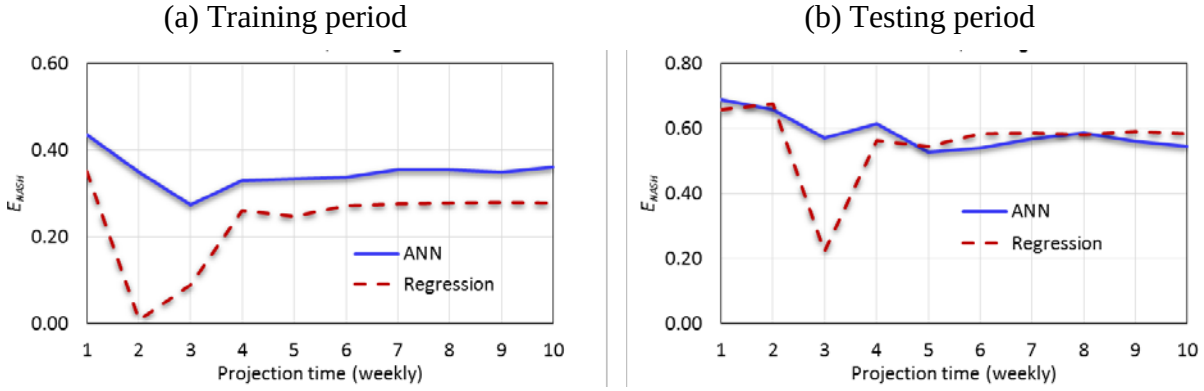

Figure 3.14. ANN and regression model performances built using lagged climate data and antecedent weekly Vector Index for (a) training period, and (b) testing period.

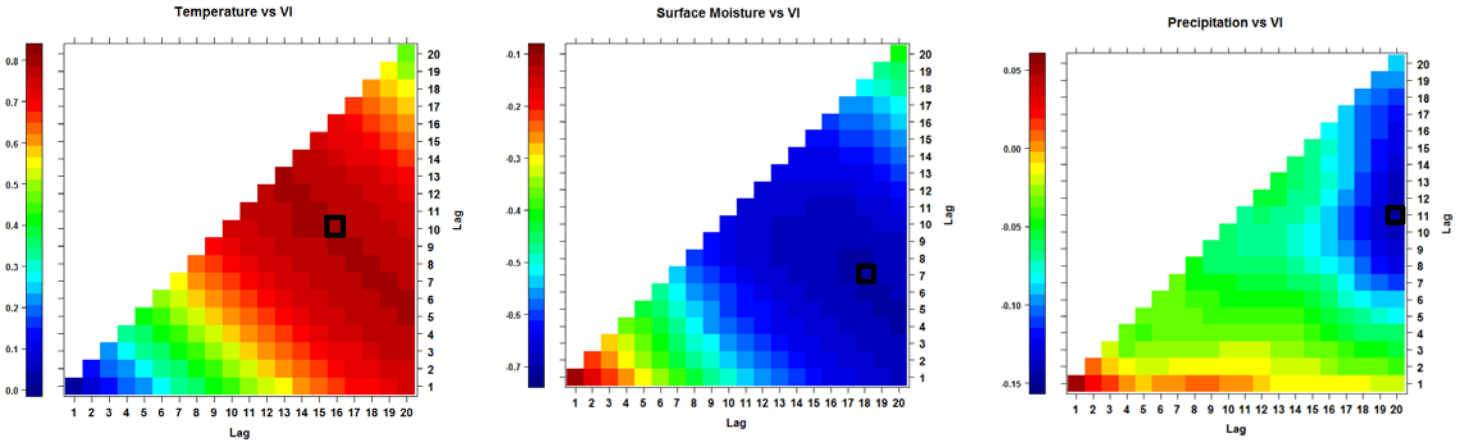

Temperature vs *Cx*. Mosquito Abundance

Surface Moisture vs *Cx*. Mosquito Abundance

Precipitation vs *Cx*. Mosquito Abundance

"Continued on next page."

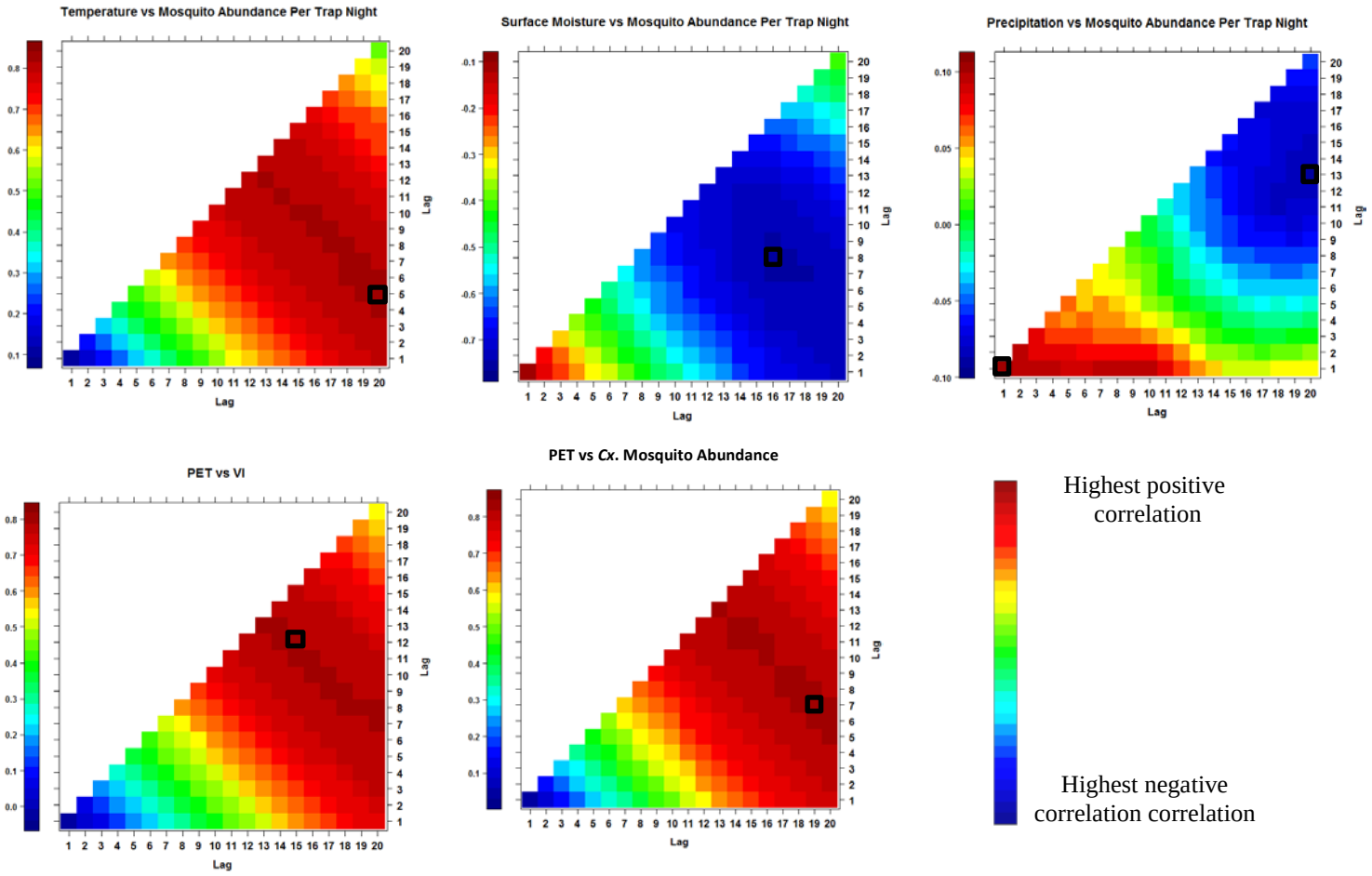

Figure 3.15. CCMs of four weeks moving average Vector Index and *Culex* mosquito abundance vs climate variables

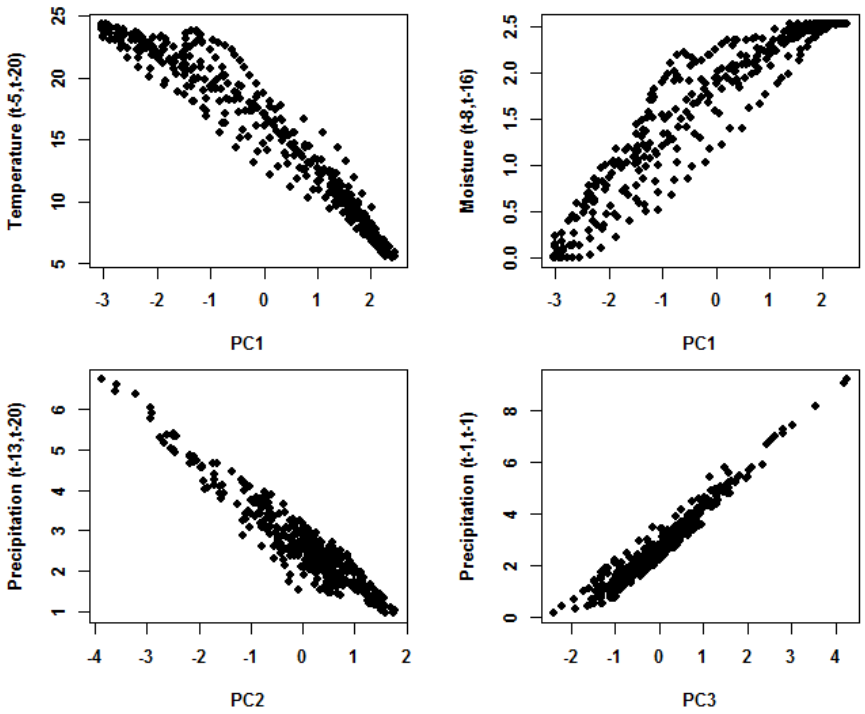

Figure 3.16. Graphs of climate variables versus each PC at four weeks moving average scale for *Culex* mosquito data.

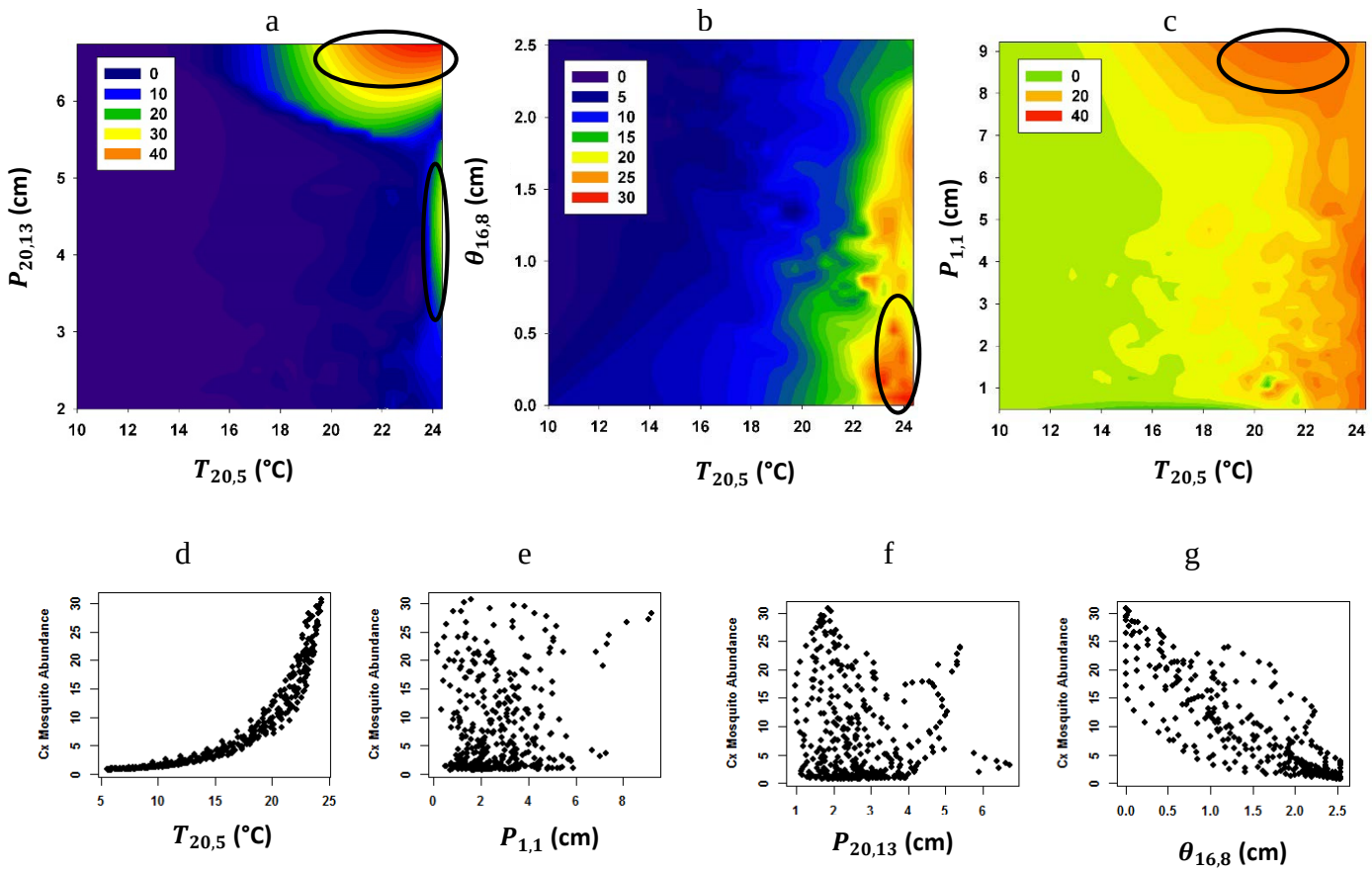

Figure 3.17. Predicted four weeks moving average female *Culex* mosquito abundance by fitted Poisson model versus climate variables. Highlighted regions correspond to high mosquito abundance.

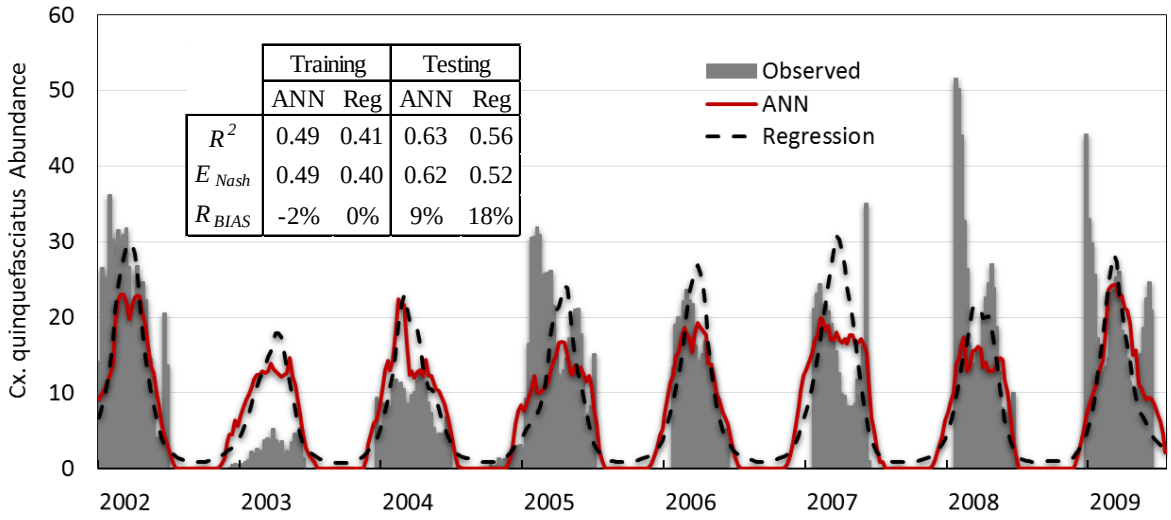

Figure 3.18. Comparison of predicted four weeks moving average *Culex* mosquito abundance by ANN and regression models vs observed data for the whole period (training + testing).

Input: Lagged climate data + $Mosq_{t-1}$

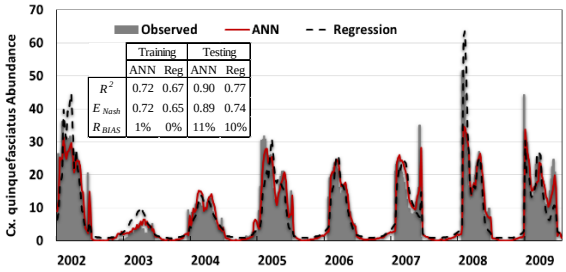

Input: Lagged climate data + $Mosq_{t-2}$

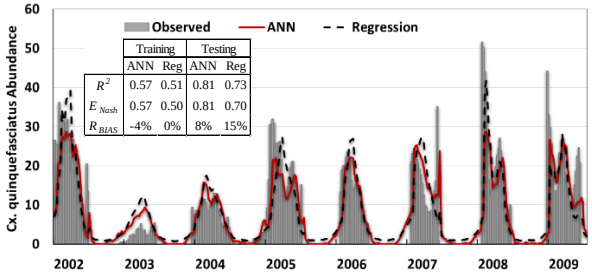

Input: Lagged climate data + $Mosq_{t-3}$

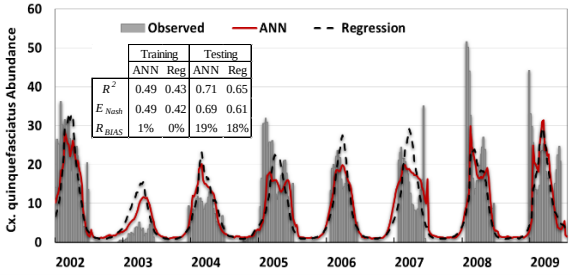

Input: Lagged climate data + $Mosq_{t-4}$

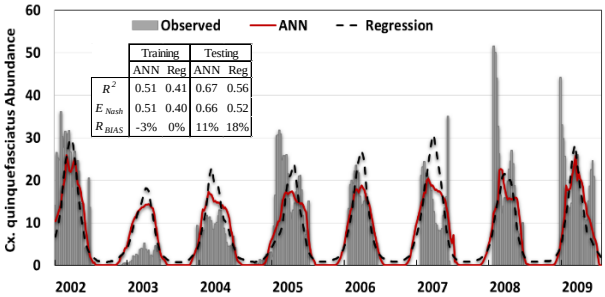

"Continued on next page."

Input: Lagged climate data + $Mosq_{t-5}$

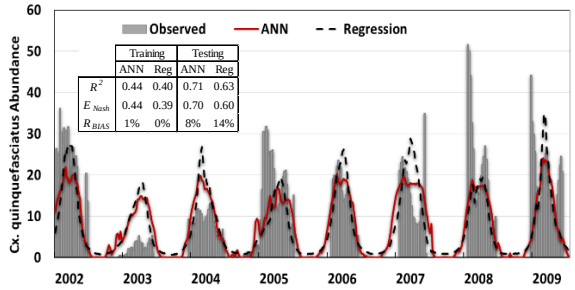

Input: Lagged climate data + $Mosq_{t-6}$

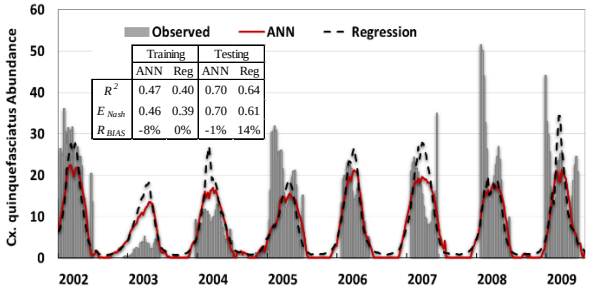

Input: Lagged climate data + $Mosq_{t-7}$

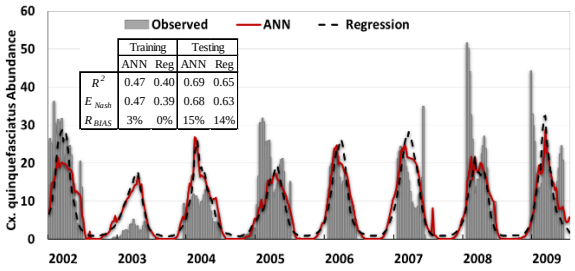

Input: Lagged climate data + $Mosq_{t-8}$

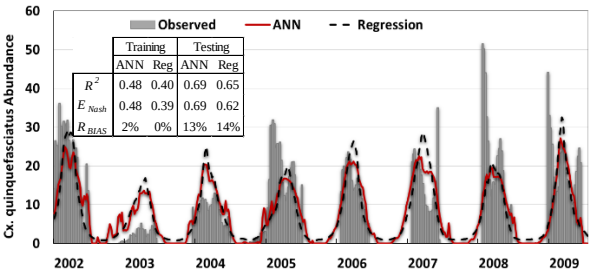

Input: Lagged climate data + $Mosq_{t-9}$

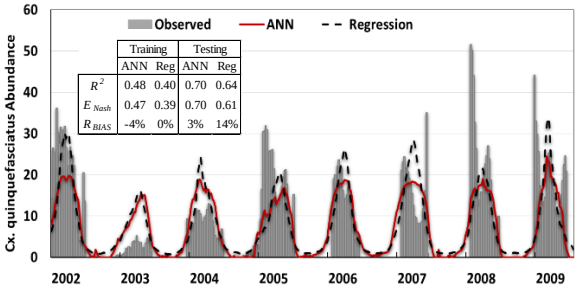

Input: Lagged climate data + $Mosq_{t-10}$

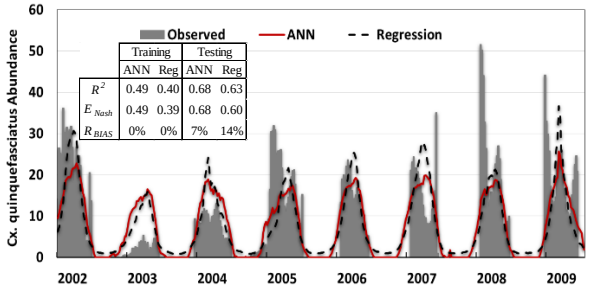

Figure 3.19. Time series of predicted four weeks moving average *Culex* mosquito abundance by ANN and regression models vs observed data using different antecedent values of mosquito abundance and lagged climate data as predictors for training and testing periods.

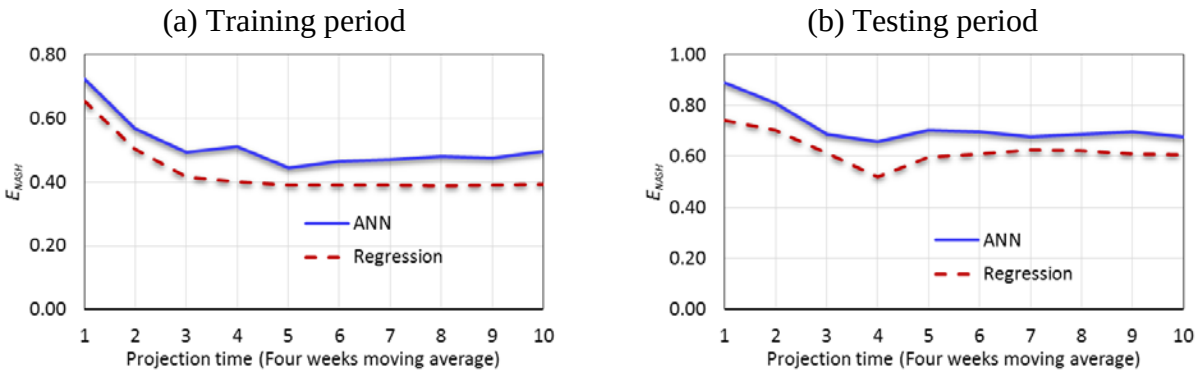

Figure 3.20. ANN and regression model performances built using interval lagged climate data and antecedent four weeks moving average *Culex* mosquito abundance for (a) training period, and (b) testing period.

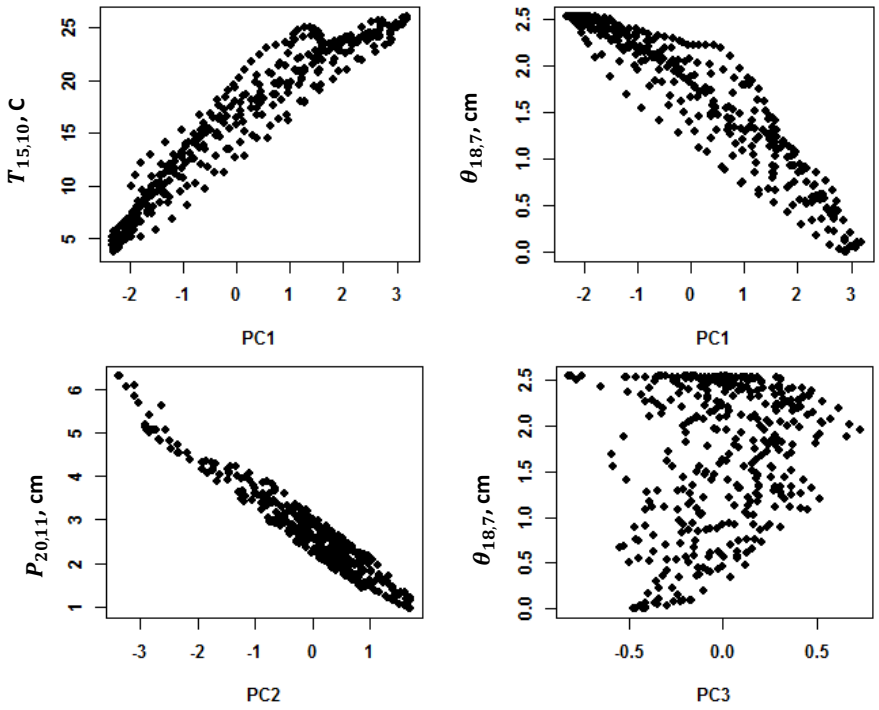

Figure 3.21. Graphs of climate variables versus each PC at four weeks moving average scale for Vector Index data.

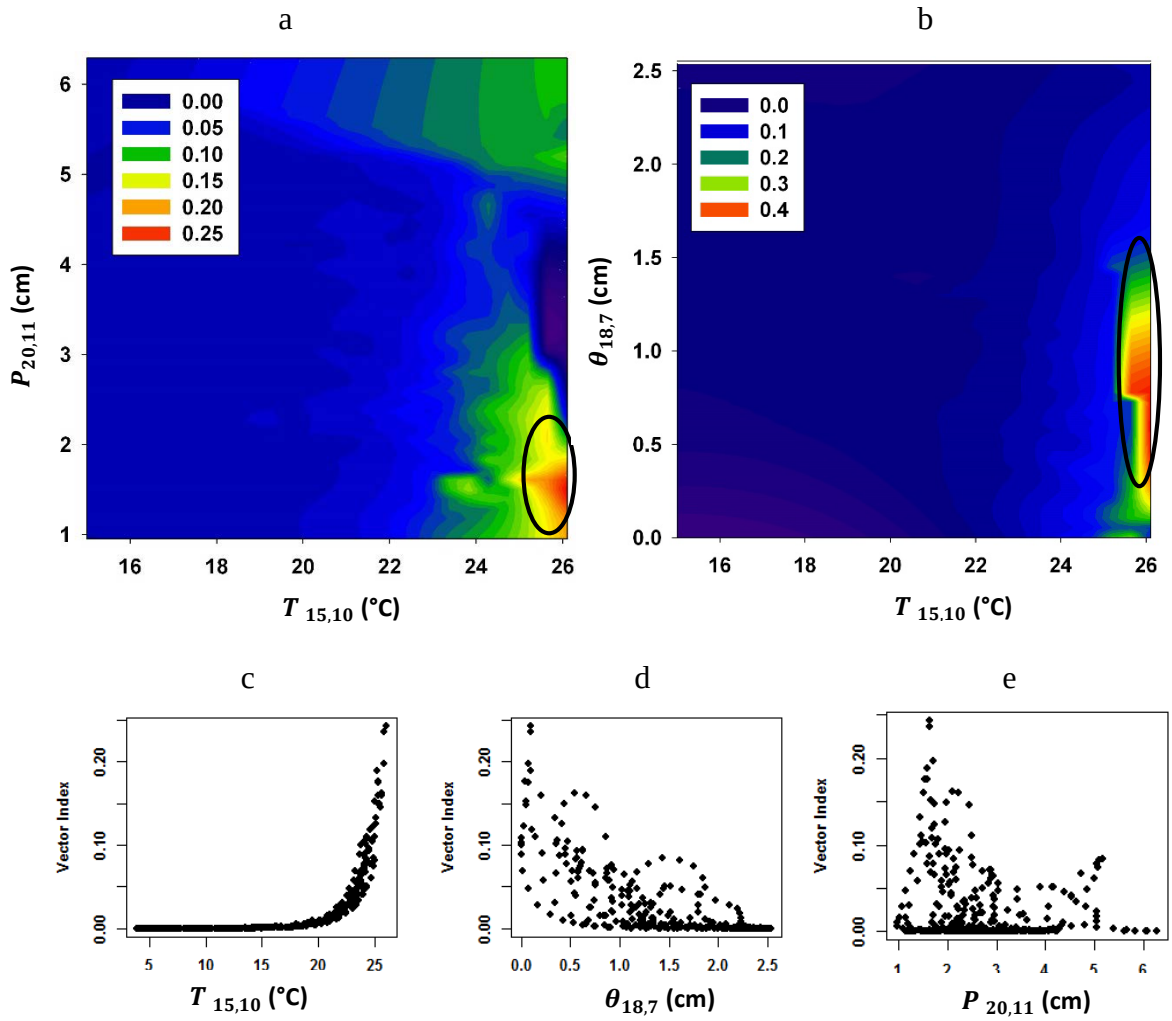

Figure 3.22. Predicted four weeks moving average Vector Index by fitted Poisson model versus climate variables. Highlighted regions correspond to high mosquito abundance.

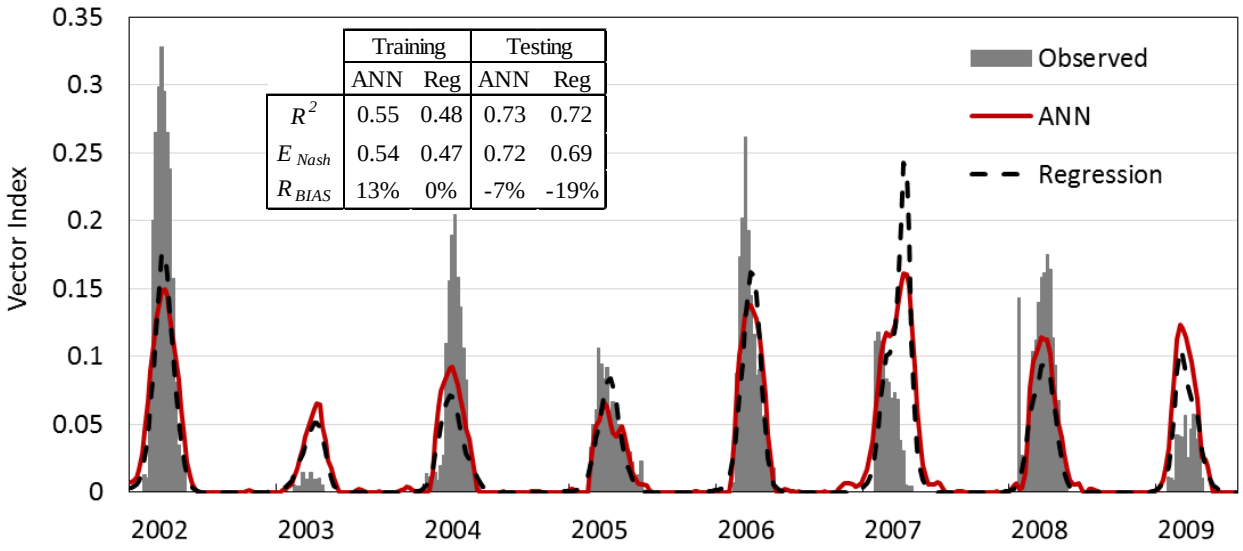

Figure 3.23. Comparison of predicted four weeks moving average Vector Index by ANN and regression models vs observed data.

Input: Lagged climate data + VI_{t-1}

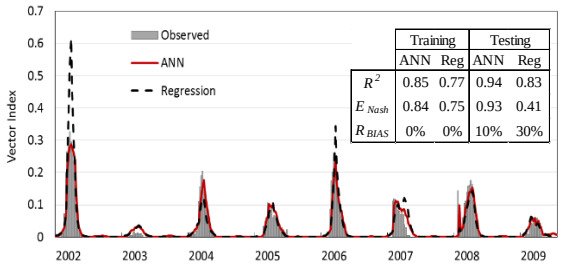

Input: Lagged climate data + VI_{t-2}

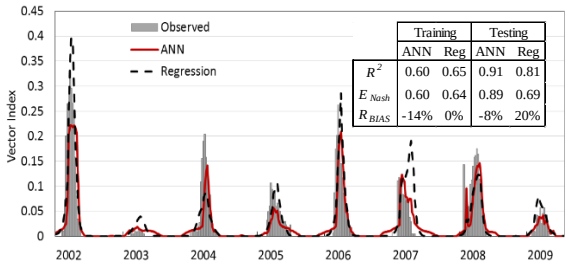

Input: Lagged climate data + VI_{t-3}

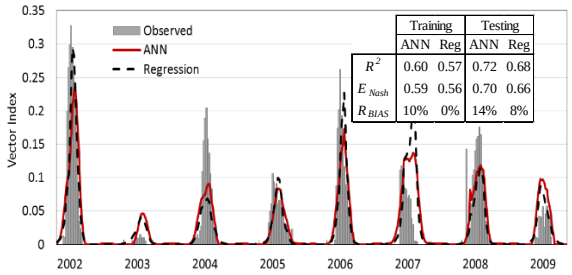

Input: Lagged climate data + VI_{t-4}

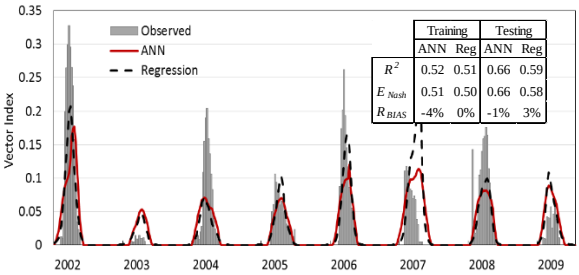

"Continued on next page."

Input: Lagged climate data + VI_{t-5}

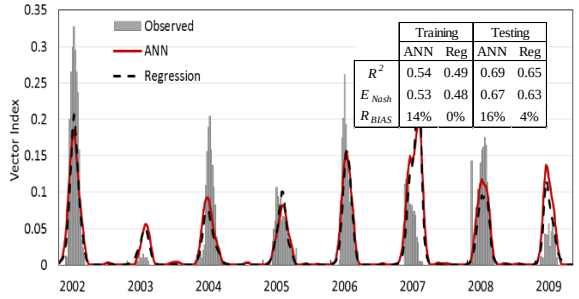

	Training		Testing	
	ANN	Reg	ANN	Reg
R^2	0.54	0.49	0.69	0.65
E_{Nash}	0.53	0.48	0.67	0.63
R_{BIAS}	14%	0%	16%	4%

Input: Lagged climate data + VI_{t-6}

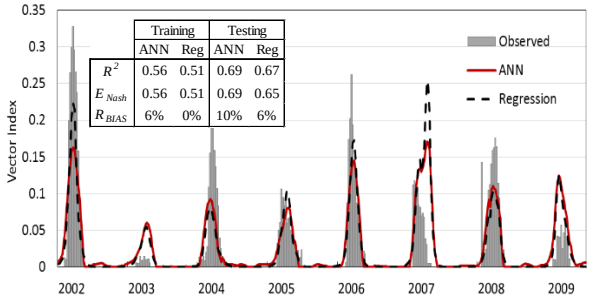

	Training		Testing	
	ANN	Reg	ANN	Reg
R^2	0.56	0.51	0.69	0.67
E_{Nash}	0.56	0.51	0.69	0.65
R_{BIAS}	6%	0%	10%	6%

Input: Lagged climate data + VI_{t-7}

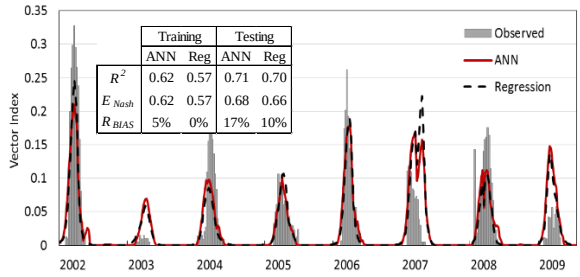

	Training		Testing	
	ANN	Reg	ANN	Reg
R^2	0.62	0.57	0.71	0.70
E_{Nash}	0.62	0.57	0.68	0.66
R_{BIAS}	5%	0%	17%	10%

Input: Lagged climate data + VI_{t-8}

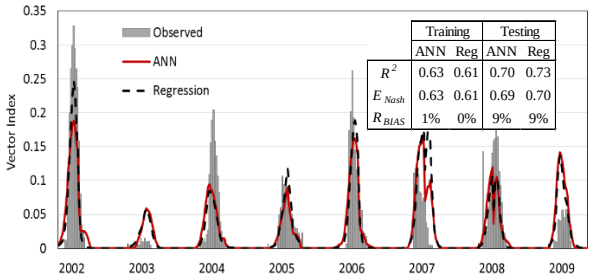

	Training		Testing	
	ANN	Reg	ANN	Reg
R^2	0.63	0.61	0.70	0.73
E_{Nash}	0.63	0.61	0.69	0.70
R_{BIAS}	1%	0%	9%	9%

Input: Lagged climate data + VI_{t-9}

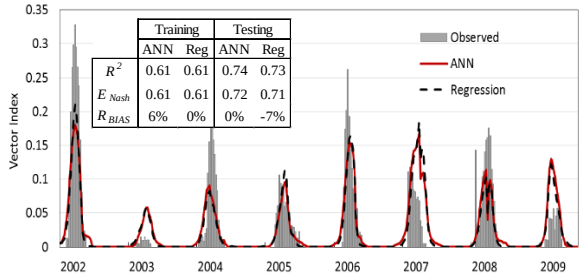

	Training		Testing	
	ANN	Reg	ANN	Reg
R^2	0.61	0.61	0.74	0.73
E_{Nash}	0.61	0.61	0.72	0.71
R_{BIAS}	6%	0%	0%	-7%

Input: Lagged climate data + VI_{t-10}

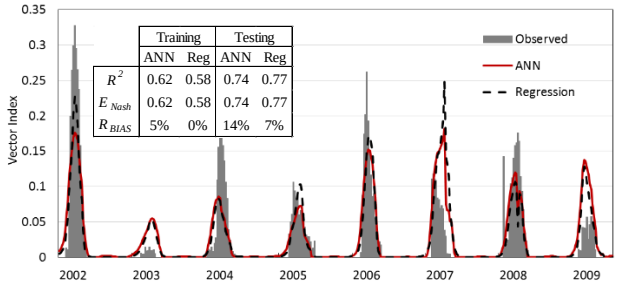

	Training		Testing	
	ANN	Reg	ANN	Reg
R^2	0.62	0.58	0.74	0.77
E_{Nash}	0.62	0.58	0.74	0.77
R_{BIAS}	5%	0%	14%	7%

Figure 3.24. Time series of predicted four weeks moving average Vector Index by ANN and regression models vs observed data using different antecedent values of mosquito abundance and lagged climate data as predictors for training and testing periods.

(a) Training period

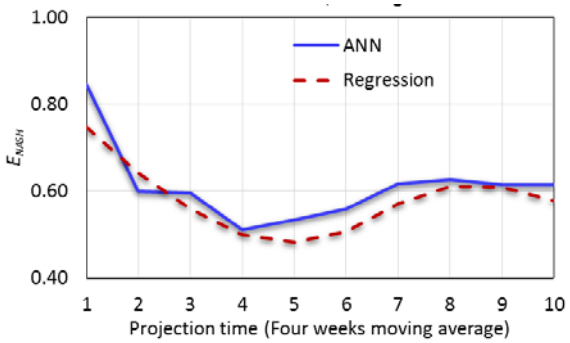

(b) Testing period

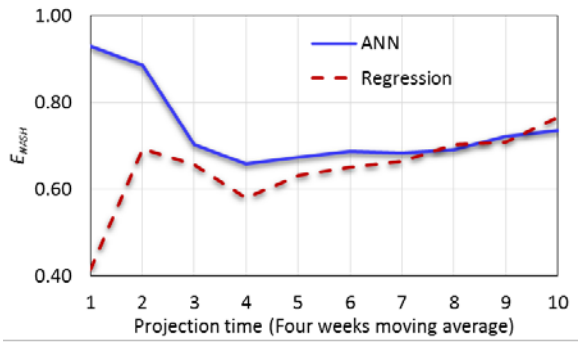

Figure 3.25. ANN and regression model performances built using interval lagged climate data and antecedent four weeks moving average Vector Index for (a) training period, and (b) testing period.

Chapter 4. Linkage between Land use/cover and water quality associated with *Culex quinquefasciatus* population in Atlanta, Georgia. U.S.A.

Abstract

Urban/suburban land use can enhance environmental conditions for the transmission of West Nile Virus. Forest to urban transition and consequently higher nutrient loads, could potentially increase the WNV risk. In the Atlanta area, high West Nile infection in humans, mosquitoes and birds reported in 2012 made this city a hotspot of WNV risk. Urbanization and shift from forest to urban in the region have increased nutrient loading into streams. Result of the mesocosm study in chapter 2 showed that depending on the type of nutrient, pre-adult mosquito abundance increases in waters with high nutrient levels. Around Atlanta, there are mosquito trap sites with high number of WNV positive pools that have no water quality data available. To examine the relationship between LULC and various water quality parameters and to predict water quality in unmonitored watersheds in the Atlanta area, an ANN-based model was applied. Streamflow and water quality data from neighboring U.S. Geological Survey (USGS) stations in the Atlanta area with *leave-one-site-out jackknifing* technique were used to build predictive models for PO_4, NH_4 and NO_3 loadings. ANN models were also developed for predicting streamflows during warm and cool seasons. First, flow was simulated using a quasi-distributed watershed model, Soil and water assessment tool (SWAT) and then the SWAT simulated flow was used as an input to ANN. NO_3,

NH_4 and PO_4 predictive models with best performance had E_{NASH} values of 0.99, 0.89, and 0.66 respectively and R_{BIAS} values of 8%, -6% and -7% respectively. No general trend was observed between percent imperviousness or percent forest cover or watershed size and the model performances. In addition, 62% of runs for predicting flow during cool season with E_{NASH} values of 0.82 to 0.50 and 83% of runs for predicting flow during warm season with E_{NASH} values of 0.79 to 0.56 had "good" to "very good" performance ratings. Coupling lumped models and semi-distributed watershed models helped to improve both ANN and the common practice of distributed model use. The developed models for predictions of water quality and streamflow in ungauged watersheds could have important implications for the control of West Nile Virus spread by *Culex* mosquito species. The findings of this study can help reduce the costs and efforts required for effective mosquito vector control by focusing on areas with lower water quality conditions.

***Keywords**:* Land use/cover (LULC), water quality, West Nile Virus, unmonitored watersheds.

Introduction

Culex quinquefasciatus, the southern house mosquito, is a cosmopolitan mosquito with worldwide distribution (Uttah et al., 2013) especially in the Southern United States and in urban area. It is a common urban mosquito (Barbosa and Regis, 2011) and also the major vector of West Nile Virus (WNV) which was detected in the United Stated in 1999. This species usually breeds in rich and polluted surface waters or artificial containers (Weinstein et al., 1997). Environmental

disturbances such as urbanization and deforestation play a key role in the emergence of many infectious diseases (Patz et al. 2004; Saleeza et al. 2011) through changing hydrological processes and water balance of river basins. Anthropogenic activities increase the number of artificial water collection reservoirs which are common aquatic habitats for *Culex quinquefasciatus* (Jacob et al. 2006, Gardner et al. 2013). Small, flooded depressions in the soil, tire tracks and shallow ditches are also suitable habitats for *Culex quinquefasciatus* (Jacob et al. 2006).

The prevalence and transmission of vector-borne pathogens are determined by the distribution and abundance of the primary vector (Reiter and LaPointe, 2007). To describe the spatial epidemiology of *Culex quinquefasciatus*, studying the spatial patterns of land cover and its impacts on hydrological factors are necessary. These parameters affect WNV risk because of their influences on mosquito habitat suitability, avian host communities and human exposure to infected mosquitoes (Chuang et al. 2012). Selection of mosquito breeding sites is the result of the recognition of physical and chemical key factors. This site selection is influenced by the presence of chemical substances of a wide range of origins (Bentley & Day 1989). Land use/ cover (LULC) changes and urbanization change concentrations of many water quality constituents due to altered sediment transport rate, chemical loads, and watershed hydrology. Urban/suburban land use can enhance environmental conditions for enzootic and bridge transmission of WNV to humans. Risk of human WNV cases is significantly associated with measures of urbanization and with percentage of forested or urban land (Brown et al., 2008). Agricultural lands and forest fragmentation significantly increase the probability of *Culex quinquefasciatus* mosquito capture

in mixed residential-agricultural community in Hawaii (Reiter and LaPointe, 2007). Forest habitat functions are source habitat for container breeding mosquito-predator communities. Connectivity of surface water in forest habitat affect the predator colonization rates (Weterings et al. 2014).

To assess the prevalence of vector-borne diseases within an area and to implement control measures, understanding the spatial and temporal dynamics of mosquito communities is vital (Buckner et al. 2010). Predicting insect abundance across a landscape is difficult (Liebhold et al. 1993, Ribeiro et al. 1996, Kitron 1998, Nansen et al. 2003); however, it can increase the efficiency and efficacy of management. Landscape characteristics for spatial prediction can be gained from existing GIS data and implemented to create target zones for management. This provides a mechanism to increase the focus of management efforts that are frequently limited by time and money. In Georgia and especially in the Atlanta metropolitan area, high West Nile infection in humans, mosquitoes and birds in 2012 reported by the Georgia Department of Public Health made Atlanta a hotspot of WNV risk. Urbanization and shifting from forest to urban in this area have increased nutrient loading into streams. As nutrients are limiting resources for bacteria and mosquitoes feed on bacteria, stream pollution is a major determinant of the abundance of mosquito vectors (Chaves et al. 2010; Calhoun et al. 2007). In this region, there are mosquito trap sites with high number of WNV positive pools that have no water quality data available. Most studies focused on trap sites near waste water treatment facilities and Combined Sewer Overflows (CSOs)-affected streams (Calhoun et al, 2007; Chaves et al. 2010; Lund et al. 2014). Nevertheless, CSOs are not the only *Culex quinquefasciatus* habitats and their development rate depends on the type

and amount of nutrients in a habitat. Our previous lab experiments indicated that emergence pattern of *Culex* mosquitoes are strongly related to certain nutrients such as NO_3, NH_4, and PO_4 and WNV risk remains even in the presence of larval habitats with low to moderate nutrient levels which are more common in the landscape than the levels characteristic of CSOs (Noori et al. 2015).

To predict water quality through the landscape in the Atlanta area under the impacts of different LULC types, modeling approaches are required. Identification and quantification of impacts of LULC changes on the hydrologic processes and water yield of a watershed and developing relationships between LULC and water quality parameters has been an area of interest to hydrologists in recent years (Paul and Meyer 2001; Kalin et al. 2010; Walsh et al. 2005, Tu 2011; Isik et al. 2012; Chadwick et. al.; 2012). Various statistical and conceptual models have been developed to help ecologists, urban planners, sociologists, administrators, and policy makers better understand the complexity of land use change patterns and evaluate the impacts of land use change on the environment, the latter of which requires large amount of data. Statistical techniques including regression models are overly simplistic and are constrained to a functional form between variables prior the analysis. On the other hand, watershed models require a lot of input data and model parameters that are often hard to predict (Palani et. al., 2008). Often, the data available to develop and apply predictive models are insufficient, even for small research catchments, which leads to the need for development of simplified models (Amiri et al. 2012).

Multivariate nature of water quality data, and a complicated nonlinear relation among the variables, make the statistical and watershed models less reliable (Chenini and Khemiri, 2009;

Nagy et. al., 2011). Due to the complexity of process of relating water quality to LULC changes using either deterministic or stochastic models, an artificial neural network (ANN) model has been applied in many studies (Ha et. al, 2003; Sahoo et. al., 2006; Singh et. al., 2009; Kalin et. al., 2010; Palani et. al., 2011; Gazzaz et. al., 2012; Isik et. al., 2012; Amiri et al. 2012). Such models have the ability to learn about the nonlinear relationships between the variables and to extract the relation between the inputs and outputs of a process without the need of a detailed understanding of its physical characteristics.

Kalin et al. (2010) developed an ANN-based model to examine the relationship between LULC and various water quality parameters and to predict water quality in unmonitored watersheds with similar characteristics. To predict water quality as a function of LULC in ungauged sites close to the mosquito trap sites in the Atlanta area, GA, Kalin et al. (2010) methodology was extended in this study. Streamflow and water quality data from neighboring USGS stations in the Atlanta area, GA were used to build the model. Streamflow was one of the input data to the model and since no streamflow data was available, a quasi-distributed watershed model, Soil and water assessment tool (SWAT), was applied to simulate streamflow. SWAT has been used widely for predicting streamflow under varying LULC and climate data (Dixon and Earls 2012; Shi et al. 2013; Fan and Shibata 2015; Glavan et al. 2015; Huang et al. 2015; Krysanova and Srinivasan 2015). However, since SWAT calibration is a complicated process and also time consuming, a separate ANN model was developed for predicting streamflow by using the SWAT simulated flow as an input to ANN. Coupling lumped and watershed models can help

overcome the limitations of each model and result in a stronger predictive model for streamflow. In this study, a hybrid model based on SWAT and ANN was developed and streamflow was first simulated by SWAT and the SWAT simulated flow was used as an input to ANN. This method reduces the time needed to calibrate and validate SWAT and also time needed to select the optimal input layer to ANN. It is hypothesized that the coupling SWAT and ANN improve the streamflow prediction accuracy and also the developed models for predicting the water quality constituents work better in urban watersheds.

Methodology

Study area and data

As WNV is endemic in Atlanta and mosquito and human cases have been reported continuously by the Georgia Department of Health since 2001, this area was selected as our case study. US Geological Survey (USGS) monitoring stations in and around the city of Atlanta, that have available water quality and instantaneous and daily streamflow data for the period 2001-2011 were considered in this study. Figure 4.1 shows the locations of selected USGS stations. Watershed areas vary from 3 to 552 km^2 and are located within the Fulton, DeKalb and Cobb counties in the state of Georgia. The study area is within the Southeastern Piedmont physiographic province of the USA. The city of Atlanta is one of the fastest growing metropolitan areas in the United States. The population of the metro area has more than tripled since the middle of the 20^{th} century, from the 1 million residents in 1950 to over 3 million by 2014, with no slowdown in sight (USGS, 2014).

The rapid development with a highly diverse LULC in this region makes it necessary to study its impact on hydrologic processes (Rose and Peters, 2001). Elevation in the study area ranges from about 157 to 513 meters above sea level. The dominant hydrologic soil group (HSG) is B which has moderate infiltration rates with silt loam to loam soil textures (Figure 4.2). The climate is warm and humid with mean annual temperature of ~16.5 °C and mean annual precipitation of ~120 cm. Dominant LULC types are impervious, evergreen forest, deciduous forest, mixed forest, pasture and urban grass, based on National Land Cover Database (NLCD, http://www.mrlc.gov/), in 2006. Summary of different LULC classes of the watersheds draining to the USGS stations shown in Figure 4.1 are given in Table 4.1. Percent imperviousness is within the range of 13%-52% and percent forest cover varies between 2% to 33%.

Water quality prediction

ANN is a black box type lumped model that has the ability to identify a relationship from given patterns which makes it possible to solve nonlinear models. ANNs can be categorized based on the direction of information flow and processing. In a feed-forward network, the connections between nodes are from an input layer, through one or more hidden layers, to an output layer (Dawson and Wilby, 2001). The most common method used to find the number of hidden layers and nodes is a trial-and-error approach (Kalin et al., 2010). In this study, the number of hidden neurons changed from 3 to 10, and number of hidden layer changed from 1 to 2. MATLAB version 7.10.0 (2010) was used for ANN model development, training and testing.

As the rates of most chemical reactions in natural waters increase with temperature (Chapra, 1997), a simplified temepratrue-dependant expression of the Arrhenius equation is used for observed values of water temperature as an input to ANN.

$$T_{eff} = \theta^{T_w - 20}$$

T_w is water temperature (°C) and θ is a dimensionless parameter which was assumed to be 1.05 in this study (Kalin et al., 2010). θ^{T_w} is the estimated Arrhenius coefficient (values above unity indicate a positive relation between the nutrient loss rate and temperature; values below unity indicate a negative relation) (Boyer et al., 2006). Water temperature was obtained from USGS stations or computed from average daily air temperature (Neitsch et al., 2005).

$$T_w = 5.0 + 0.75\,\bar{T}_{av}$$

$\bar{T}_{av}$, average daily air temperature (°C), was obtained from National Climatic Data Center (NCDC) stations in the city of Atlanta (Figure 4.1).

Nutrient loads per unit area (yield) (kg ha^{-1} d^{-1}) were calculated and used in the ANN network as outputs. Natural logarithms of water quality parameters were used in the network to avoid zero outputs (Kalin et al. 2010). All data were normalized within the range of 0.1 to 0.9 before training the network using the equation below:

$$z_i = 0.1 + 0.8\frac{(x_i - x_{min})}{(x_{max} - x_{min})}$$

where z_i is the normalized value, x_i is the log-transformed observed data point, and x_{max} and x_{min} are the minimum and maximum values among all the data points. Multiple ANN runs were

conducted for each nutrient using *leave-one-site-out jackknifing* technique (Sefick et al. 2015). For each run, out of n stations, one station was excluded for testing purposes and the model was trained to the remaining (n-1) stations. Model performances were assessed with the Nash–Sutcliffe efficiency (E_{NASH}) (Nash and Sutcliffe, 1970), and bias ratio (R_{BIAS}) (Salas et al., 2000). Moriasi et al. (2007) proposed some guidelines for the evaluation of model simulation related to streamflow, sediment and nutrients for a monthly time step. Considering that our time scale is smaller (daily), the adjusted ratings in evaluating the ANN model performance developed by Kalin et al. (2010) were adopted in this study:

Very good: $E_{NASH} \geq 0.70$; $|R_{BIAS}| \leq 0.25$

Good: $0.50 \leq E_{NASH} < 0.70$; $0.25 < |R_{BIAS}| \leq 0.50$

Satisfactory: $0.30 \leq E_{NASH} < 0.50$; $0.50 < |R_{BIAS}| \leq 0.70$

Unsatisfactory: $E_{NASH} < 0.30$; $|R_{BIAS}| > 0.70$

Streamflow prediction

SWAT is a quasi-distributed watershed model simulating the movement of water, sediment, nutrient, crop growth, nutrient cycling, etc. in a watershed. It is a conceptual hydrologic model, operating at daily and sub-daily steps (Arnold et al. 1998). SWAT has widely been used for assessing water resources and nonpoint source pollution problems. Input information for each sub-watershed includes weather, soil properties, topography, and vegetation. The sub-watersheds are divided to hydrologic response units or HRUs which are lumped land areas with unique land use, soil type and slope combinations.

SWAT considers watershed hydrology in two parts. The first part is composed of the watershed land areas that controls the water transported to the channels together with sediment, nutrients and pesticide in each sub-watershed. The second part includes the movement of water through the stream network to the watershed outlet (Cibin et al., 2010). The climatic variables required by SWAT include precipitation, temperature, wind speed, solar radiation and relative humidity. These data can be input to the model as observed data or generated during the simulation. Three potential evapotranspiration (PET) methods have been incorporated into SWAT: Penman–Monteith (Monteith 1965), Hargreaves (Hargreaves et al., 1985) and Priestley–Taylor (Priestley and Taylor 1972). Also, a data set of daily PET values can be supplied to the model if a different PET method is preferred. In this study, PET was calculated externally through the Hamon method (Hamon, 1961) and provided to the SWAT model as input. This method which has been shown to work well in the southeastern United States (Lu et al., 2005), calculates PET based on mean air temperature and hours of daylight for a given day. SWAT allows the user to specify a warm-up period during the simulation process to stabilize or calculate values that become initial values for the period of interest. In this study, one year was used as warm-up period.

LULC data from 2006 NLCD, soil data from Soil Survey Geographic Database (SURRGO, http://websoilsurvey.sc.egov.usda.gov/App/HomePage.htm), daily air temperature data from National Climatic Data Center (NCDC, http://www.ncdc.noaa.gov/), stations in Atlanta area and daily precipitation data from North American Land Data Assimilation Systems (NLDAS, http://ldas.gsfc.nasa.gov/index.php) were used as inputs to the SWAT model. To consider the

seasonal changes in vegetation and evapotranspiration and to study their impact on flow individually, the SWAT simulated flow was separated into cool and warm seasons. Warm season was considered to be May through October and cool season was considered to be November through April. To improve streamflow predictions, an ANN model was coupled with SWAT. This is a loose coupling where SWAT-simulated baseflow and direct flow are used as inputs to the ANN models. Separate ANN models were developed for cool and warm seasons. Multiple runs were conducted for each model using *leave-one-site-out jackknifing* technique.

Results

Water quality prediction

Different combinations of data were examined as input to the ANN model to identify the optimal input layer. For all three water quality parameters, combination of LULC, streamflow and temperature generated better results than other combinations. 15, 13 and 25 stations containing sampled NO_3, PO_4 and NH_4 data respectively, were used for prediction purposes. Data from all stations except one, were used for training the model and the one left was used for testing the developed model.

NO_3 prediction

Delineated watersheds of USGS stations that were used for predicting NO_3 load had low percentage of pasture and urban grass, between 0 to 1%, therefore they were not included in the

input group. Most watersheds were highly urbanized with percent imperviousness of 18% to 51%. 15 sets of run were conducted for NO_3 prediction and each time one watershed was excluded for testing and 14 watersheds were considered for training the model. E_{NASH} values are given in Figure 4.3 for each run. Average E_{NASH}, and absolute R_{BIAS} values over all 15 runs were 0.89 and 7% respectively. Overall, the model performances were "very good". Log scale scatterplots of simulated versus observed NO_3 loadings for all runs are shown in Figure 4.4. Based on the scatter plots, the runs for the test watersheds #2336644, #2336517 and #2336240 had the best performances with E_{NASH} values of 0.99, 0.99 and 0.98 and R_{BIAS} values of 8%, -12% and -6% respectively. The area of these watersheds varied from 10 to 71 km^2. In terms of LULC, they have 21% to 45% Imperviousness and 4% to 25% forest cover. The instantaneous NO_3 loading value ranged from 0 to 4.5 kg ha^{-1} d^{-1} among these three watersheds. To visualize the selected model performances, the log scaled load duration curve of observed versus simulated NO_3 are given in Figure 4.5. Since these watersheds are mostly urbanized, the developed models work better in the developed watershed. Figure 4.6 shows no general trend between percent forest or imperviousness or size of the test watershed and relative E_{NASH} values.

NH_4 prediction

25 USGS stations which had available NH_4 data were used for developing the predictive model (Table 4.1). The watershed sizes varied from 3 to 552 km^2 and with the percent imperviousness of 13% to 52%. Total forest cover for these watersheds ranged from 2% to 33%.

25 models were developed and the E_{NASH} was estimated to measure the performance of each model (Figure 4.7). Averages of E_{NASH} and absolute R_{BIAS} values for the 25 runs were 0.62 and 14% respectively. The overall performance rating of models varied from "good" to "very good". Considering the scatter plots of ANN generated versus observed NH_4 loadings for each station (Figure 4.8), models developed for testing USGS stations #2207185, #2207220, and #2207385 with E_{NASH} values of 0.89, 0.88, and 0.86, and R_{BIAS} values of -6%, -5% and -8% respectively had the highest performance accuracy. The test watersheds relative to these models had 16% to 21% imperviousness and 24% to 30% forest cover. The area of these watersheds varied from 26 to 552 km^2. Also, NH_4 loadings ranged from 0 to 0.48 kg ha^{-1} d^{-1}. The log scaled load duration curves of observed versus simulated NH_4 for the models with the best performance are given in Figure 4.9. There is no general trend between percent LULC types in a watershed and its developed predictive model accuracy. The model performances do not decrease or increase with changing the percentage development or forest cover in the test watersheds (Figure 4.10). However, in the model with the lowest performance accuracy, Station #2207400, 11% of the test watershed is covered by pasture. This indicates that the developed models do not predict NH_4 loadings for pastoral watersheds with an acceptable level of accuracy.

PO_4 prediction

Out of 29 USGS stations, 13 stations with sampled unfiltered PO_4 and measured streamflow data available for the period 2005-2011 were used to develop an ANN predictive model. The area

of these watersheds ranged from 3 to 420 km^2 with the percent imperviousness of 13% to 52% and percent forest cover of 2% to 33%. All the stations are located in the Gwinnett County. 13 runs were conducted and the model performances are given in Figure 4.11. The performance ratings of 10 out of 13 models varied from "satisfactory" to "good". Average values of E_{NASH} and absolute value of R_{BIAS} among 13 models were 0.43 and 17% respectively. Considering these values and also looking at the scatter plots of observed versus ANN generated PO_4 loadings (Figure 4.12), three models with best performances were those developed for stations #2208150, #2334578, and #2336030. The E_{NASH} values of these three models were 0.66, 0.65 and 0.50 respectively and their R_{BIAS} values were -7%, -23% and -0.17% respectively. The log scaled load duration curves of observed versus ANN generated PO_4 of these three test watersheds are given in Figure 4.13. The area of these watersheds varied from 4 to 80 km^2. In terms of LULC, they had 13% to 52% imperviousness and 2% to 26% forest cover. No trends were identified between percent imperviousness or forest cover or size of test watersheds and the relative model performance (Figure 4.14). Among 13 developed ANN models, the watershed with the highest percent forest cover had the lowest E_{NASH} value and under prediction at -44%. Also watershed #2207400, with 11% pasture cover, had a weak performance too. This indicates that the developed models work better for urbanized watersheds.

Streamflow prediction

In order to predict water quality in ungauged watersheds, streamflow data as an input was needed. Therefore, An ANN model was developed based on the neighboring watersheds delineated for USGS to predict streamflow in unmonitored watersheds. The streamflow was simulated using the SWAT model first and was used as an input to ANN. No calibration or sensitivity analysis was conducted for SWAT. SWAT simulated baseflow and directflow of 29 USGS stations were fed to the ANN model as inputs to predict the observed daily streamflow. Two sets of runs for warm and cool seasons were developed and in each set, 29 runs were conducted using *one-site-out jackknifing* technique. In each run, data of 28 sites were used for training the model and one station left out, was used for testing the developed model. Note that each run corresponds to a different ANN model where one of the 29 sites was tested. Out of the total 29 runs, two of them had E_{NASH} values below zero during cool season simulations. Those two are not shown on the figures for clarity (Figure 4.15). Overall, 62% of runs for predicting flow during the cool season and 83% of runs for predicting flow during the warm season had “good” to “very good” performance ratings. The average E_{NASH} and absolute R_{BIAS} values during the warm season runs were 0.59 and 14% respectively and during the cool season runs were 0.55 and 9% respectively. The top 10 runs with best prediction accuracy were selected for each season and the scatter plots of observed versus ANN generated daily streamflow of the related watersheds are given in Figure 4.16. For the warm season (Figure 4.16 (a)), there were two outliers that were removed from the scatter plot.

During the warm season, test watersheds of the top 10 models with the high performance had the percent imperviousness of 13% to 52% and percent forest cover of 2% to 33%. The area of these watersheds varied from 4 to 90 km^2. During the cool season, the area of test watersheds of the top 10 models varied from 4 to 69 km^2 with 13% to 52% imperviousness and 2% to 25% forest cover. Developed models for warm season performed better than those for cool seasons as predicted values are close to 1:1 line, except a few values which are underestimated (Figure 4.16). Since most of selected watersheds are urbanized, the ANN predictive models worked better for developed watersheds. In general, as the percent forest cover or the area of test watershed increased, the model performances gradually decreased for both warm and cool season predictions. Also, the test watershed with higher percent imperviousness had a better model performance for the cool season flow prediction. This indicates that the developed models work better in urbanized watersheds with the size of 200 km^2 or less (Figure 4.17).

Discussion

This study provides further evidence that ANNs can predict water quality loadings in ungauged watersheds using data from the neighboring watersheds with similar characteristics. This approach has been previously demonstrated for west Georgia by Kalin et al. (2010) and Isik et al. (2012). In the present study, similar model was developed for water quality prediction in the Atlanta metropolitan area and also ANN was run several times for each nutrient using *leave-one-site-out jackknifing* technique. The inputs to the water quality models were streamflow, water

temperature and LULC percentages. The main purpose was to predict NO_3, NH_4 and PO_4 loadings for rivers passing by mosquito trap sites around the Atlanta area, and also to link the predicted water quality parameters to *Culex quinquefasciatus* abundance for the future work. The developed ANN models could predict NO_3 and NH_4 loadings with "good" to "very good" level of accuracy. The developed models for PO_4 loadings under-predicted the peak observed values with the performance rate of "satisfactory" to "good" which could be due to the flashy behavior of the watersheds and lack of flow measurement during high-flow periods. For missing instantaneous flow data, average daily streamflow from USGS discharge was used as input to ANN.

In addition, ANN and SWAT were combined to predict streamflow using the SWAT simulated flow. By coupling ANN and SWAT a hybrid approach was introduced for predicting daily streamflow in unmonitored watersheds. Combining ANN and SWAT could enrich the modeling environment by excluding the calibration and sensitivity analysis to adjust the SWAT model parameters and by narrowing down the number of inputs to ANN. SWAT outflow was the only input to ANN and in each run a watershed was left out for testing the model. The information and knowledge obtained from each model, were coupled together and facilitated addressing the problem and predicting the streamflow. Since in this approach, SWAT was not calibrated, the proposed method also can help parameter transferability. Assume SWAT was calibrated and validated in the neighboring watersheds. To apply the calibrated model to an ungauged nearby watershed having similar characteristics, the developed model parameters need to be transferred to the target watershed (Wang et al. 2014). SWAT-ANN could be considered another

regionalization approach to predict flow in ungauged watersheds because it uses all the information from nearby watersheds and comes up with a universal model. The developed ANN models for predicting flow during warm and cool seasons had “good” to “very good” accuracy in most test watersheds. The developed models in this study work better in an urban watershed than a forested watershed, which would be helpful for linking streams water quality conditions near mosquito trap sites in the Atlanta area to the *Culex* mosquito population.

Although artificial intelligence techniques usually provide appropriate efficiency despite data shortage in a watershed, the performance of these models is highly dependent upon utilizing patterns in their training, and if an event was beyond their training scope, the performance of the model would be extremely poor at predicting the required phenomenon (Jajarmizadeh et al. 2015). In this study, the SWAT model calibration was aided by incorporating ANN and combining ANN and SWAT resulted in a stronger and with higher accuracy predictive model for streamflow.

Conclusions

The developed models for predictions of water quality and streamflow in ungauged watersheds could have important implications for the control of West Nile Virus spread by *Culex* mosquito species. Since water quality sampling for a large area is time consuming and expensive, predictive models provide a revolutionary techniques to estimate water quality for the area of interest. However, how accurate and reliable the models are always the major discussion. Results of this study reveals that if water quality and LULC data are available from neighboring watersheds

with similar characteristic, a predictive model for unmonitored watersheds with an acceptable level of accuracy can be developed if streamflow data exist or can be estimated. In this study, we were able to generate daily streamflow by coupling SWAT and ANN models. This helps to predict continuous water quality data in the Atlanta area. However, wherever observed instantaneous streamflow data was missing, average daily flow for USGS stations were used, which can cause error in our prediction. Having more reliable streamflow data, and also providing a more accurate LULC map instead of NLCD, can improve the model performance. Also predicting nutrient concentrations instead of loadings could be the next step of this study.

The findings of this study can help reduce the costs and efforts required for effective mosquito vector control by focusing on areas with lower water quality conditions. However, water quality is one of the environmental factors affecting mosquito development. A broader study needs to be conducted to combine the different risk factors and to investigate their impacts on transmission of WNV for future studies.

References

Amiri, B.J., Sudheer, K.P., Fohrer, N., 2012. Linkage between in-stream total phosphorus and land cover in Chugoku district, Japan: an ANN approach. J. Hydrol. Hydromech. 60 (1), 33–44.

Arnold, J.G., Srinivasan, R., Muttiah, R.S., Williams, J.R. 1998. Large area hydrologic modeling and assessment: part I. Model development. JAWRA. 34 (1), 73–89.

Barbosa, R.M.R., Regis, L.N. 2011. Monitoring temporal fluctuations of *Culex quinquefasciatus* using oviposition traps containing attractant and larvicide in an urban environment in Recife, Brazil. Mem Inst Oswaldo Cruz, Rio de Janeiro, Vol. 106(4): 451-455.

Boyer, E.W., Alexander, R.B., Patron, W.J., Li, Ch., Butterbach-Bahi, K., Donner, S.D., Skaggs, R.W., Del Grosso, S.J. 2006. Modeling denitrification in terrestrial and aquatic ecosystems at regional sales. Ecol. Appl. 16 (6), 2123-2142.

Brown, H.E., Childs, J.E., Diuk-Wasser, M.A., Fish, D. 2008. Ecological factors associated with West Nile Virus transmission, northeastern United States. Emerg Infect Dis. Vol. 14, No. 10. 1539-1545.

Buckner, E.A., Blackmore, M.S., Golladay, S.W., Covich, A.P. 2010. Weather and landscape factors associated with adult mosquito abundance in southwestern Georgia, U.S.A. J Vector Ecol. 36(2): 269-278.

Calhoun, L.M., Avery, M., Jones, L., Gunarto, K., King, R., Roberts, J., Burkot, T.R. 2007. Combined Sewage Overflows (CSO) Are Major Urban Breeding Sites for *Culex quinquefasciatus* in Atlanta, Georgia. Am. J. Trop. Med. Hyg. 77: 478–484.

Chadwick, M.A., Thiele, J.E., Huryn, A.D., Benke, A.C., Dobberfuhl, D.R. 2012. Effects of urbanization on macroinvertebrates in tributaries of the St. Johns River, Florida, USA. Urban Ecosyst, Springer. 15:347-365.

Chapra, S.C. 1997. Surface water quality modeling. McGraw-Hill, New York.

Chaves, L.F., Keogh, C.L., Nguyen, A.M., Decker, G.M., Vazquez-Prokopec, G.M., Kitron, U.D. 2010. Combined sewage overflow accelerates immature development and increases body size in the urban mosquito *Culex quinquefasciatus*. J Appl. Entomol. 135: 611–620.

Chenini, I. and Khemiri, S. 2009. Evaluation of ground water quality using multiple linear regression and structural equation modeling. Int. J. Environ. Sci. Tech. 6 (3), 509-519.

Chuang, T.W., Ionides, E.L., Knepper, R.G., Stanuszek, W.W., Walker, E.D., Wilson, M.L. 2012. Cross-Correlation Map analyses show weather variation influences on mosquito abundance patterns in Saginaw County, Michigan, 1989–2005. J Med Entomol, 49(4):851-858.

Cibin, R., Sudheer, K.P., Chaubey, I. 2010. Sensitivity and identifiability of stream flow generation parameters of the SWAT model. Hydrol. Process. 24(9): 1133–1148.

Dawson, C.W., and Wilby, R.L. 2001. Hydrologic modeling using artificial neural networks. Prog. Phys. Geog. 25 (1), 80-108.

Dixon, B., and Earls, J. 2012. Effects of urbanization on streamflow using SWAT with real and simulated meteorological data. Applied Geography, 35, 174-190.

Fan, M., and Shibata, H. 2015. Simulation of watershed hydrology and stream water quality under land use and climate change scenarios in Teshio River watershed, northern Japan. Ecological Indicators, 50: 79-89.

Gardner, A.M., Anderson, T.K., Hamer, G.L., Johnson, D.E., Varela, K.E., Walker, E.D., Ruiz, M.O. 2013. Terrestrial vegetation and aquatic chemistry influence larval mosquito abundance in catch basins, Chicago, USA. Parasit Vectors. 6:1-11.

Gazzaz, N.M., Yusoff, M.K., Aris, A.Z., Juahir, H., Ramli, N.F. 2012. Artificial neural network modeling of the water quality index for Kinta River (Malaysia) using water quality variables as predictors. Mar Pollut Bull. 64(11):2409-20.

Glavan, M. Ceglar, A. Pintar, M. 2015. Assessing the impacts of climate change on water quantity and quality modelling in small Slovenian Mediterranean catchment lesson for policy and decision makers. Hydrol. Process. John Wiley & Sons, Ltd.

Ha, H., Stenstrom, M.K. 2003. Identification of land use with water quality data in stormwater using a neural network. Water Res. 37, 4222-4230.

Hamon, W.R. 1961. Estimating potential evapotranspiration. Journal of Hydraulics Division, Proceedings of the American Society of Civil Engineers. 871: 107–120

Hargreaves, G. L, Hargreaves G. H., Riley, J.P. 1985. Agricultural benefits for Senegal River basin. J. Irrig. Drain. Eng, ASCE. 111(2): 113–124.

Huang, J., van den Dool, H., Georgakakos, K.P., 1996. Analysis of model-calculated soil moisture over the United States (1931-93) and application to long-range temperature forecasts. J. Clim. 9(6): 1350-1362.

Isik, S., Kalin, L., Schoonover, J., Srivastava, P., Lockaby, B.G. 2012. Modeling Effects of Changing Land Use/Cover on Daily Streamflow: An Artificial Neural Network and Curve Number based Hybrid Approach. J. Hydrol. 485: 103-112.

Jacob, B.G., Shililu, J. , Muturi, E.J., Mwangangi, J.M., Muriu, S.M., Funes, J., Githure, J., Regens, J.L., Novak, R.J. 2006. Spatially targeting *Culex quinquefasciatus* aquatic habitats on modified land cover for implementing an Integrated Vector Management (IVM) program in three villages within the Mwea Rice Scheme, Kenya. Int J Health Geogr. 5: 1-9.

Jajarmizadeh, M., Lafdani, E.K., Harun, S., Ahmadi, A. 2015. Application of SVM and SWAT models for monthly streamflow prediction, a case study in south of Iran. KSCE Journal of Civil Engineering, 19(1):345-357.

Kalin, L., Isik, S., Schoonover, J.E., Lockaby, B.G. 2010. Predicting Water Quality in Unmonitored Watersheds Using Artificial Neural Networks. JEQ. 39(4):1429-1440.

Kitron, U. 1998. Landscape ecology and epidemiology of vector-borne diseases: tools for spatial analysis. J. Med. Entomol. 35: 435-445.

Krysanova, V. and Srinivasan, R. 2015. Assessment of climate and land use change impacts with SWAT. Reg Environ change, 15:431-434.

Liebhold, A. M., R. E. Rossi, and W. P. Kemp. 1993. Geostatistics and geographic information systems in applied insect ecology. Annu. Rev. Entomol. 38: 303-327

Lu, J., Sun, G., McNulty, S.G., Amatya, D.M., 2005. A comparison of six potential evapotranspiration methods for regional use in the Southeastern United States. J. Am. Water Resour. Assoc. JAWRA. 41 (3), 621-633.

Lund, A., McMillan, J., Kelly, R., Jabbarzadeh, Sh., Mead, D.G., Burkot, Th.R., Kitron, U.D., Vazquez-Prokopec, G.M. 2014. Long term impacts of combined sewer overflow remediation on water quality and population dynamics of *Culex quinquefasciatus*, the main urban West Nile virus vector in Atlanta, GA. Environ. Res. 129: 20-26.

Monteith, J. L. 1965. Evaporation and the environment. In The State and Movement of Water in Living Organisms. 19th Symp Soc Exp Biol. Cambridge University Press. Cambridge, U.K. 205–234.

Moriasi, D.N., Arnold, J.G., Van Liew, M.W., Bingner, R.L., Harmel, R.D., Veith, T.L. 2007. Model evaluation guidelines for systematic quantification of accuracy in watershed simulations. Trans. ASABE. 50:885–900.

Neitsch, S.L., Arnold, J.G., Kiniry, J.R., Williams, J.R., King, K.W. 2005. Soil and water assessment toll theoretical documentation. Version 2005. Temple, TX.

Nagy, C., Lockaby, B.G., Kalin, L., Anderson, C. 2011. Effects of Urbanization on Stream Hydrology and Water Quality: The Florida gulf Coast, Hydrol. Process. 26:2019-2030.

Nansen, C., Campbell, J. F., Phillips, T.W., Mullen, M.A. 2003. The impact of spatial structure on the accuracy of contour maps of small data sets. J. Econ. Entomol. 96:1617-1625.

Nash, J.E., and Sutcliffe, J.V. 1970. River flow forecasting through conceptual models: Part I. A discussion of principles. J. Hydrol. 10:282–290.

Noori, N., Lockaby, G.B., Kalin, L. 2015. Larval development of *Culex quinquefasciatus* in water with low to moderate pollution levels. J. Vector Ecol. Vol. 40 (2).

Patz, J.A., Daszak, P., Tabor, G.M., Aguirre, A.A., Pearl, M., Epstein, J., Wolfe, N.D., Kilpatrick, A.M., Foufopoulos, J., Molyneux, M., Bradley, D.J. 2004. Unhealthy landscape: policy recommendations on land use change and infectious disease emergence. Environ. Health Perspect. 112: 1092-2098.

Palani, S., Liong, Sh-Y., Tkalich, P. 2008. An ANN application for water quality forecasting. Mar Pollut Bull, Elsevier. 56:1586-1597.

Palani, S., Tkalich, P., Balasubramanian, R., Palanichamy, J. 2011. ANN application for prediction of atmospheric nitrogen deposition to aquatic ecosystems. Mar Pollut Bull, Elsevier. 62, 1198–1206.

Paul, M.J. and Meyer, J.L. 2001. Streams in the urban landscape. Annu. Rev. Ecol. Syst. 32: 333-365.

Priestley, C.H.B., Taylor, R. J. 1972. On the assessment of surface heat flux and evaporation using large-scale parameters. Mon. Wea. Rev. 100(2): 81–92.

Reisen, WK., Milby, M.M., Meyer, R.P., Pfuntner, A.R., Spohele, J., Hazerlrigg, J.E., Webb, J.P. 1991. Mark-release-recapture studies with Culex mosquitoes (Diptera: Culicidae) in Southern California. J Med Entomol. 28(3):357-71.

Reisen, WK., Milby, M.M., Meyer, R.P. 1992. Population dynamics of adult Culex mosquitoes (Diptera Culicidae) along the Kern River, Kern County, California, in 1990. J Med Entomol. 29(3): 531-543.

Reiter, M. and LaPointe, D.A. 2007. Landscape factors influencing the spatial distribution and abundance of Mosquito Vector *Culex quinquefasciatus* (Diptera: Culicidae) in a mixed residential–agricultural community in Hawai‘i. J. Med. Entomol. 44(5): 861-868.

Ribeiro, J.M.C., Seulu, F., Abose, T., Kidane, G., Teklehaimanot, A. 1996. Temporal and spatial distribution of anopheline mosquitoes in an Ethiopian village: implications for malaria control strategies. Bull. W.H.O. 74: 299-305.

Rose, S., Peters, N.E., 2001. Effects of urbanization on streamflow in the Atlanta area (Georgia, USA): a comparative hydrological approach. Hyrol Process, 15, 1441-1457.

Sahoo, G.B., Ray, C., De Carlo, E.H. 2006. Use of neural network to predict flash flood and attendant water qualities of a mountainous stream on Oahu, Hawaii. J. Hydrol. 327, 525-538.

Salas, J.D., M. Markus, and A.S. Tokar. 2000. Streamflow forecasting based on artificial neural networks. p. 23–51. In R.S. Govindaraju and A.R. Rao (ed.) Artificial neural networks in hydrology. Kluwer Academic, Dordrecht, the Netherlands.

Saleeza, S.N.R., Norma-Rashid, Y., Azirun, M.S. 2011. Mosquitoes larval breeding habitat in urban and suburban areas, Peninsular Malaysia. WASET. 58: 569-573.

Sefick, S.A., Kalin, L., Kosnicki, E., Schneid, B.P., Jarrell, M.S., Anderson, Ch.J., Paller, M.H., Feminella, W., 2015. Emperical estimation of stream discharge using channel gemoerty in low-gradient, sand-bed streams of the Southeastern plains. JAWRA.

Shi, P., Ma, X., Hou, Y., Li, O., Zhang, Zh., Qu, S., Chen, Ch., Cai, T., Fang, X. 2013. Effects of Land-Use and Climate Change on Hydrological Processes in the Upstream of Huai River, China. Water Resour Manage. 27:1263-1278.

Singh, K.P., Basant, A., Malik, A., Jain, G. 2009. Artificial neural network modeling of the river water quality: A case study. Ecol. Model. 220:888–895.

Tu, J. 2011. Spatial and temporal relationships between water quality and land use in northern Georgia, USA. J Integr. Environ. Sci. 8: 151-170.

U.S. Geological Survey, 2014. The effects of urbanization on water quality: population growth.

Uttah, E.,C., Wokem, G.N., Okonofua, Ch. 2013 .The Abundance and Biting Patterns of *Culex uinquefasciatus* Say (Culicidae) in the Coastal Region of Nigeria. Hindawi Publishing Corporation, ISRN Zoology. Volume 2013, Article ID 640691, pages: 1-7.

Walsh, A.S., Glass, G.E., Lesser, C.R., Curriero, F.C. 2008. Predicting seasonal abundance of mosquitoes based on off-season meteorological conditions. Environ Ecol Stat. 15:279–291.

Weinstein, P., Laird, M., Browne, G. 1997. Exotic and endemic mosquitoes in New Zealand as potential arbovirus vectors. Wellington, Ministry of Health.

Weterings, R., Umponstira, Ch. Buckley, H.L. 2014. Container-breeding mosquitoes and predator community dynamics along an urban-forest gradient: The effects of habitat type and isolation. Basic Appl. Ecol. 15. 486-495.

Wang, R., Kalin, L., Kuang, W., Tian, H. 2013. Individual and combined Effects of land use/cover and climate change on Wolf Bay watershed streamflow in southern Alabama. Hydrol Process. 28, 5530-5546.

Table 4.1. Watershed characteristics of selected USGS sites.

								Number of Samples		
Station ID	IM	DF	EF	MF	PA	UG	Area (km^2)	NO_3	PO_4	NH_4
2203603	46%	4%	5%	0%	0%	0%	6	70	-	21
2203655	36%	7%	8%	1%	0%	0%	58	143	-	40
2203700	34%	7%	4%	1%	2%	0%	27	110	-	19
2205522	28%	5%	9%	0%	1%	1%	19	-	39	35
2207120	23%	10%	10%	0%	1%	1%	420	-	48	95
2207185	16%	12%	17%	0%	4%	0%	26	-	49	97
2207220	21%	12%	12%	0%	2%	1%	552	-	-	57
2207385	16%	8%	17%	0%	6%	2%	45	-	54	101
2207400	16%	6%	13%	1%	11%	4%	21	-	57	95
2208150	18%	15%	11%	1%	6%	4%	80	-	46	102
2217274	14%	20%	5%	0%	7%	4%	3	-	55	93
2218565	17%	17%	6%	1%	2%	2%	15	-	49	92
2334480	13%	24%	9%	0%	2%	3%	24	-	59	95
2334578	13%	19%	6%	0%	4%	3%	13	-	58	
2334885	18%	21%	8%	1%	5%	1%	122	-	53	107
2335350	37%	7%	5%	0%	1%	1%	23	-	55	99
2335870	20%	8%	13%	1%	1%	0%	80	121	-	104
2336030	52%	2%	0%	0%	0%	0%	4	-	57	94
2336120	30%	6%	9%	0%	0%	0%	90	113	-	35
2336240	24%	8%	9%	1%	0%	0%	71	112	-	33
2336300	31%	6%	8%	1%	0%	0%	225	115	-	38
2336313	51%	8%	2%	0%	0%	1%	7	93	-	93
2336360	26%	8%	10%	1%	0%	0%	69	124	-	32
2336410	22%	12%	12%	1%	0%	0%	98	116	-	31
2336517	45%	2%	2%	0%	0%	0%	20	32	-	
2336526	34%	7%	6%	0%	1%	1%	35	100	-	26
2336658	18%	11%	11%	1%	0%	0%	17	45	-	
2336728	18%	16%	16%	1%	0%	0%	88	88	-	24
2336644	21%	7%	18%	0%	0%	1%	10	27	-	-

** IM= imperviousness, DF: Deciduous Forest, EF: Evergreen Forest, MF: Mixed Forest, PA: Pasture, UG, Urban Grass*

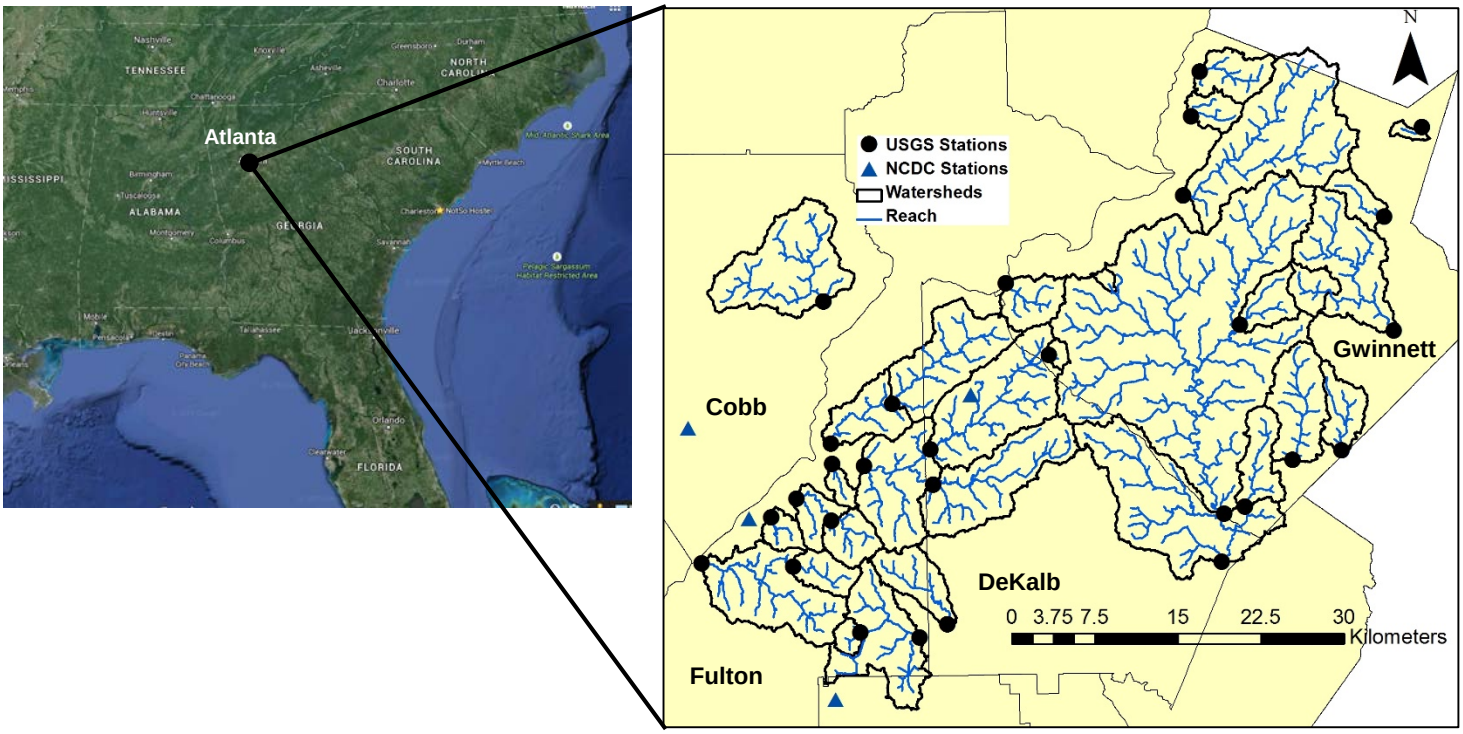

Figure 4.1. Delineated watersheds for USGS stations in the Atlanta area. Black circles show the streamflow stations, blue triangles show climate stations.

(a) Topographic map (b) LULC 2006 (c) Hydrologic soil group map

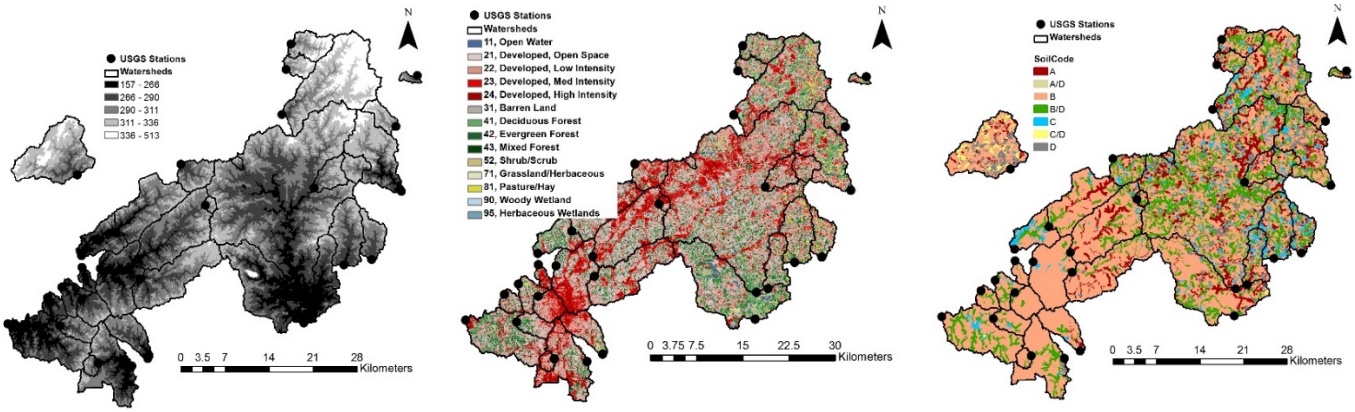

Figure 4.2. Topographic (in meter), LULC and soil maps of watersheds around Atlanta, GA.

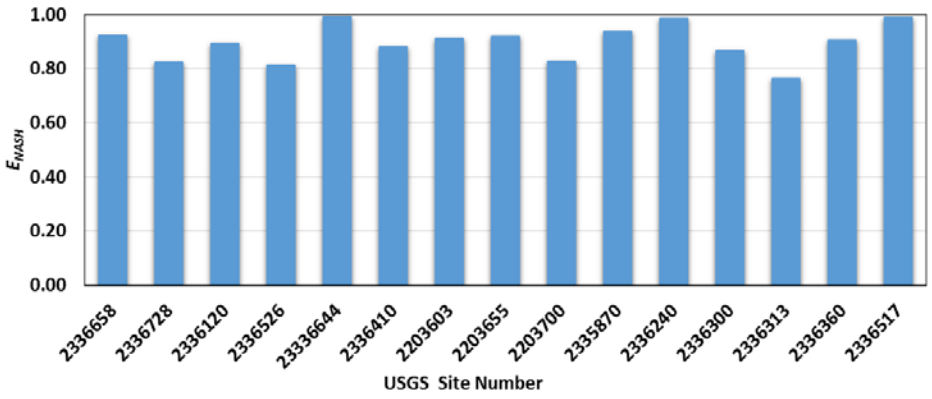

Figure 4.3. E_{NASH} values for each set of run conducted for NO_3 prediction.

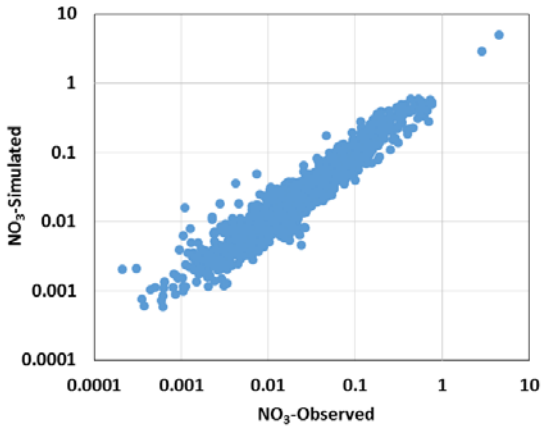

Figure 4.4. Log scaled scatter plots of observed versus ANN generated NO_3 loading (kg ha^{-1} d^{-1}) for the test watersheds.

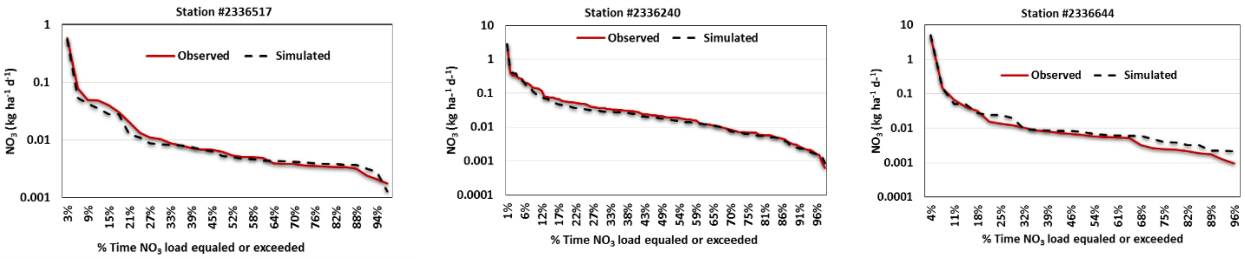

Figure 4.5. Log scaled load duration curve of observed versus ANN generated NO_3 for watersheds with high performance accuracy.

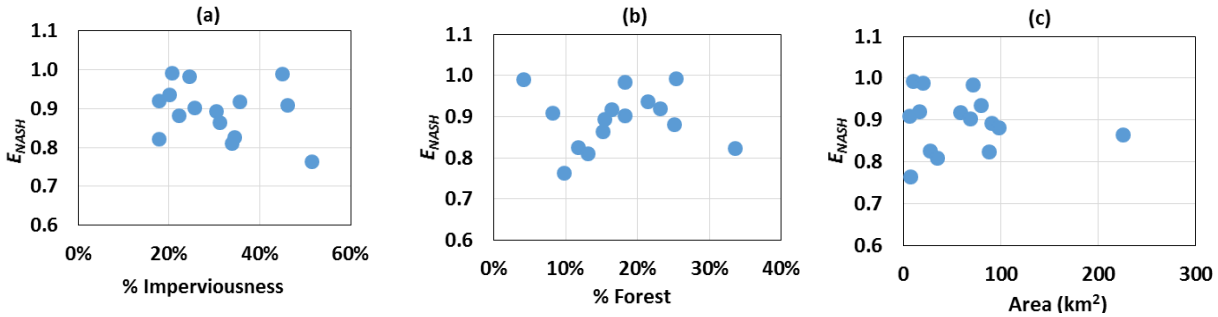

Figure 4.6. E_{NASH} values of NO_3 predictive models versus (a) percent imperviousness, (b) percent forest and (c) area of the test watersheds.

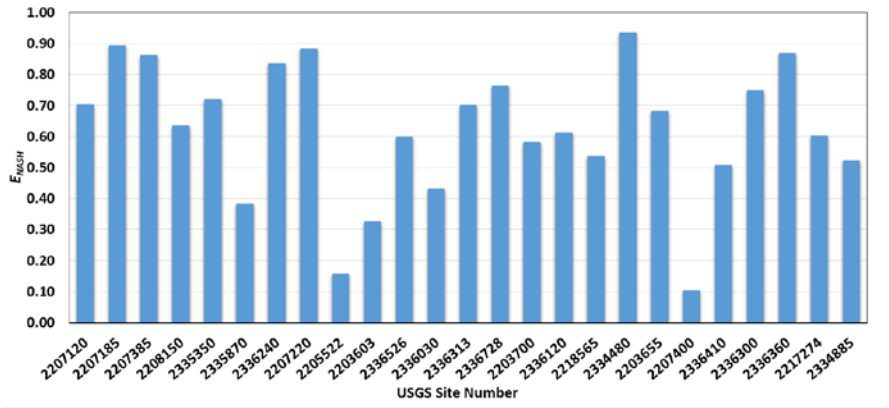

Figure 4.7. E_{NASH} values for each set of run conducted for NH_4 prediction.

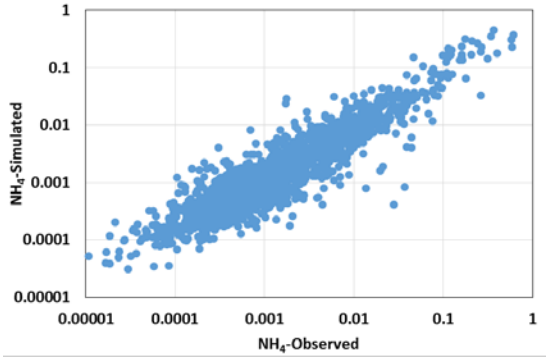

Figure 4.8. Log scaled scatter plots of observed versus ANN generated NH_4 loading (kg ha^{-1} d^{-1}) for test watersheds.

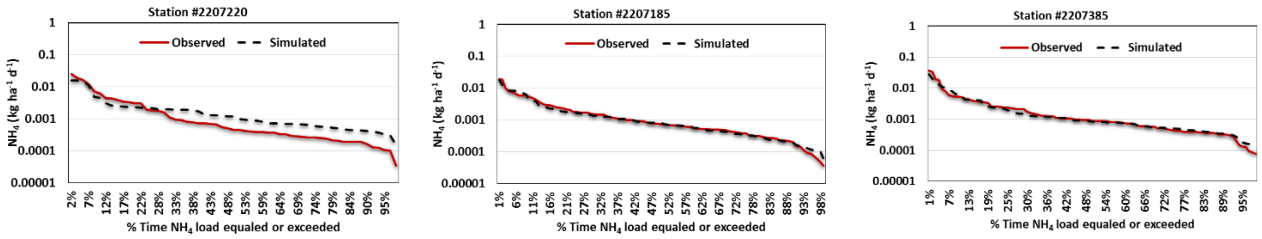

Figure 4.9. Log scaled load duration curve of observed versus ANN generated NH_4 for watersheds with high performance accuracy.

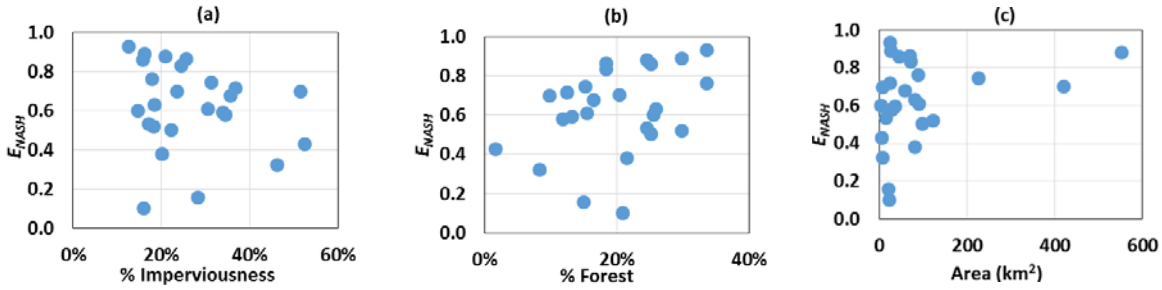

Figure 4.10. E_{NASH} values of NH_4 predictive models versus (a) percent imperviousness, (b) percent forest and (c) area of the test watersheds.

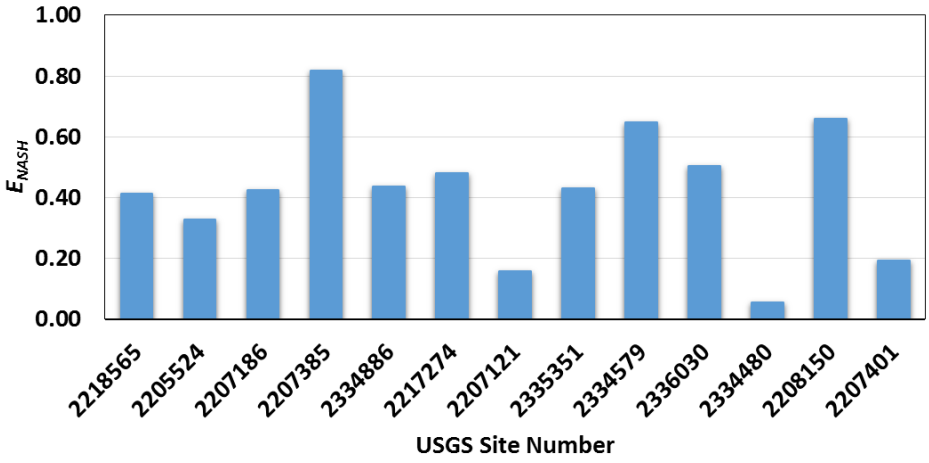

Figure 4.11. E_{NASH} values for each set of run conducted for PO_4 prediction.

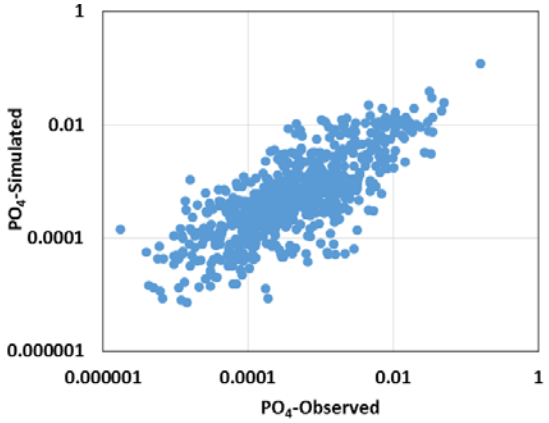

Figure 4.12. Log scaled scatter plots of observed versus ANN generated PO_4 loading (kg ha^{-1} d^{-1}) for test watersheds.

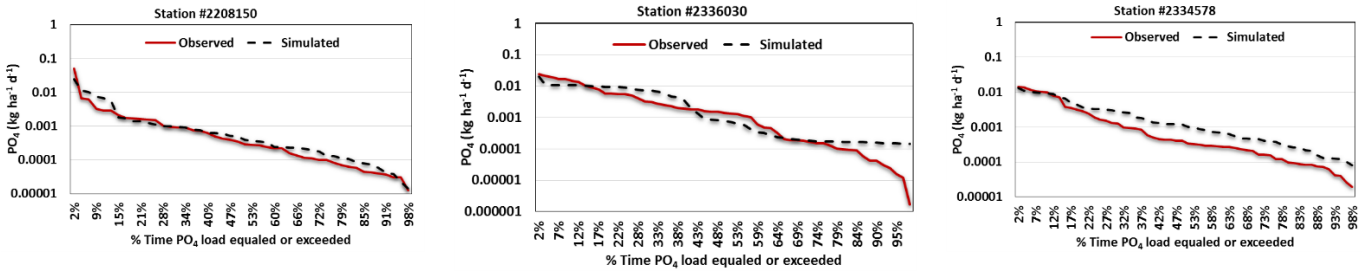

Figure 4.13. Log scaled load duration curve of observed versus ANN generated PO_4 for watersheds with high performance accuracy.

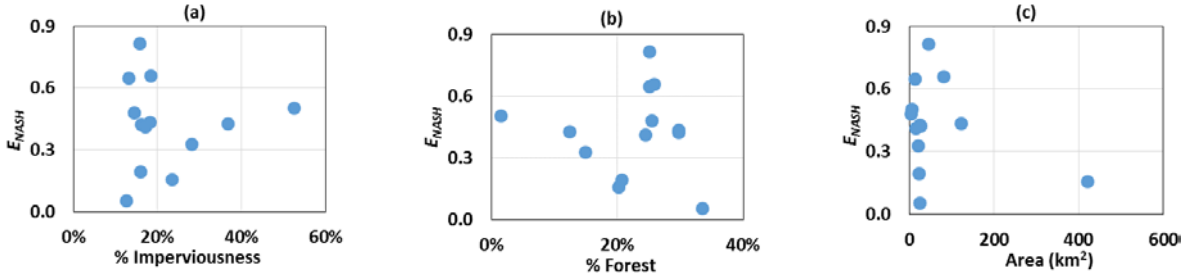

Figure 4.14. E_{NASH} values of PO_4 predictive models versus (a) percent imperviousness, (b) percent forest and (c) area of the test watersheds.

(a) Warm Season

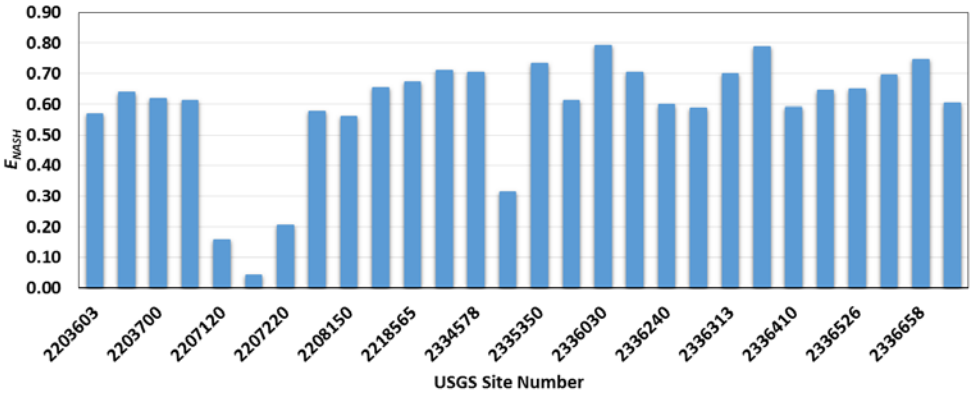

(b) Cool Season

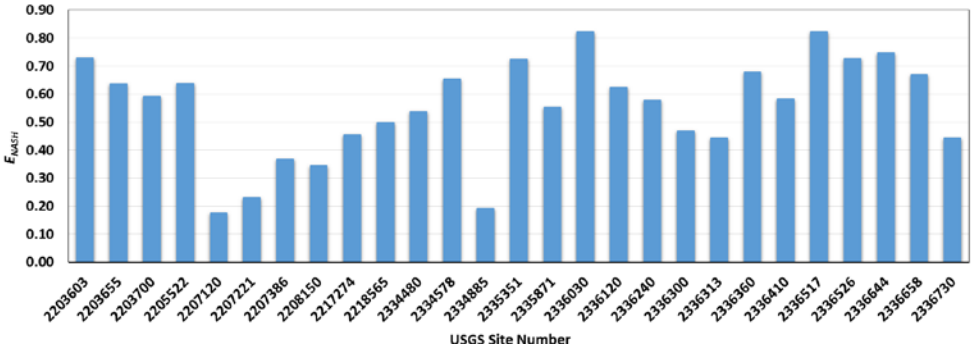

Figure 4.15. E_{NASH} values for each set of run conducted during (a) warm and (b) cool seasons flow predictions.

(a) Warm Season (b) Cool Season

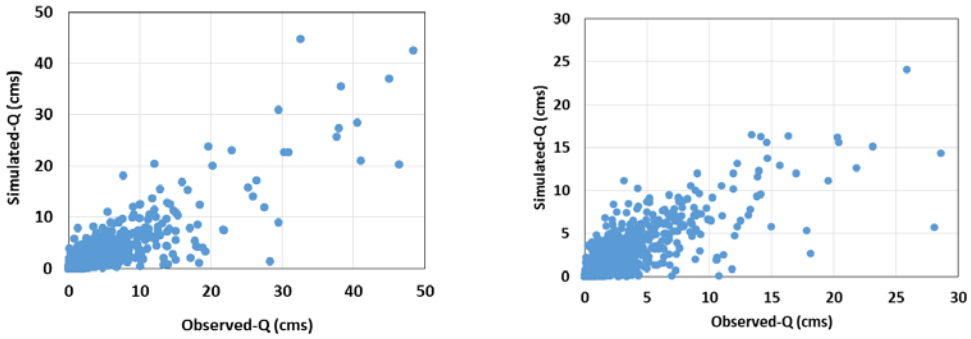

Figure 4.16. Scatter plots of observed versus ANN generated daily streamflow for (a) warm season, (b) cool season.

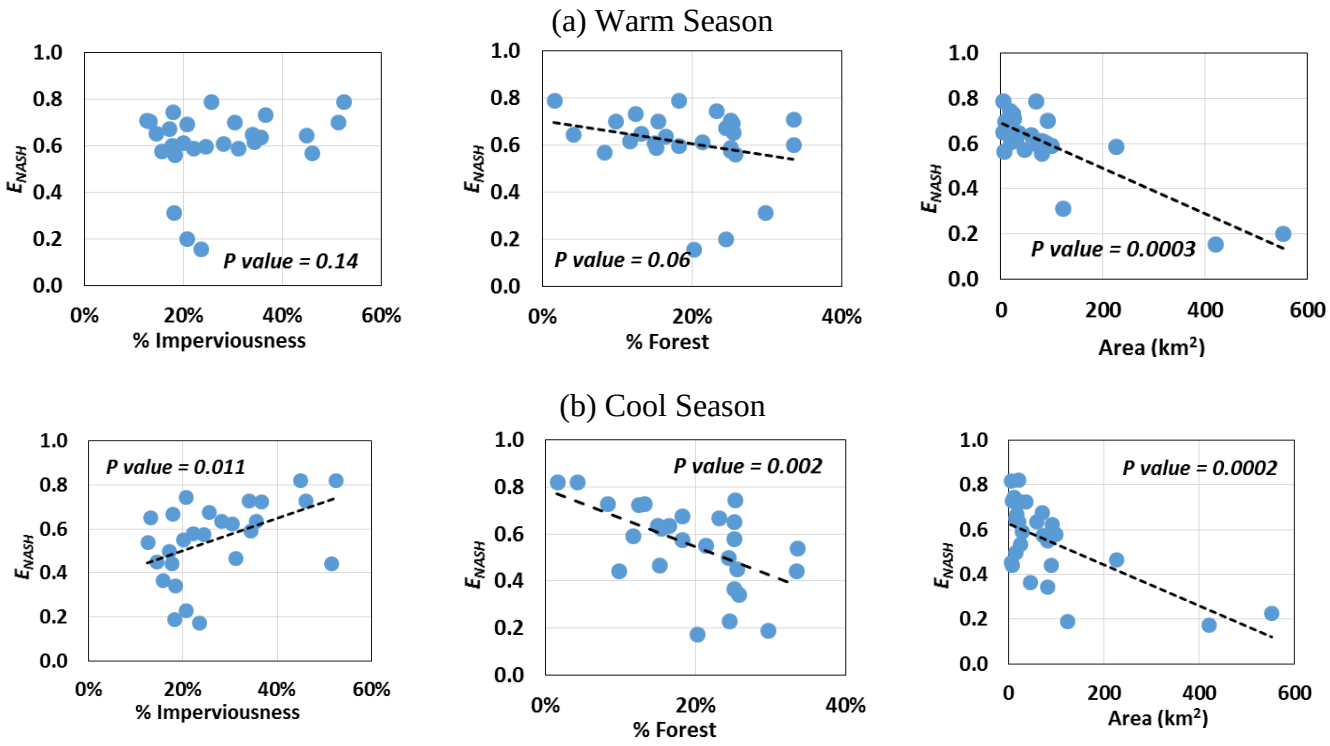

Figure 4.17. E_{NASH} values of streamflow predictive models for (a) warm season and (b) cool season versus percent imperviousness, percent forest and area of the test watersheds.

Chapter 5. Environmental predictors of *Culex quinquefasciatus* abundance associated with West Nile Virus

Abstract

West Nile Virus (WNV) is a mosquito-borne infectious disease of global public health concern. The occurrence of this virus is influenced by many risk factors such as climate variability, land use/cover (LULC) characteristics and hydrologic and water quality conditions. The combined role of these environmental factors on *Culex quinquefasciatus* abundance and potential WNV outbreak in Atlanta area, Georgia, U.S.A. were examined and discussed in this chapter. Considering findings from previous chapters and linking them together helped assess the virus risk in a broader view and investigate the combined impacts of those factors on mosquito population and the consequent WNV risk. Detailed assessment of environmental risk factors would help predict spatial patterns of human WNV risk in the Atlanta metropolitan area. It will also be effective for early warning of WNV risk outbreaks by directing surveillance activities and environmental monitoring and public health interventions.

Keyword: West Nile Virus, mosquito population, Environmental factors, climate, water quality, land use, hydrology.

Introduction

West Nile Virus (WNV) is the most widespread flavivirus in the world, distributed in Africa, Eurasia, and the Americas (Tran et al. 2014). This virus is transmitted between birds as the principal hosts via mosquito vectors. In the southeast U.S., over 96% of the West Nile Virus positive mosquito pools reported to the CDC from 1999 to 2010 have been obtained from *Culex* mosquitoes, among which 65% were from *Culex quinquefasciatus* (Andreadis, 2012). The state of Georgia, and especially the metro Atlanta area has been a hotspot of WNV incidence in 2012 with 117 WNV human cases, 6 deaths and 125 WNV positive mosquito pools (among which over 81% were from *Culexquinquefasciatus*) reported by the Georgia Department of Public Health. Feeding behaviors of these mosquitoes can affect transmission, amplification and geographic distribution of this virus (Munoz et al. 2012). Biotic and abiotic conditions affect mosquito behaviors and consequently the risk of WNV epidemics (Paz et al. 2013). The occurrence of this virus is impacted by many risk factors such as the presence of susceptible avian hosts, infected birds, mosquito abundance that feed on birds and human or horses, and the interaction of the vector with the biotic and abiotic environment. The most important environmental factors influencing the maintenance of WNV are climate variability, land use/cover (LULC) characteristics, water quality conditions of mosquito breeding sites and socio-economic conditions. Understanding the ecology of the vectors, suitable habitats and preferential hosts is important for predicting the amplification of WNV infection (Bisanzio et al. 2011).

Climate is the main driver of the vector abundance carrying this virus (Roiz et al., 2014). *Culex* species display a seasonal behavior. Their activity reaches its minimal level in the winter, then rises in the spring to the peak levels of summer and continues until mid-fall (Strickman, 1988). Elevated temperatures accelerate the growth rates of vector populations, decrease the interval between blood meal and speed the development of viruses within the mosquito carriers (Epstein, 2001; Patz et. al., 2008; Wang et. al., 2010). Rainfall and the surface moisture also prepare potential breeding habitats for female mosquitoes to lay their eggs (Shaman et al., 2002).

Characteristics of LULC, forest to urban conversion and its impact on water quality also affect the virus incidence by preparing suitable conditions for mosquitoes to develop through the landscape. Urbanization and shifting from forest to urban cause increase in nutrient loading into the urban streams. As nutrients are limiting resources for bacteria and mosquito larvae feed on bacteria, stream pollution is a major determinant of the abundance of mosquito vectors (Chaves et al. 2010; Calhoun et al. 2007). The selection of mosquito breeding sites is the result of the recognition of key physical and chemical factors. Sites with higher nutrient concentrations provide greater microbial food resources and mitigate resource competition (Dowling et al. 2013).

Spatial analysis of epidemiological data can help identify the geographic locations of populations at risk. Temporal analysis can also clarify inter-annual and seasonal variation of the vector abundance, and long-term predictions of shifts in mosquito abundance which can help identify high-risk periods for WNV. These analyzes can facilitate the development of hypotheses

about the epidemiological and ecological processes that drive these patterns (Rezaeian et al. 2007; Zeger et al. 2004; Wimberly et al. 2013).

The mosquito population density is a function of all the above environmental determinants and the complex nature of each of the drivers makes the impacts of potential future changes difficult to quantify (Paz et al. 2013). The geographic and seasonal patterns of *Culex* mosquito density can shift toward a specific region or occur earlier in the transmission season (Wimberly et al. 2013). The impacts of spatially heterogeneous environmental and ecological factors on mosquito population dynamics are complex and understanding the inter-relationships between vectors, hosts, and their environment can provide valuable information for identifying conditions suitable for pathogen transmission (Bisanzio et al. 2011).

In the previous chapters, a set of environmental conditions including the climate variability, LULC characteristics and water quality conditions favorable for *Culex* mosquito developments were identified and predictive models were developed for each factor separately. The main goal of this chapter is to discuss the significance of above environmental drivers of WNV, in a broader view and to investigate the combined impacts of those factors on mosquito population and the consequent WNV risk. This will lead to a better integration of environmental monitoring and to build a virus risk map based on the updated variations of abiotic factors.

Methodology

WNV for the first time was detected in 2001 in Georgia and has caused human disease each year since it arrived in Georgia. Continuous mosquito and human cases reported to the Georgia Department of Health since 2001 followed by a recent outbreak in 2012, made the virus endemic in this state and particularly in Atlanta. In this study, for a better integration of environmental monitoring, the combined impacts of environmental factors on mosquito abundance in Atlanta area was discussed. Figure 5.1 shows a schematic of the methodology followed.

LULC and water quality and *Culex quinquefasciatus* Population

To characterize the water quality conditions of streams around Atlanta and to link it to distribution of WNV transmission risk, mosquito trap sites that have been used at least 10 times in Fulton, DeKalb and Cobb counties and were located near a stream network with the distance of 1 km or less were selected (Figure 5.2). 58 sites were selected in the Atlanta metropolitan area and 1 km radius around each field site was considered based on the maximum distance traveled per day of *Culex quinquefasciatus* (Reisen et al. 1991, 1992). Watersheds were delineated for each trap site with a water body inside a 1 km radius using SWAT. To link the water quality conditions in streams near selected mosquito traps to the mosquito abundance, daily streamflow and nutrient loadings were predicted using the ANN models developed in chapter 4. Watersheds were delineated for each trap site using the Soil and Water Assessment Tools (SWAT) and streamflow was simulated. The simulated streamflows were divided into warm and cool seasons and were

used as inputs to ANN models. The predicted flow along with the percentage of different LULC types and water temperature were used as inputs to the ANN models for predicting PO_4, NH_4 and NO_3 loadings. Average daily air temperature was obtained from National Climatic Data Center (NCDC) stations in the city of Atlanta (Figure 5.2) and temepratrue-dependant expression of the Arrhenius equation was used as an input to ANN (refer to chapter 4).

The predicted water quality constituents were linked to the developed regression models in chapter 2 to estimate *Culex quinquefasciatus* population under water quality conditions in Atlanta area from 2002 to 2010.

Results and discussion

Watersheds delineated for the mosquito trap sites are shown in Figure 5.2 and the watersheds characteristics are also given in Table 5.1. Percent imperviousness ranged from 0% to 68% and percent forest cover ranged from 0% to 100%. Also the area of these watersheds varied from 0.01 km^2 to 325.25 km^2. For daily flow during cool and warm seasons, the top 5 predictive models with best performance accuracy were chosen and to summarize the data, median value of monthly streamflow averaged through all 100 watersheds for the period 2002-2010 and their 95% upper and lower bounds were given in Figure 5.3. Among all the watersheds, the total daily predicted streamflow ranged from 0.005 to 139.4 m^3/s.

The predicted daily streamflow along with the percent LULC types and T_{eff} were used as inputs to the developed ANN models to predict PO_4, NO_3 and NH_4 loadings. The top three ANN models

with high performance accuracy were selected for each nutrient. Since the climate-mosquito data in the previous chapter was analyzed in four weeks moving average scale, the nutrient loadings were also estimated in the same scale and the log scaled values are given in Figure 5.4. The median and 95% upper and lower bounds of loading values for the period 2002-2010 along watersheds nearby 58 mosquito trap sites were calculated. The predicted loading values ranged from 0 to 2.28 kg ha^{-1} d^{-1} for NO_3, 0 to 1.22 kg ha^{-1} d^{-1} for NH_4 and 0 to 0.16 kg ha^{-1} d^{-1} for PO_4. There are high fluctuations in PO_4 values for watersheds nearby mosquito trap sites, this could be due to lower performance of the developed predictive model for PO_4 loadings compared to the other two models.

To show how much nutrient actually exists in the stream water regardless of the size of the watershed, the nutrient load was predicted in this study. To link the predicted nutrient values around the Atlanta area to the mosquito population, the dose-response relationships between larval development and nutrients developed through a mesocosm experiment were applied here. The predicted nutrient yield by the best developed ANN model were converted to concentration and were linked to the dose-response curves. Four weeks moving average nutrient concentrations were calculated and are given in Figure 5.5. Median of nutrient concentrations and the 95% upper and lower bounds along the watersheds for the period 2002 to 2010 are shown in this figure. Since flow was one of the input to the nutrient predictive models and the streamflow model performances gradually decreased as the watershed size increased (Figure 4.16), large watersheds were excluded. The highest mean NO_3 concentrations over the period 2002-2010 for four weeks moving average

scale was 2.7 mg/L and belonged to the watershed #37 with the size of 73 km^2, 31% imperviousness and 17% forest cover. The watershed #22 with the area of 3.8 km^2 and percent imperviousness of 21 and percent forest cover of 25 had the second highest mean NO_3 concentration of 2.6 mg/L. Based on the mesocosm experiment, high NO_3 concentrations favor the development of male mosquitoes and suppresses the development of female mosquitoes. Therefore, sites #37 and #22 could have less number of female *Culex quinquefasciatus* in comparison to other sites.

The highest mean NH_4 concentrations over the period 2002-2010 was 0.40 mg/L and belonged to watersheds #40. The area of this watershed was 11 km^2 with 14% imperviousness and 29% forest cover. Findings of chapter 2 revealed that for adult males, increased NH_4 concentrations decreased pupation time. Therefore, NH_4 enhances the rate of development of male mosquitoes. Also higher NH_4 concentrations increases the number of surviving mosquito larvae and the number of larvae successfully pupating. In above mentioned sites, the abundance of *Culex quinquefasciatus* should be higher due to high NH_4 concentrations.

For PO_4, the highest mean predicted concentration levels belonged to watersheds with percent imperviousness of less than 10% or percent forest cover above 40%, and since they were outside the ranges of delineated watersheds of USGS stations (see Figure 4.16) and extrapolation reduces the model accuracy, these watersheds were considered as outliers. Excluding these outliers, the highest PO_4 concentrations averaged over the period 2002-2010 for four weeks moving average scale were 2.6 and 0.44 mg/L for watersheds #1-1 and #37 respectively. The area of these

watersheds varied from 0.27 to 73 km^2. In terms of LULC, they had 50% to 17% forest cover and13% to 31% imperviousness. PO_4 concentration exerts a positive influence on late aquatic stages of mosquito larvae. This nutrient plays a significant role in keeping larvae alive longer but inhibits pupation in absence of NO_3 or NH_4. Moreover, the mesocosm experiment showed that in containers with the combinations of either PO_4 and NO_3 or PO_4 and NH_4, fewer days are required for both females and males to emerge than other groups. The high PO4 concentration level in highly forested watershed indicates that the potential breeding habitats for *Culex* mosquito development can be found even in non-developed areas. However, the predicted PO_4 values for watersheAds nearby mosquito trap sites had high fluctuations with a wide 95% bound as shown in Figure 5.5. This could be due to lower performance of the developed predictive model for PO_4 loadings compared to the other two models. Also, the developed predictive model for the test watershed with the highest percent forest cover had the weakest performance indicating that it is less reliable to apply the model to forested watersheds for prediction purposes.

The results of water quality prediction indicated that the breeding sites with high nutrient concentrations can occur in both forested and urban areas and the developed models can be applied in watersheds similar to the watersheds delineated for USGS stations which were used for developing predictive water quality and streamflow models. These watersheds had the percent imperviousness of 13% to 52% and percent forest cover of 2% to 33%. Also, as the watershed size increased, the streamflow model performances gradually decreased (Figure 4.16). This indicates

that the developed models are reliable to be applied in watersheds with the size of less than 200 km^2 (See Figure 4.16) and with LULC types within the mentioned ranges.

Conclusions

Applying developed predictive models to the urbanized watersheds around Atlanta can help us identify potential mosquito breeding sites through the landscape. Due to urbanization and deforestation in the Atlanta area and increase in surface runoff, the suitability of breeding mosquitoes has improved. Also animal communities that serve as hosts and vectors for pathogens are modified due to LULC changes. Loss of bird habitat due to forest fragmentation can increase avian densities within remaining fragments and may facilitate the transmission and amplification of WNV (Wang et al. 2010). In addition, climate alters pathogen and vector demographic rates (Kilpatrick 2011). Climate variability influences landscape through drought or flooding or through dry and wet period. Drought can affect the nutrient concentrations especially in standing waters through evaporation. During drought conditions, the reduced water flow creates stagnant water pools which become richer in organic material ideal for breeding mosquitoes (Aharonson-Raz et al. 2014). This may bring the mosquitoes and birds into close contact and around small water holes and thus facilitate the virus circulation. When drought ends and water resource increase, infected mosquitoes and bird disperse, initiating the early transmission phase of WNV cycle (Shaman et al. 2002). Also, intense spring or summer rain or floods, provide pools for mosquitoes to breed along the stream bank and if the stream water is polluted, it would help mosquitoes to develop faster

which can lead to an outbreak. The rise and fall of the water table in the land surface determines where and when pools of water form at the land surface, creating potential larval mosquito habitats (Shaman et al. 2005 & 2010). The virus could occur in inundated lowland habitats in floodplain forest ecosystem (Hubalek 2008). Our findings from chapter 3 are in an agreement with the above statements. Combining the findings of chapters 3 and 4 indicates that areas with higher PO_4 or lower NO_3 level coupled with above average total weekly rain events over March to April and mild spring, provide favorable conditions for mosquito development in mid-July. However, more detailed studies need to be conducted to develop an integrated model for predicting mosquito population under the combined impacts of the most important WNV risk factors. There are large uncertainties that need to be clarified regarding the linkage of each environmental factor and mosquito development. Also the accuracy and reliability of the identified relationships play an important role in understanding and predicting the dynamic of mosquito population. Detailed assessment of environmental risk factors would help predict spatial patterns of human WNV risk. WNV human risk map may assist with selecting surveillance sites, guiding preventive control measures such as catch basin, and determining the thresholds for initiating responsive control activities in the highest risk areas. Early warning and identification of outbreaks is critical to limiting the animal and human losses to this disease (Valiakos et al. 2014). Targeted surveillance and control efforts prioritized for high WNV risk areas should start earlier in the season or after detection of WNV enzootic activity and should lead to increased public health protection during

outbreaks while reducing costs, labor, and environmental impacts associated with these measures (Rochlin et al. 2011).

To identify the hotspots of WNV, birds behavior also needs to be accounted since this virus is maintained in a bird-mosquito transmission cycle (Bisanzio et al. 2011). Local movements of resident birds and long-range travel of migratory birds may contribute to pathogen dispersion (Valiakos et al. 2014). Determining area that provide favorable habitats for local and migratory birds along with abundant larval breeding sites for local mosquito species would help understand the spatial distribution of *Culex* species. Human behaviors such as time spent outdoors and use of repellants, must also align. To understand the distribution of WNV risk in an area, both landscape as well as socio-economic attributes need to be considered. Socio-economic conditions, particularly housing age and income create elevated WNV transmission risk at particular sites. Areas with high poverty rates appear to face a greater threat from WNV (Tackett et al. 2006). Spatial patterns of disease risk may be associated with socioeconomic factors due to effects of urbanization on the natural environment (Ruiz et al. 2007). An understanding of why certain populations are more vulnerable may can provide a stronger basis for decisive action by public health practitioners.

References

Aharonson-Raz K, Lichter-Peled A, Tal S, Gelman B, Cohen D, et al. (2014) Spatial and Temporal Distribution of West Nile Virus in Horses in Israel (1997–2013) - from Endemic to Epidemics. PLoS ONE 9(11): e113149. doi:10.1371/journal.pone.0113149

Andreadis, Th.G., 2012. The contribution of *Culex pipens* complex mosquitoes to transmission and persistence of West Nile Virus in North America. The American Mosquito Control Association, Inc. Vol. 28, No. 4, page: 137-151.

Bisanzio, D., Giacobini, M., Bertolotti, L., Mosca, A., Balbo, L., Kitron, U., Vazquez-Prokopec, G.M., 2011. Spatio-temporal patterns of distribution of West Nile virus vectors in eastern Piedmont Region, Italy. *Parasites & Vectors*. 4:230.

Calhoun, L.M., M. Avery, L. Jones, K. Gunarto, R. King, J. Roberts, and T.R. Burkot. 2007. Combined Sewage Overflows (CSO) Are Major Urban Breeding Sites for *Culex quinquefasciatus* in Atlanta, Georgia. Am. J. Trop. Med. Hyg. 77: 478–484.

Chaves, L.F., C.L. Keogh, A.M. Nguyen, G.M. Decker, G.M. Vazquez-Prokopec, and U.D. Kitron. 2010. Combined sewage overflow accelerates immature development and increases body size in the urban mosquito *Culex quinquefasciatus*. J Appl. Entomol. 135: 611–620.

Dowling, Z., Sh.L. Ladeau, P. Armbruster, D. Biehler, and P.T. Leisnham. 2013. Socioeconomic Status Affects Mosquito (Diptera: Culicidae) Larval Habitat Type Availability and Infestation Level. J Med Entomol. 50:764-772

Epstein, P. R., 2001. West Nile Virus and the Climate. *Journal of Urban Health: Bulletin of the New* York Academy of Medicine. Vo. 78, No, 2.

Hubalek, Z. 2008. Mosquito-borne viruses in Europe. *Parasitol Res* (Suppl 1) 103:S29–S43. DOI 10.1007/s00436-008-1064-7.

Kilpatrick, A.M. 2011. Globalization, Land Use, and the Invasion of West Nile Virus. *Science* 334, 323.

Munoz, J., Ruiz, S., Soriguer, R., Alcaide, M., Viana, D.S., Roiz, D., Vazquez, A., Figuerola, J. 2012. Feeding Patterns of Potential West Nile Virus Vectors in South-West Spain. PLoS ONE. Vol. 7:6, 1:9.

Paz, Sh., Semenza, J.C. 2013. Environmental Drivers of West Nile Fever Epidemiology in Europe and Western Asia—A Review. *Int. J. Environ. Res. Public Health*. 10, 3543-3562; doi:10.3390/ijerph10083543.

Patz, J.A., Olson, S.H., Uejio, Ch. K., Gibbs, H.K., 2008. Disease Emergence from Global Climate and Land Use Change. *Med Clin N Am* 92, 1473–1491.

Rezaeian, M.; Dunn, G.; St Leger, S.; Appleby, L. 2007. Geographical epidemiology, spatial analysis and geographical information systems: A multidisciplinary glossary. *J. Epidemiol. Commun. Health, 61*, 98–102.

Rochlin, I., Turbow, D., Gomez, F., Ninivaggi, D.V., Campbell, S.R. 2011. Predictive Mapping of Human Risk for West Nile Virus (WNV) Based on Environmental and Socioeconomic Factors. *PLoS ONE*. Vol. 6: 8. 1:10.

Roiz, D., Ruiz, S., Soriguer, R., Figuerola, J., 2014. Climatic effects on mosquito abundance in Mediterranean wetlands. Parasites & Vectors, 7:333.

Ruiz, M.O., Walker, E.D., Foster, E.S., Haramis, L.D., Kitron, U.D. 2007. Association of West Nile virus illness and urban landscapes in Chicago and Detroit. Int J Health Geogr, 6: 10.

Shaman, J., Stieglitz, M., Stark, C., Blancq, S. L., Cane, M., 2002. Using a Dynamic Hydrology Model to Predict Mosquito Abundances in Flood and Swamp Water. *Emerging Infectious Diseases Journal,* Vol. 8, No. 1.

Shaman, J., Day, J.F., Stieglitz, M., 2005. Drought-Induced Amplification and Epidemic Transmission of West Nile Virus in Southern Florida. *Journal of Medical Entomology*, 42(2): 134-141.

Shaman, J., Day, J.F. Komar, N. 2010. Hydrologic Conditions Describe West Nile Virus Risk in Colorado. *Int. J. Environ. Res. Public Health, 7,* 494-508; doi:10.3390/ijerph7020494.

Strickman, D., 1988. Rate of oviposition by *Culex Quinquafasciatus* in San Antonio, Texas, during three years. *Journal of the American Mosquito Control Association*. Vol 4, No. 3. 339-344.

Tackett, J., Charnigo, R., Caldwell, G. 2006. Relating West Nile Virus case fatality rates to demographic and surveillance variables. Public Health Rep. 121(6): 666–673.

Tran, A. Sudre, B., Paz, Sh., Rossi, M., Desbrosse, A., Chevalier, V., Semenza, J.C. 2014. Environmental predictors of West Nile fever risk in Europe. International Journal of Health Geographics. 13:26. Pages 2:11.

Valiakos, G., Papaspyropoulos, K., Giannakopoulos, G., Birtsas, B., Tsiodras, S., Hutchings, M.R., Spyrou, V., Pervanidou, D., Athanasiou, L.V., Papadopoulos, N., Tsokana, C., Baka, A., Manolakou, K., Chatzopoulos, D., Artois, M., Yon, L., Hannant, D., Petrovska, L., Hadjichristodoulou, Ch., Billinis, Ch. 2014. Use of Wild Bird Surveillance, Human Case Data and GIS Spatial Analysis for Predicting Spatial Distributions of West Nile Virus in Greece. *PLOS ONE*. Vol. 9:5. 1:8.

Wang, G., Minnis, R.B., Belant, J.R., Wax, Ch.R., 2010. Dry weather induces outbreaks of human West Nile virus infections. *BMC Infectious Diseases*, 10:28.

Wimberly, M.C., Giacomo, P., Kightlinger, L., Hildreth, M.B. 2013. Spatio-Temporal Epidemiology of Human West Nile Virus Disease in South Dakota. *Int. J. Environ. Res. Public Health*, *10*, 5584-5602; doi:10.3390/ijerph10115584

Zeger, S.L.; Irizarry, R.A.; Peng, R.D. 2004. On time series analysis of public health and biomedical data. Annu. Rev. Public Health, 27, 57–69.

Table 5.1. Watersheds characteristics of selected mosquito trap sites.

Site Number	IM	DF	EF	MF	PA	UG	Area (km2)
3	11%	16%	12%	0%	0%	0%	2.50
4	32%	6%	12%	4%	0%	0%	9.83
7	8%	30%	13%	0%	9%	8%	7.06
11	18%	7%	12%	1%	0%	0%	21.48
12	22%	3%	24%	3%	0%	7%	2.48
14	49%	1%	1%	0%	1%	0%	10.03
15	20%	11%	13%	1%	0%	0%	73.13
16	17%	0%	0%	0%	8%	0%	1.19
18	10%	19%	16%	2%	5%	0%	3.83
22	21%	5%	15%	5%	0%	0%	3.76
28	29%	9%	12%	0%	0%	0%	8.48
29	27%	8%	11%	1%	0%	0%	35.07
30	20%	9%	9%	0%	0%	0%	3.91
35**	31%	7%	9%	1%	0%	0%	225.33
36	31%	6%	6%	0%	0%	0%	1.38
37-1	31%	7%	10%	0%	0%	0%	73.16
39	21%	3%	9%	2%	0%	0%	5.73
40	14%	11%	15%	2%	10%	2%	10.94
42	53%	6%	2%	0%	0%	0%	4.24
44	36%	8%	8%	0%	0%	0%	5.83
47	27%	3%	8%	0%	0%	0%	3.69
51**	15%	24%	8%	1%	6%	3%	325.25
52	21%	4%	25%	1%	3%	0%	6.17
55	17%	23%	9%	1%	2%	0%	13.52
56	12%	23%	10%	0%	8%	0%	4.73
57	7%	11%	16%	0%	3%	3%	3.58
10-1	30%	0%	0%	0%	0%	0%	0.42
10-2	17%	0%	20%	0%	0%	0%	0.46
10-3	13%	29%	29%	0%	0%	0%	0.62
10-4	6%	50%	13%	0%	0%	0%	0.68
10-5	47%	0%	0%	0%	0%	0%	0.38
1-1	13%	50%	0%	0%	25%	0%	0.27
1-2	11%	9%	9%	9%	0%	0%	1.00

"Continued on next page."

1-3	8%	22%	0%	0%	22%	0%	0.75
13-1	27%	5%	10%	0%	2%	0%	17.70
13-2	10%	14%	7%	0%	0%	0%	1.22
13-3	6%	0%	0%	0%	0%	0%	0.32
1-4	1%	60%	0%	0%	20%	0%	0.56
17-1	17%	6%	12%	2%	0%	0%	12.85
17-2	8%	0%	44%	0%	0%	0%	0.85
19-1	39%	2%	0%	0%	0%	0%	4.85
19-2	34%	14%	7%	0%	0%	0%	1.23
19-3	28%	0%	0%	0%	0%	0%	0.21
20-1	52%	0%	0%	0%	0%	0%	0.50
20-2	68%	0%	0%	0%	0%	0%	0.41
2-1	10%	14%	43%	0%	14%	5%	1.84
2-2	16%	5%	38%	0%	0%	3%	3.19
23-1 & 24 & 21	51%	0%	1%	0%	0%	0%	3.35
23-2	16%	6%	6%	0%	0%	0%	3.22
25-1	19%	4%	13%	0%	0%	0%	2.30
25-2	20%	0%	5%	0%	0%	0%	1.63
26-1	40%	11%	6%	0%	0%	0%	1.71
26-2	26%	7%	17%	0%	1%	0%	8.27
26-3	24%	14%	14%	7%	0%	0%	1.13
27-1	46%	7%	2%	0%	0%	0%	3.97
27-2	6%	0%	0%	0%	0%	0%	0.36
32-1	33%	3%	8%	0%	0%	0%	9.75
32-2	27%	4%	13%	0%	0%	0%	22.53
33-1**	28%	11%	10%	1%	0%	0%	300.56
33-2	35%	10%	6%	0%	1%	1%	31.86
34-1	42%	29%	0%	0%	0%	0%	0.52
34-2	10%	33%	0%	0%	0%	0%	0.52
34-3	3%	25%	25%	0%	0%	0%	0.25
37-2	9%	21%	21%	0%	0%	0%	1.38
38-1	20%	4%	10%	0%	0%	0%	4.68
38-2	20%	14%	10%	0%	0%	0%	3.70
41-1	2%	0%	75%	0%	0%	0%	0.39
41-2	10%	15%	15%	0%	0%	0%	3.53

“Continued on next page.”

43-1	43%	0%	10%	0%	0%	0%	0.93
43-2	18%	17%	17%	0%	0%	0%	1.00
45-1	29%	10%	0%	0%	0%	0%	1.08
45-2	36%	0%	0%	0%	0%	0%	0.27
45-3	3%	0%	0%	0%	25%	0%	0.30
45-4	52%	0%	0%	0%	0%	0%	0.01
46-1	22%	15%	11%	0%	0%	0%	0.43
46-2	28%	7%	7%	0%	0%	0%	2.41
46-3	10%	33%	67%	0%	0%	0%	1.37
48-1	16%	7%	21%	0%	7%	0%	0.18
48-2	8%	22%	11%	0%	0%	0%	0.11
49-1	28%	20%	0%	0%	0%	0%	1.41
49-2	3%	0%	33%	0%	0%	0%	1.74
49-3	11%	20%	13%	0%	0%	0%	0.56
49-4	22%	0%	0%	0%	0%	0%	0.26
49-5	18%	15%	0%	0%	0%	0%	1.24
50-1	27%	0%	17%	0%	0%	0%	0.34
50-2	12%	11%	21%	0%	0%	0%	1.16
5-1	1%	37%	26%	0%	0%	5%	0.49
5-2	4%	53%	0%	0%	16%	0%	9.99
53-1	29%	7%	2%	0%	0%	0%	1.59
53-2	22%	25%	0%	0%	0%	0%	1.74
54-1	19%	5%	8%	0%	0%	0%	5.03
54-2	24%	6%	24%	0%	0%	0%	0.80
58-1	3%	47%	28%	0%	0%	6%	3.68
58-2	1%	25%	25%	0%	25%	0%	1.53
6-1	23%	10%	19%	0%	0%	0%	1.81
6-2	12%	11%	29%	0%	0%	0%	2.52
8-1	0%	25%	46%	0%	10%	7%	6.24
8-2	0%	29%	18%	0%	6%	24%	1.40
9-1	43%	0%	0%	0%	0%	0%	1.04
9-2	28%	20%	0%	0%	0%	0%	0.57
Average	21%	12%	12%	0%	2%	1%	13.75
Maximum	68%	60%	75%	9%	25%	24%	325.25
Minimum	0%	0%	0%	0%	0%	0%	0.01

"Continued on next page."

STDEV***	0.15	0.14	0.15	0.02	0.06	0.04	57.74

** IM= imperviousness, DF: Deciduous Forest, EF: Evergreen Forest, MF: Mixed Forest, PA: Pasture, UG: Urban Grass*

*** Watersheds with large areas were considered as outliers.*

****Standard deviation*

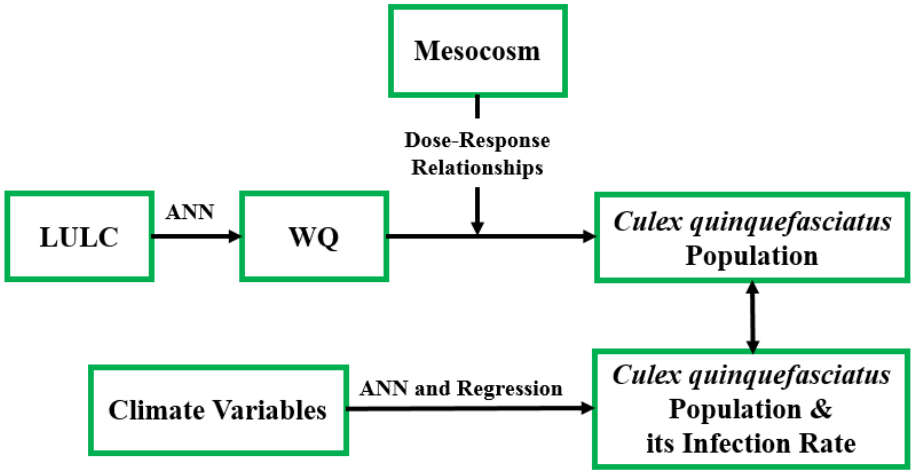

Figure 5.1. Schematic of methodology.

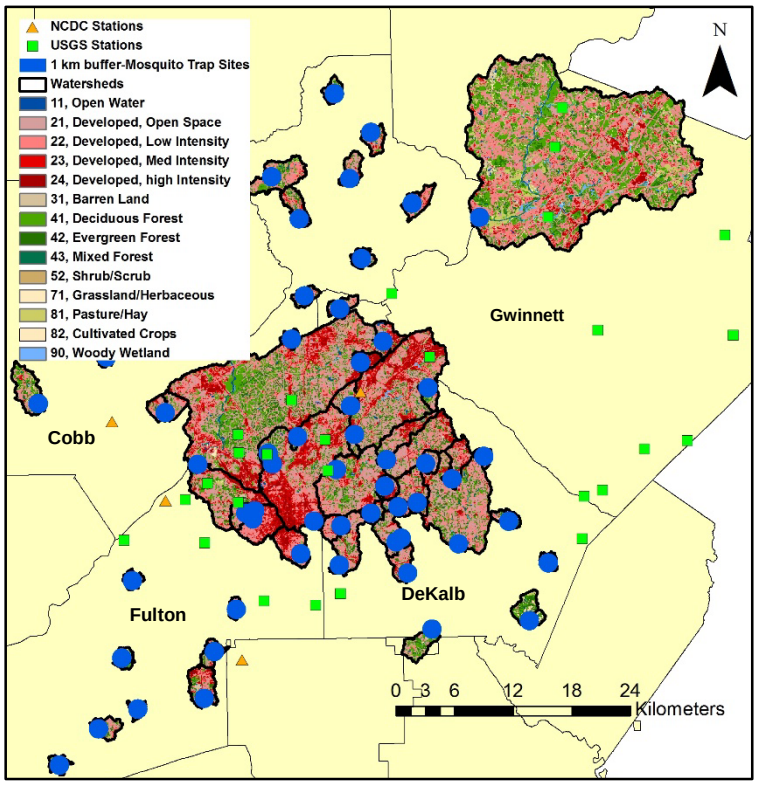

Figure 5.2. Delineated watersheds for 58 selected mosquito trap sites in the Atlanta area.

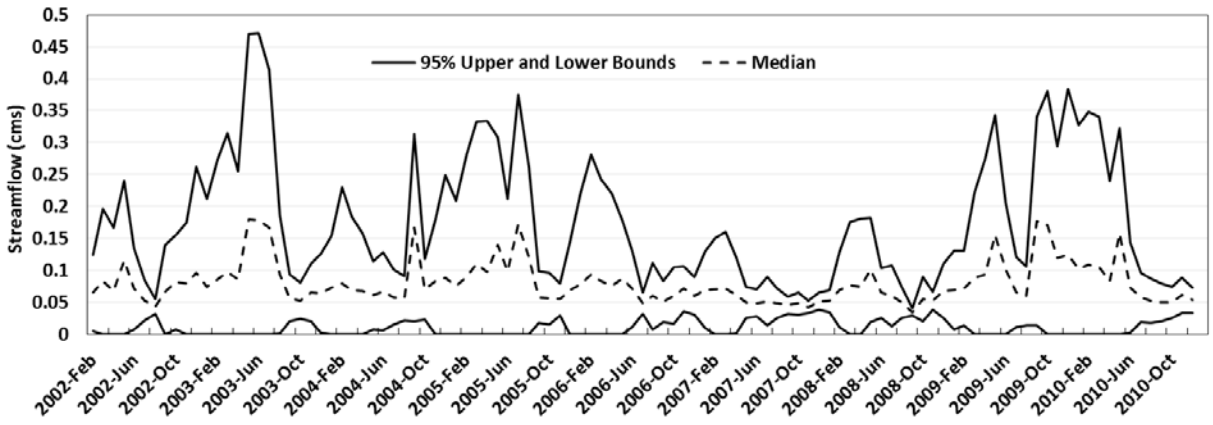

Figure 5.3. Predicted average monthly streamflow obtained from top 5 ANN models with best performances along 100 watersheds nearby mosquito trap sites.

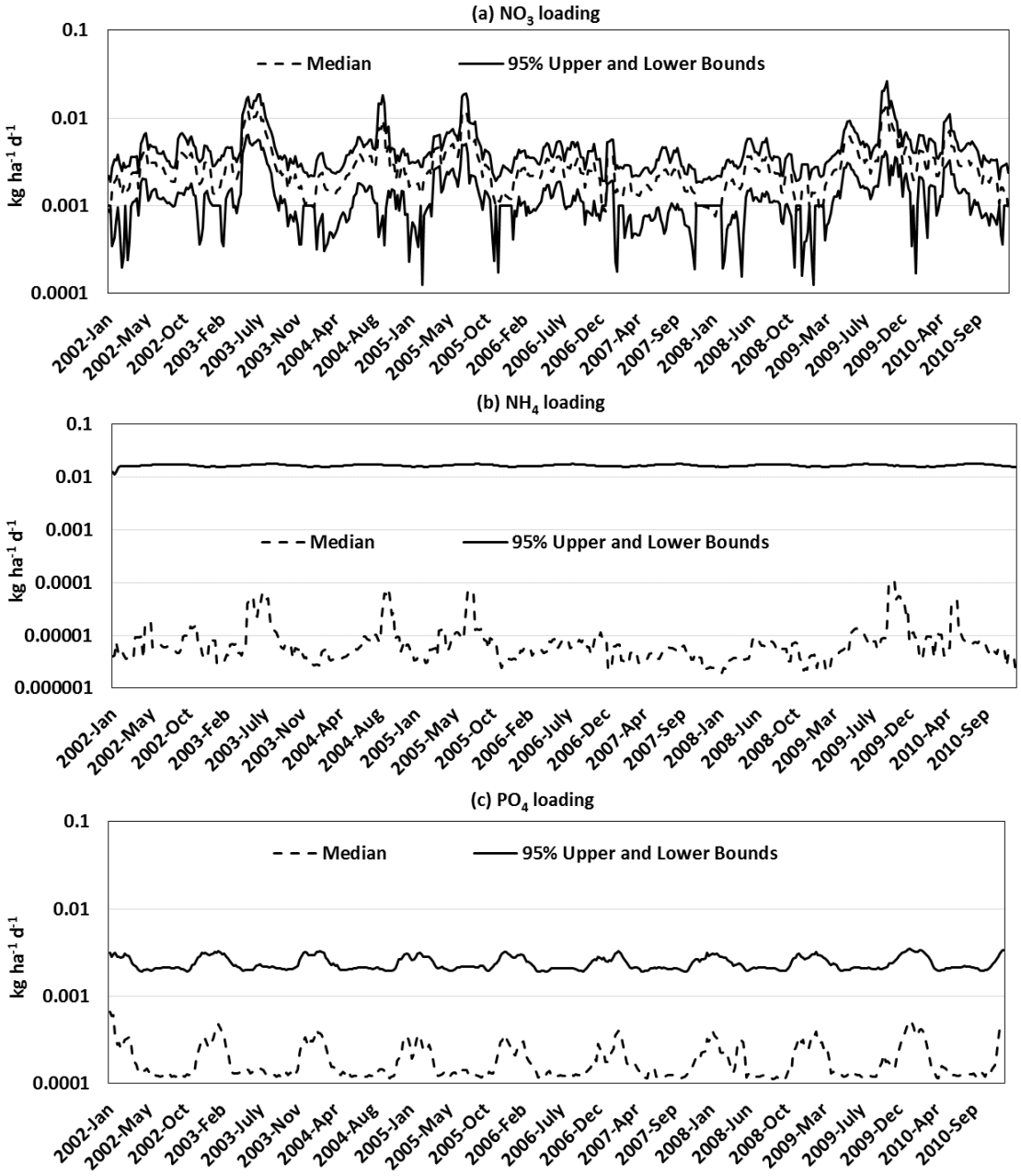

Figure 5.4. Log scaled predicted four weeks moving average (a) NO_3, (b) NH_4, and (c) PO_4 loadings using ANN models with best performances for watersheds nearby mosquito trap sites.

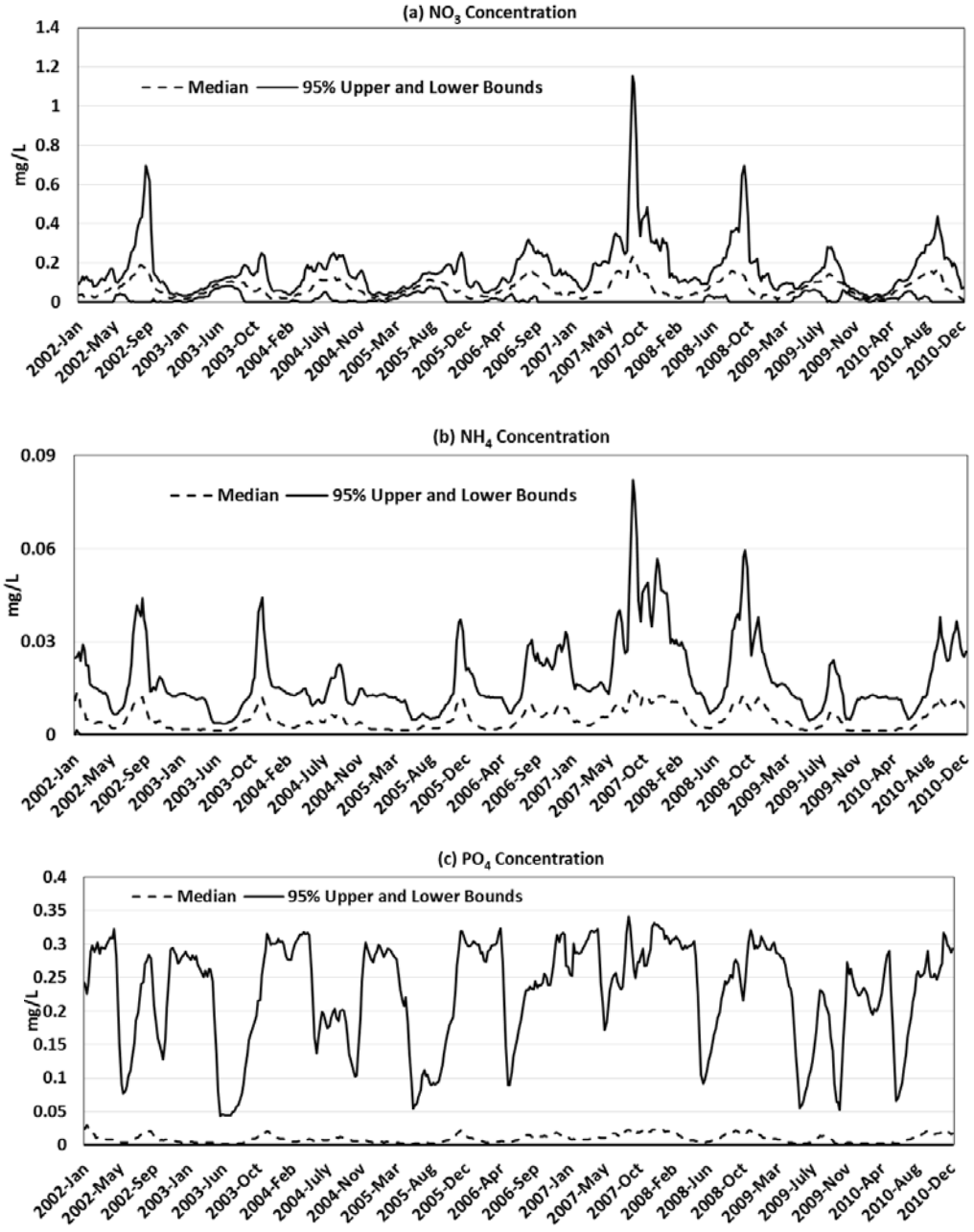

Figure 5.5. Predicted four weeks moving average and 95 % upper and lower bounds (a) NO_3, (b) NH_4, and (c) PO_4 concentrations along all watersheds.

Chapter 6. Conclusion

Summary and Conclusions

WNV transmission risk depends on different ecological and environmental factors (Chevalier et al. 2014). Biotic and abiotic conditions affect mosquito behaviors and consequently the risk of WNV epidemics (Paz et al. 2013). Several elements of biological and ecological knowledge are still missing and experimental studies are needed to quantify key parameters. To assess the prevalence of vector-borne diseases within an area and to implement control measures, understanding the spatial and temporal dynamics of mosquito communities is vital (Buckner et al. 2010). To do so, developing predictive models that link environmental variables and insect abundance is essential to increase the efficiency and efficacy of management. The main goal of this research was to advance our understanding of the transmission of mosquito-borne arboviruses under the influence of different environmental and climatic drivers of WNV disease. The most important findings of this research and the study implications are highlighted below.

Water quality and *Culex quinquefasciatus* population

The mesocosm experiment results have demonstrated the impacts of nutrients on mosquito pre-adult development and the quantitative relationships between specific nutrient concentrations in water and developmental parameters. The major findings of this experiment were:

1) Increased NO_3 levels alone in the larval habitat favors the development of male mosquitoes and suppresses the development of female mosquitoes. However, those adult females that do emerge, develop faster in containers with the NO_3 constituent compared to the reference group. Female mosquitoes are larger than males and also their development time is longer than males, therefore, they need more food than males.

2) Addition of PO_4 alone to the larval habitat increases the larval development time. The increase in the developmental time occurs in the absence of nitrogen. Nitrogen is required for chitin development and severely limiting for larval growth. Therefore, the combination of NO_3 and PO_4 or NH_4 and PO_4 nutrients in the container favors mosquito development and shortens pupation time.

These findings should promote the development of targeted larviciding interventions, thus reducing the costs and efforts required for effective mosquito vector control. The results of this experiment may also help identify specific larval habitats for *Culex* mosquitoes by predicting which water quality conditions in urban landscapes are most likely to support mosquito development, which could lead to improved control of WNV transmission. However, it is important to take into account the accuracy of the developed dose-response relationships and their uncertainties when applying them to the real world and real cases.

Climatic variability and *Culex quinquefasciatus* abundance and its infection rate

This study clarified the temporal patterns (inter-annual variations and deviations from expected seasonal cycles) of *Culex* mosquito population and its infection rate anomalies and their application to predict future WNV risk and to identify high-risk periods and to suggest new hypotheses about the drivers of temporal variability at different scales. The major findings of this study were:

1) Elevated temperature and PET averaged over late winter and spring were associated with increased abundance of *Culex quinquefasciatus* and their related infection rate in summer. Also, drier than normal condition during spring with low available moisture in surface layers creates favorable conditions for the development of *Culex* vectors in summer.

2) Rain events of 6 cm and higher averaged over March to April in weekly scale combined with mild spring with average weekly temperature of 20 to 24 °C, favor mosquito development in mid-July. Also, total weekly rain events of 2 cm or less in March through May coupled with temperature around 26 °C, increases the chance of getting higher number of infectious mosquitoes in mid-July.

3) Addition of 1 week antecedent mosquito count data to the ANN model as a predictor increased the E_{NASH} value from 0.54 to 0.68 and from 0.62 to 0.89 respectively for weekly and four weeks moving average scales. For the Vector Index, addition of the antecedent infection rate one week prior the capture increased the ANN model performance accuracy and the E_{NASH} value

changed from 0.54 to 0.69 and from 0.72 to 0.93 respectively for weekly and four weeks moving average scales.

These findings and the developed models can be used to estimate the size of vector populations that are likely to be seen in summer and to monitor the possible abnormalities in the increase of rates of WNV infection. Also, long-term predictions of shifts in mosquito abundance and in WNV risk can be estimated by modeling the significant climate factors under future warming conditions. These information can be used for an early detection of virus circulation in mosquitoes and to provide early warning for WNV outbreaks. However, more detailed climate analysis and data mining are needed to understand the variance in mosquito population and their infection rate year to year. Also considering other climate variables such as wind speed and humidity as predictors and selecting the optimal input layer to the model can lead to a more powerful prediction with reduced uncertainty.

Linkage between LULC and water quality

This study revealed that water quality can be predicted with Artificial Neural Networks in ungauged watersheds using data from the neighboring watersheds with similar characteristics. In addition, simulating the streamflow by SWAT and using the simulated flow as input to the ANN model, resulted in a stronger model with higher predictive power.

1) The developed ANN models could predict NO_3 and NH_4 loadings with “good” to “very good” level of accuracy. The performance of the developed predictive model for PO_4 loadings was

lower than the other two models, however, the model could provide a useful degree of predictive power.

2) The developed ANN models for predicting flow during warm and cool seasons had “good” to “very good” accuracy in most test watersheds.

3) No general trend was observed between percent imperviousness or percent forest cover or watershed size and the water quality model performances. However for the streamflow predictive models, as the percent forest cover or the size of test watershed increased, the model performance gradually decreased.

The developed models for predictions of water quality and streamflow in ungauged watersheds could help identify where an increase in vector population size and associated WNV transmission risk should be expected. Based on this information, implementation of risk-based surveillance programs could be conducted to better assess the virus outbreak. The significance of developing predictive water quality models become more evident for a large area due to time consuming and expensive process of water quality sampling. However, the developed models are not reliable to be applied in large watersheds (> 200 km^2) with high percentage forest cover. Applying a more accurate LULC map and more reliable instantaneous streamflow data can help improve the model performance. Also predicting nutrient concentrations by coupling SWAT and ANN models can lead to more powerful and accurate prediction.

Environmental predictors of *Culex quinquefasciatus* abundance associated with West Nile Virus

In this part of the study, daily streamflow and nutrient loadings were predicted in streams near selected mosquito traps in Atlanta using the developed ANN models from chapter 4 to link the water quality conditions to the mosquito abundance. Also for a better integration of environmental monitoring, the combined impacts of environmental factors on mosquito abundance was discussed. Major findings of this part of the study were:

1) The predicted loading values along the 58 sites ranged from 0 to 2.28 kg ha^{-1} d^{-1} for NO_3, 0 to 1.22 kg ha^{-1} d^{-1} for NH_4 and 0 to 0.16 kg ha^{-1} d^{-1} for PO_4.

2) Sites #37 and #22 had the highest four weeks moving average NO_3 concentrations averaged over the period 2002-2010. Based on the findings of the mesocosm experiment, these sites could have less number of female *Culex quinquefasciatus* in comparison to other sites.

3) The highest mean NH_4 concentrations over the period 2002-2010 was 0.40 mg/L and belonged to watersheds #40. Findings of chapter 2 revealed that for adult males, increased NH_4 concentrations decreased pupation time. Therefore in this site, the abundance of *Culex quinquefasciatus* should be higher due to high NH_4 concentrations.

4) The highest PO_4 concentrations averaged over the period 2002-2010 for four weeks moving average scale were 2.6 and 0.44 mg/L for watersheds #1-1 and #37 respectively. This nutrient plays a significant role in keeping larvae alive longer but inhibits pupation in absence of NO_3 or NH_4.

Findings from previous chapters and linking them together helped assess the virus risk in a broader view. Information from epidemiological surveillance should be integrated with environmental monitoring to provide more effective predictions of the likelihood of future WNV outbreak (Wimberly et al. 2013). However, the developed models had weak performance for highly forested watersheds, therefore, it is safer to apply them to urbanized watersheds for water quality and streamflow prediction purposes. Because of all these uncertainties, can should be taken in interpreting results from these models.

Future research

The potential future study that could be conducted as an extension of this work is modeling the impacts of preceding climate conditions over a range of time on *Culex* vector species under climate change scenarios so that long-term predictions of shifts in mosquito abundance can be estimated. Also the linkage between El Nino Southern Oscillation (ENSO) and the mosquito count data can be studied.

For streamflow prediction, wherever observed instantaneous streamflow data was missing, average daily flow for USGS stations were used, which can cause error in our prediction. Having more reliable streamflow data, and also providing a more accurate LULC map instead of NLCD, can improve the model performances. Also lumped and semi-distributed models can be coupled for predicting water quality concentrations by simulating the nutrients using SWAT and applying the simulated values as inputs to the ANN model.

In addition, to determine the WNV human risk, the socio-economic conditions need to be studied. Selection of risk factors characterized socio-economic conditions relevant to human ecology such as education, housing and income can help predict spatial patterns of WNV human cases. The risk of WNV to humans can be reduced by combining mosquito control and targeted health education outreach. Finally, there is a need to develop an integrated physically-based model by combining both temporal and spatial environmental factors and to investigate their impacts together on transmission of WNV. This could help properly predict the dynamic of *Culex* mosquitoes carrying this virus and consequently human risk at a given location and to implement adapted surveillance systems.

References

Buckner, E.A., Blackmore, M.S., Golladay, S.W., Covich, A.P. 2010. Weather and landscape factors associated with adult mosquito abundance in southwestern Georgia, U.S.A. Journal of Vector Ecology. Vol. 36, No.2. 269-278.

Chevalier, V., Tran, A., Durand, B. 2014. Predictive Modeling of West Nile Virus Transmission Risk in the Mediterranean Basin: How Far from Landing? *Int. J. Environ. Res. Public Health*, *11*, 67-90; doi: 10.3390/ijerph110100067.

Paz, Sh., Semenza, J.C. 2013. Environmental Drivers of West Nile Fever Epidemiology in Europe and Western Asia—A Review. *Int. J. Environ. Res. Public Health*. 10, 3543-3562; doi:10.3390/ijerph10083543.

Wimberly, M.C., Giacomo, P., Kightlinger, L., Hildreth, M.B. 2013. Spatio-Temporal Epidemiology of Human West Nile Virus Disease in South Dakota. *Int. J. Environ. Res. Public Health*, *10*, 5584-5602; doi:10.3390/ijerph10115584